Addressing Challenges in Pulsar Science in the Era of Multi-messenger Astronomy

Christo Venter

Centre for Space Research, North-West University, Potchefstroom

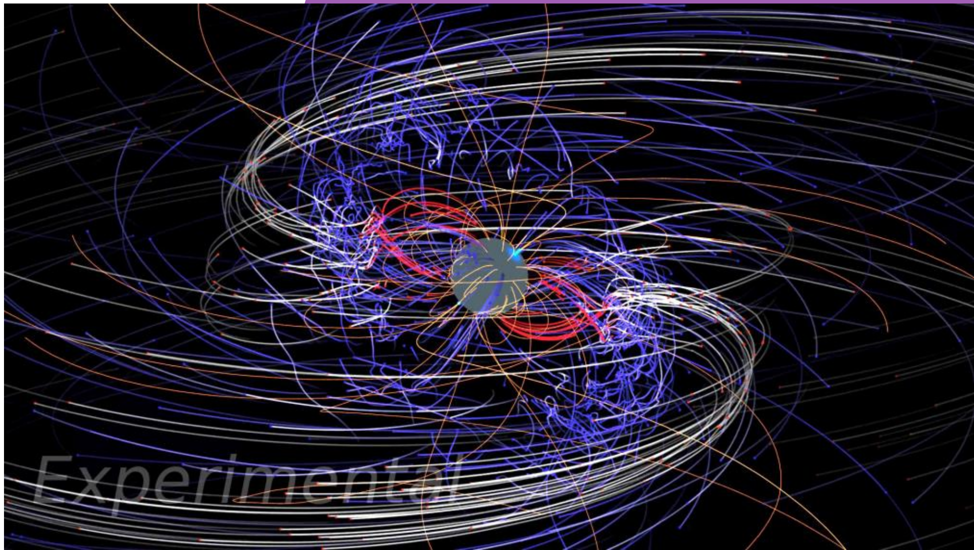

Applications of Quantum Information in Astrophysics and Cosmology, 24–26 April 2023, Cape Town

Setting the Scene

Quantum Information Theory

Astrophysics

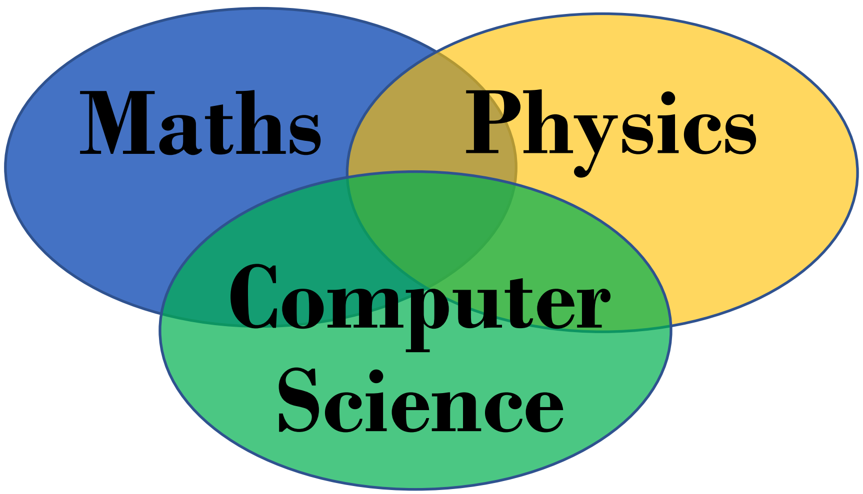

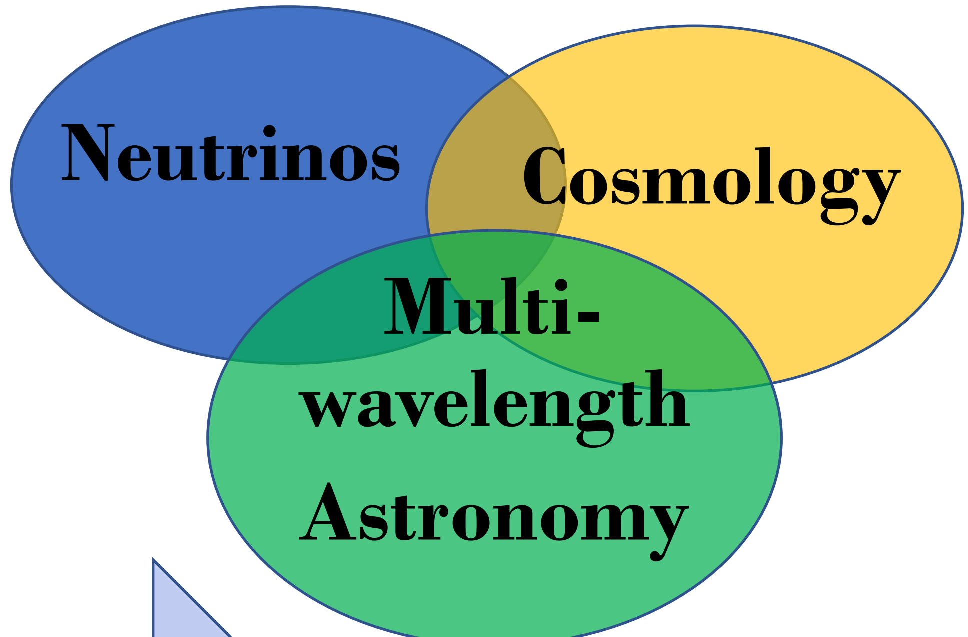

Applications?

Setting the Scene

Quantum Information Theory

Astrophysics

Multi-wavelength Astronomy

Physics

Pulsars

Overlaps?

https://plantura.garden/uk/insects/bees/bee-pollination

Astronomical Facilities

MeerKAT Radio Telescope

- **Inaugurated in July 2018 in Carnarvon, Northern Cape**
- **64 dishes; 13.5 m diameter**
- **Modes: Continuum, spectral lines, timing, polarisation, transient searches**
- **Receivers:**
  0.58 – 1.015 GHz;
  0.9 – 1.67 GHz;
  8 – 14.5 GHz
- **SKA Pathfinder**
- **MeerKAT Extended: 84 dishes (MPIFR)**
- **Massive computing and digital processing systems on site**

Southern African Large Telescope (SALT)

- Largest single optical telescope in Southern Hemisphere
- Located at SAAO outside Sutherland
- 11 m hexagonal primary mirror array
- 320 – 1700 nm
(near UV- near IF)
- Imaging, spectra, polarisation, transients
- Legacy Survey of Space and Time (LSST): South African involvement; 10-year survey of Southern Sky; 15 TB / night

NICER

- Neutron star Interior Composition Explorer
- NASA's payload (372 kgs) on the ISS since 2017
- Planned: 18 months
- X-ray timing instrument: array of 56 X-ray photon detectors
- Soft (0.2–12 keV) X-ray band
- Unprecedented sensitivity
- Science goals:
  - ✓ Fundamental investigation of extremes in gravity, material
  - ✓ density, and EM fields
  - ✓ Better understanding of the extreme nature and composition of neutron stars (NSs)
  - ✓ Constrain EOS to high precision

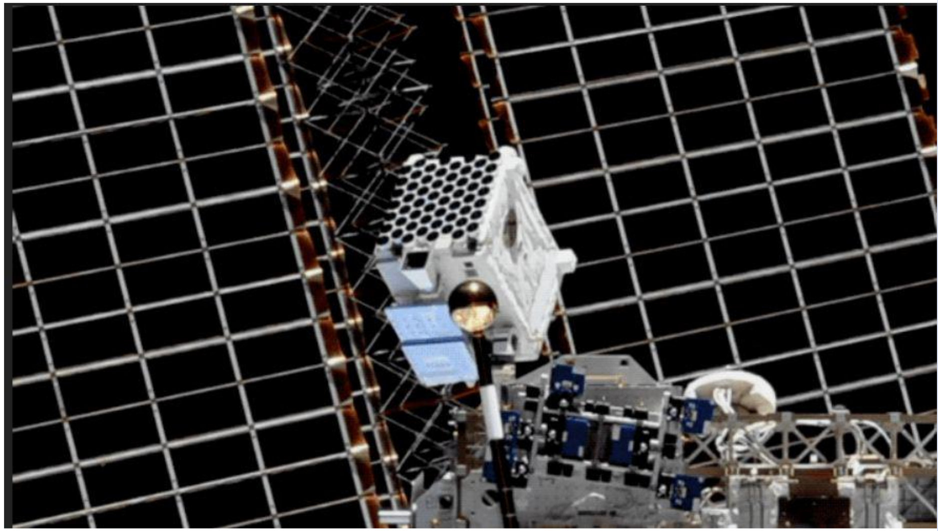

https://heasarc.gsfc.nasa.gov/docs/nicer

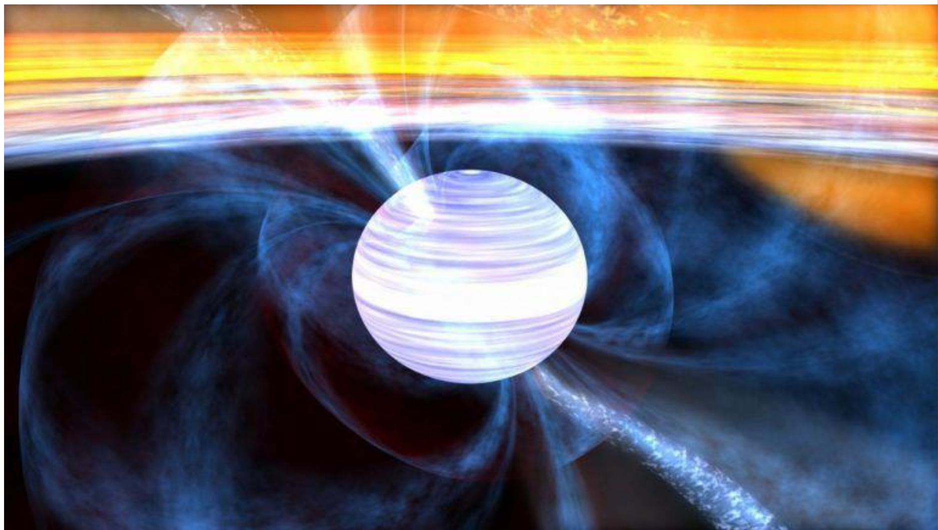

Fermi Large Area Telescope (LAT)

- Launched in June 2008
- Low-Earth orbit
- Pair-conversion instrument
- FoV > 2 sr (20% of sky)
- Scans whole sky every 3 h
- 20 MeV – 300 GeV (gamma rays)
- > 8000 cm^2 effective area
- Pulsars, nebulae, novae, supernova remnants, active galaxies, globular clusters, GRBs, Fermi Bubbles, Galactic Centre, cosmic rays, terrestrial flashes, sun, etc.

H.E.S.S. Telescopes

- High Energy Stereoscopic System
- Ground-based Imaging Atmospheric (Air) Cherenkov Telescopes (IACTs)
- Very-high-energy gamma-ray photons (50 GeV to 100 TeV)
- 4 x 12-m and 1 x 28-m telescopes
- PWNe, AGNe, SNRs, GRBs, binaries, galaxies, haloes, MM follow-up…
- And now also pulsars!
- Next: Cherenkov Telescope Array (CTA)

Multi-messenger Astronomy

GW170817:

- Binary neutron star merger
- Gravitational waves by LIGO
- *Fermi* GBM: short GRB
- Bright optical transient
- X-ray and radio emission
- No VHE gamma rays / neutrinos

(Abbott et al. 2017)

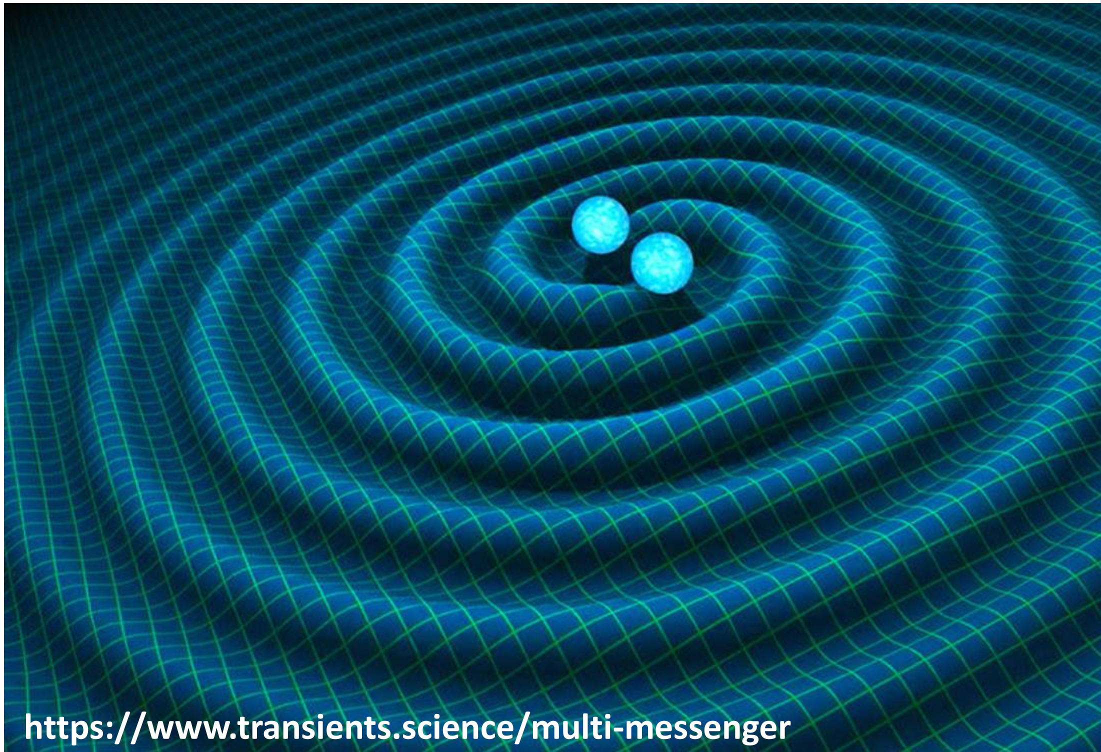

Multi-messenger Astronomy

TXS 0506+056:

- IceCube Neutrino Telescope detected a 290 TeV neutrino passing through deep South Pole Ice on 22/09/2017
- Flaring Blazar (VHE)
- Archival data: excess of neutrino events
- Solved century-old riddle as to the source of cosmic rays

(Aartsen et al. 2018)

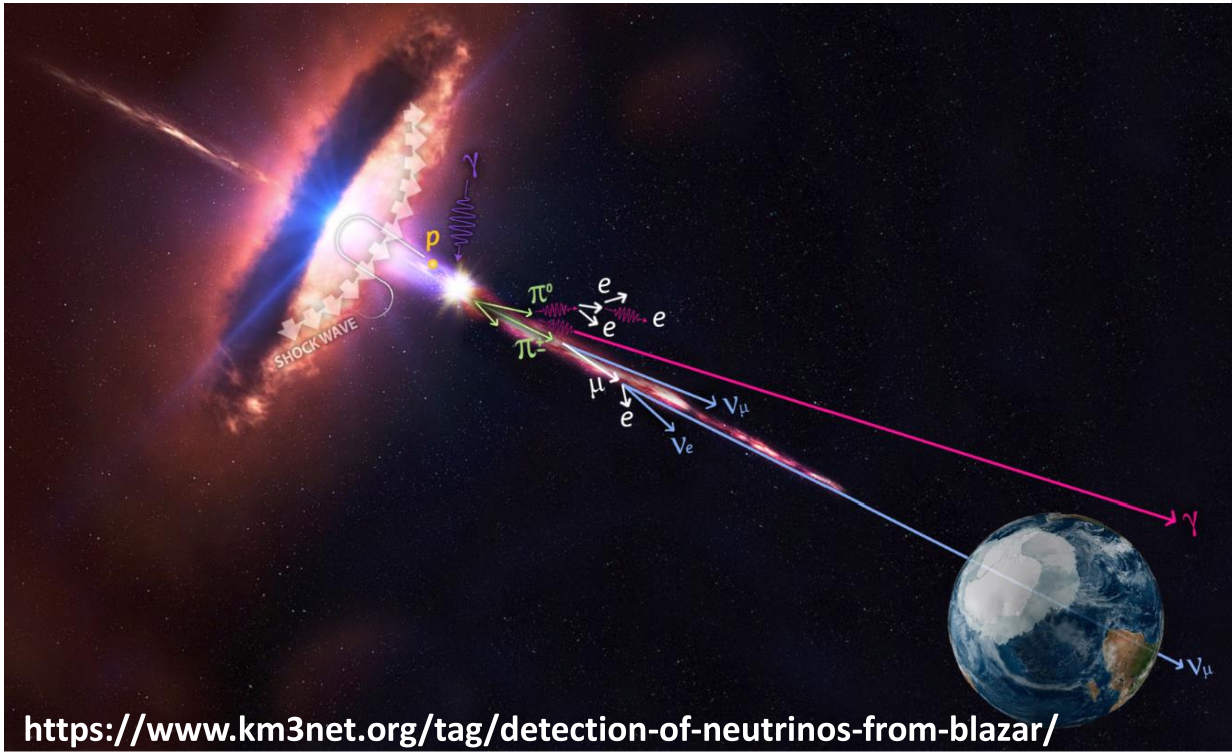

Pulsars

Pulsars

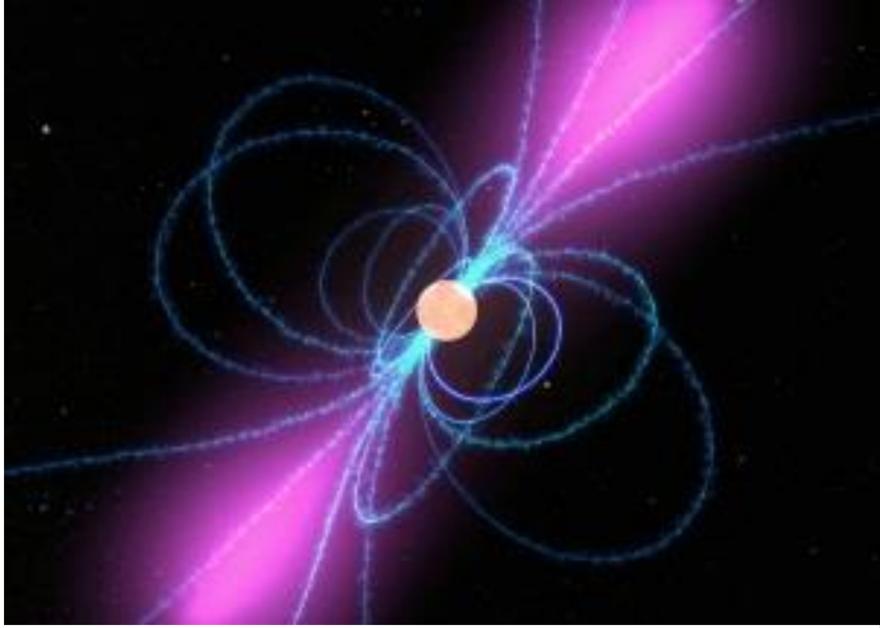

- Rapidly-rotating, highly-magnetised neutron stars
- Progeny of supernova explosions
- Spin-modulated, beamed pulsations across the EM band, wind of particles
- ~2 500 in radio, ~270 in GeV, also tens in X-rays, optical.
- “Pulsar zoo”: magnetars, RRATs, MSPs, binaries, MeV pulsars, transitional systems, etc.

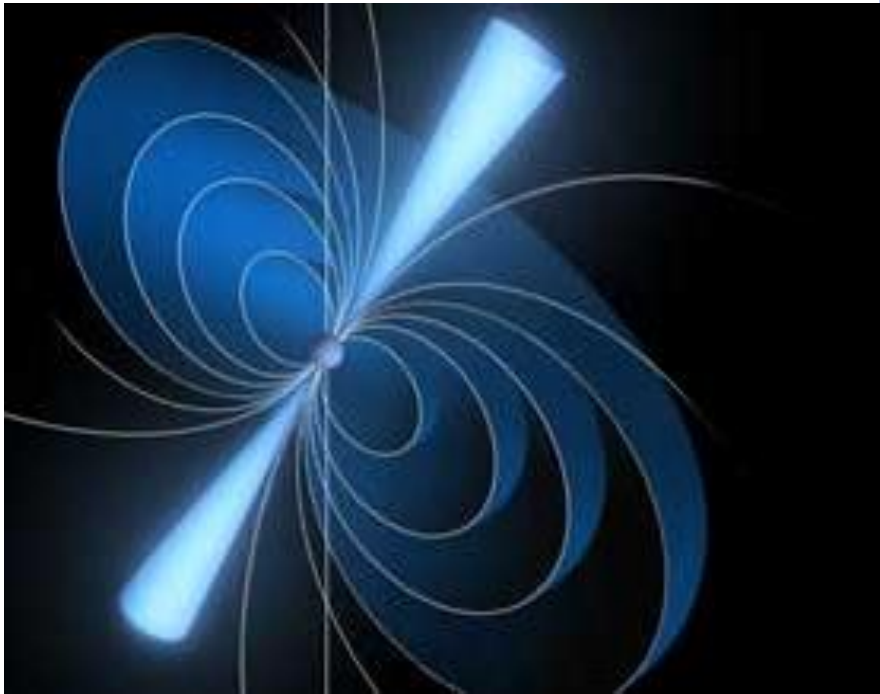

Observational Highlights

Fermi LAT Observations

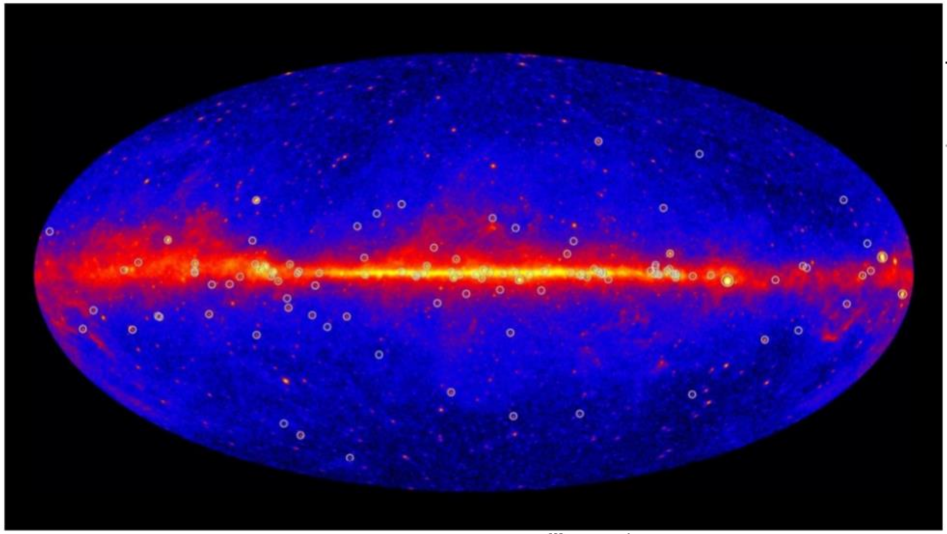

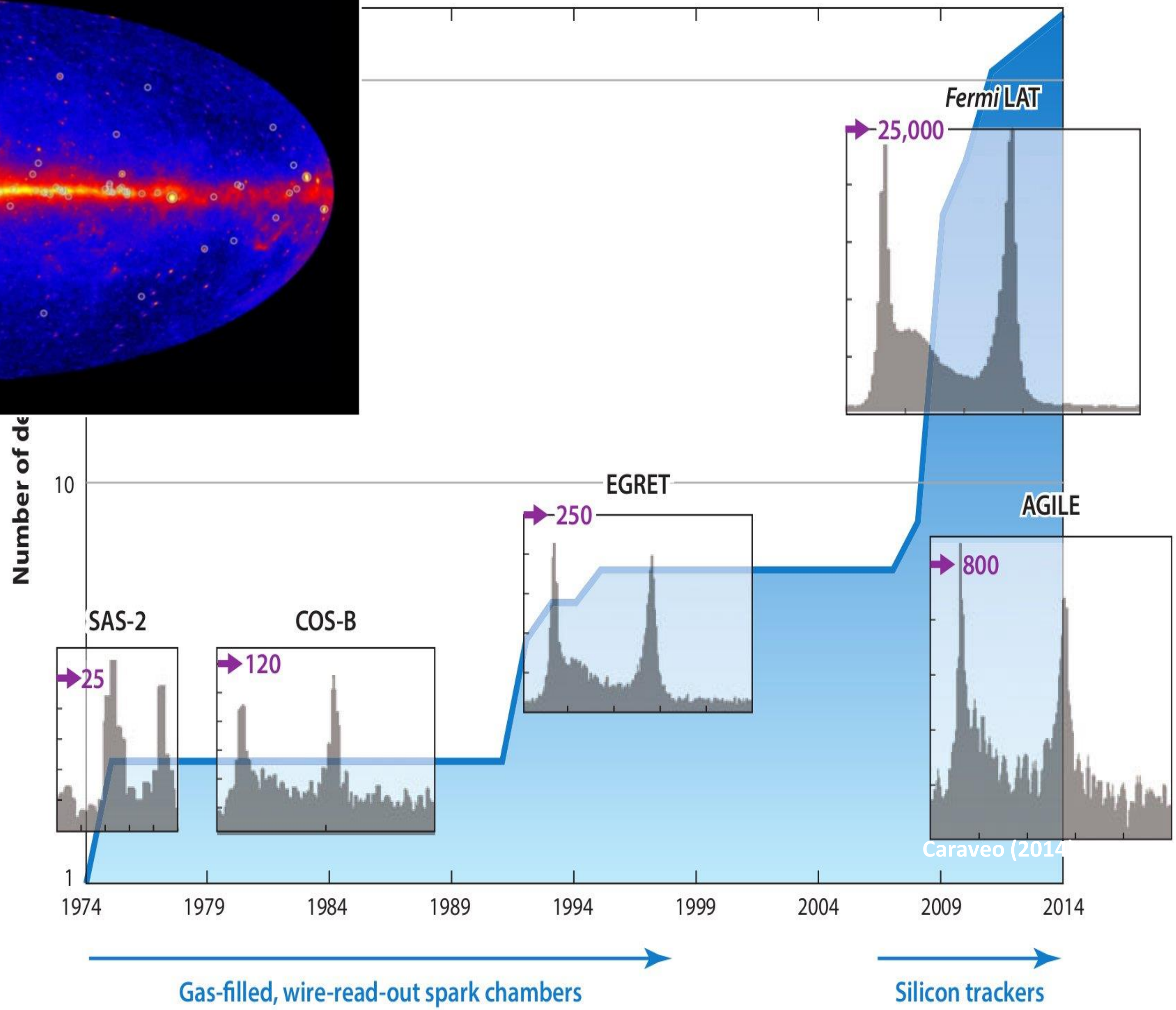

- Revolution in pulsars science
- >250 pulsars, 118 MSPs
- 3PC in production: Light curves, spectra, trends

Observations

Abdo et al. (2009)

- **Diversity of light curves (LC)**
- **3PC**

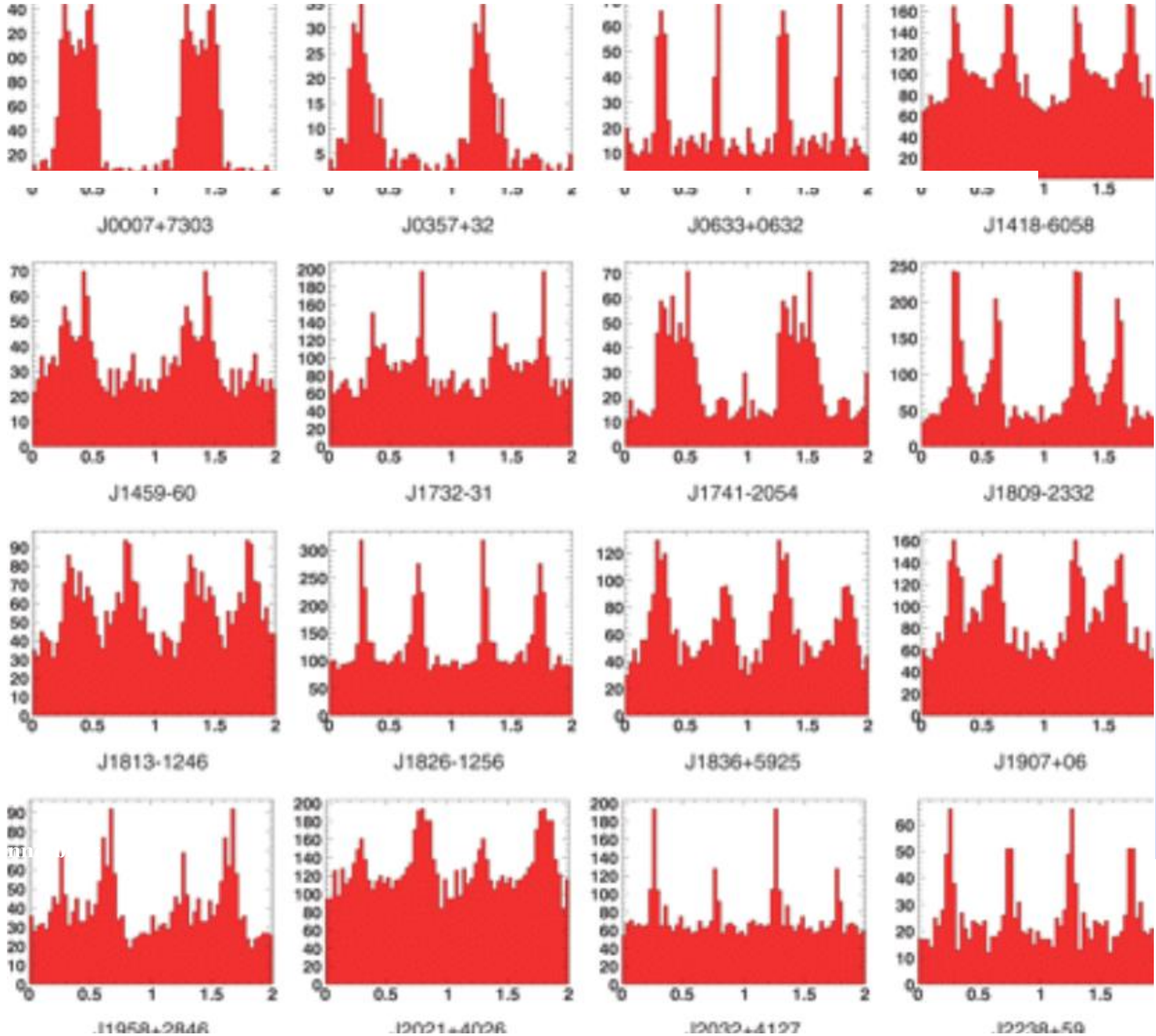

Observations

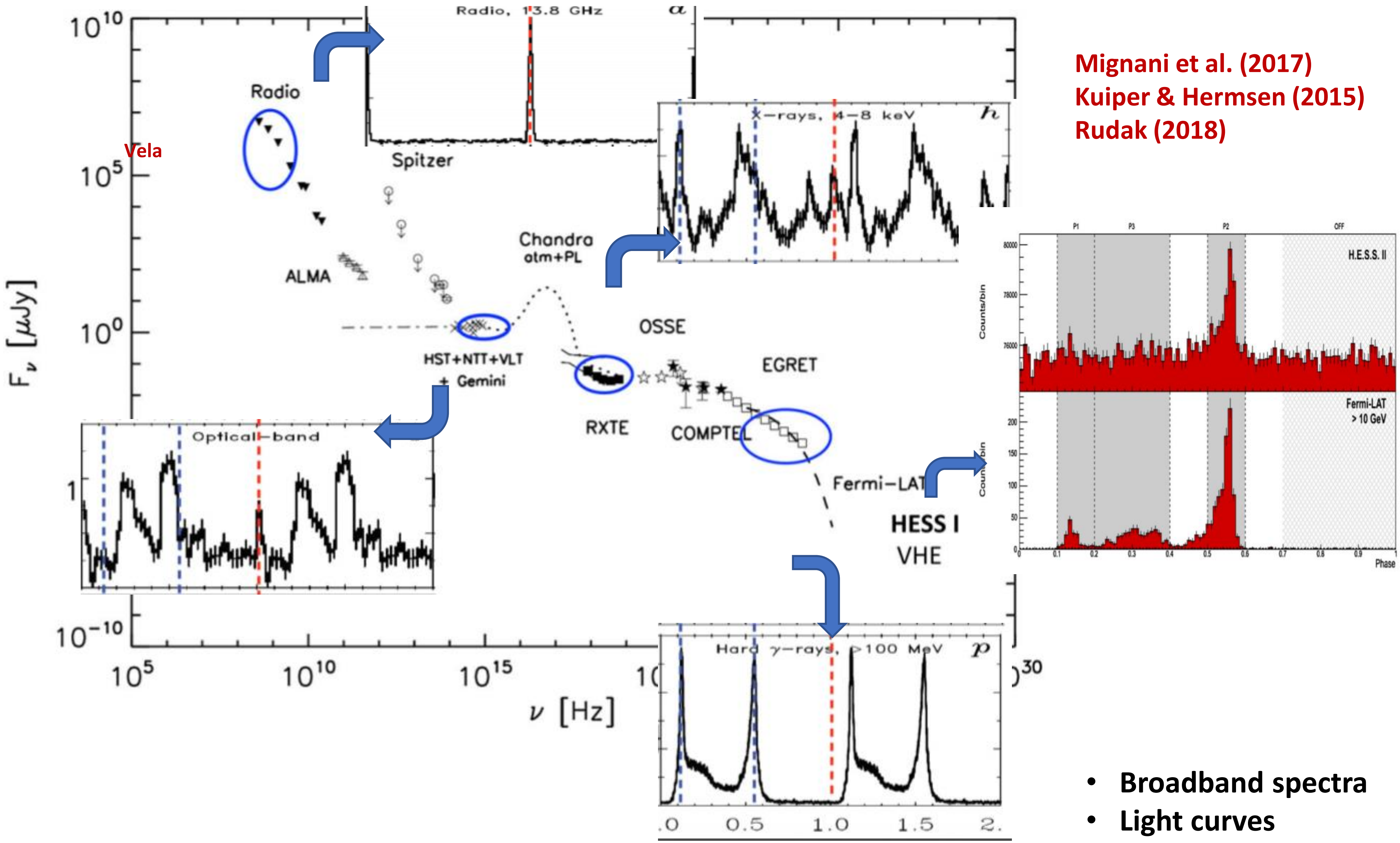

Mignani et al. (2017)
Kuiper & Hermsen (2015)
Rudak (2018)

- **Broadband spectra**
- **Light curves**

Observations

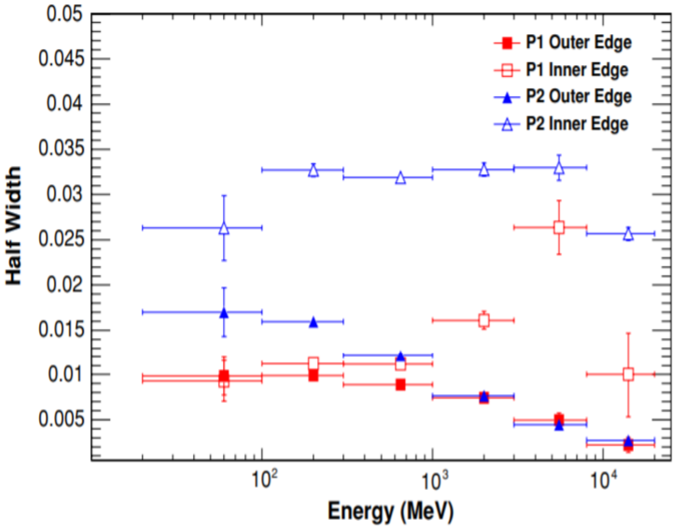

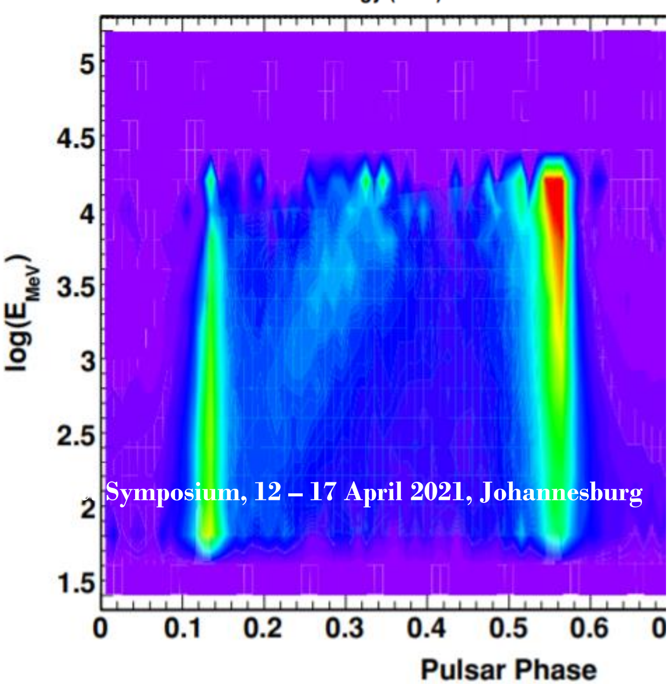

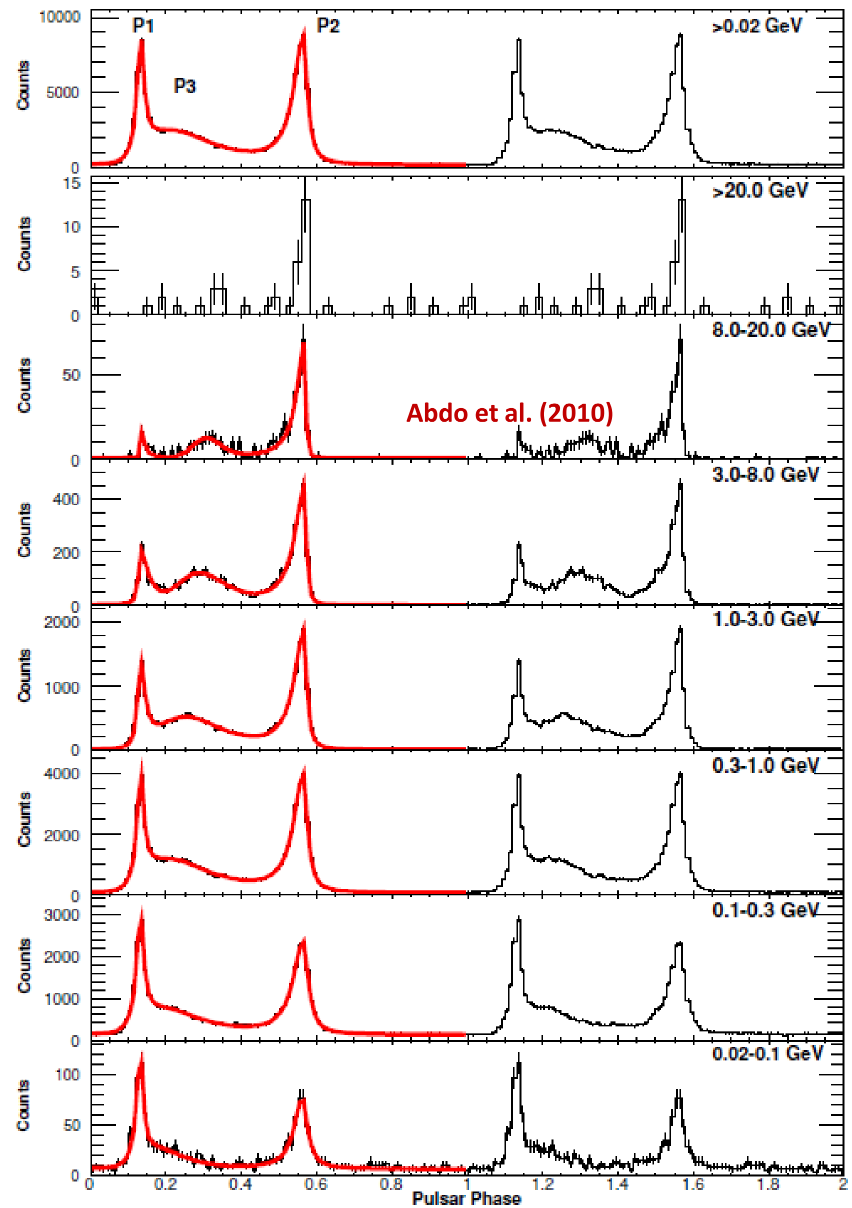

Models

Model Overview

- **Traditional models**
- **Striped-wind models**
- **Separatrix / current sheet models**
- **PIC models**

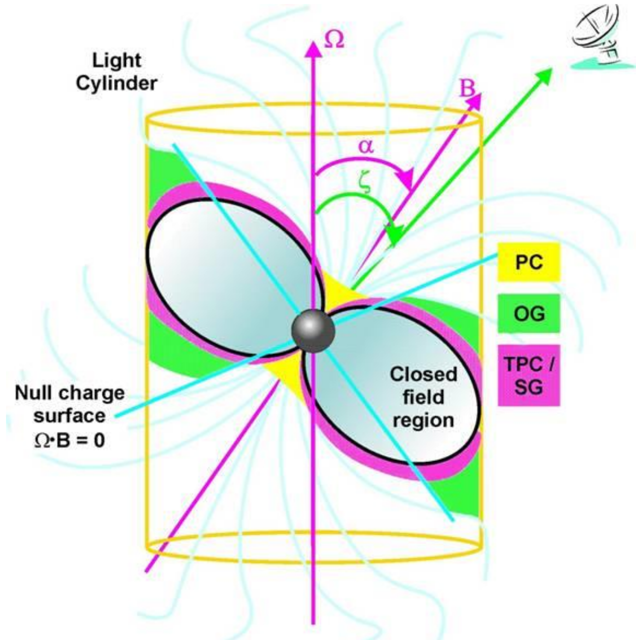

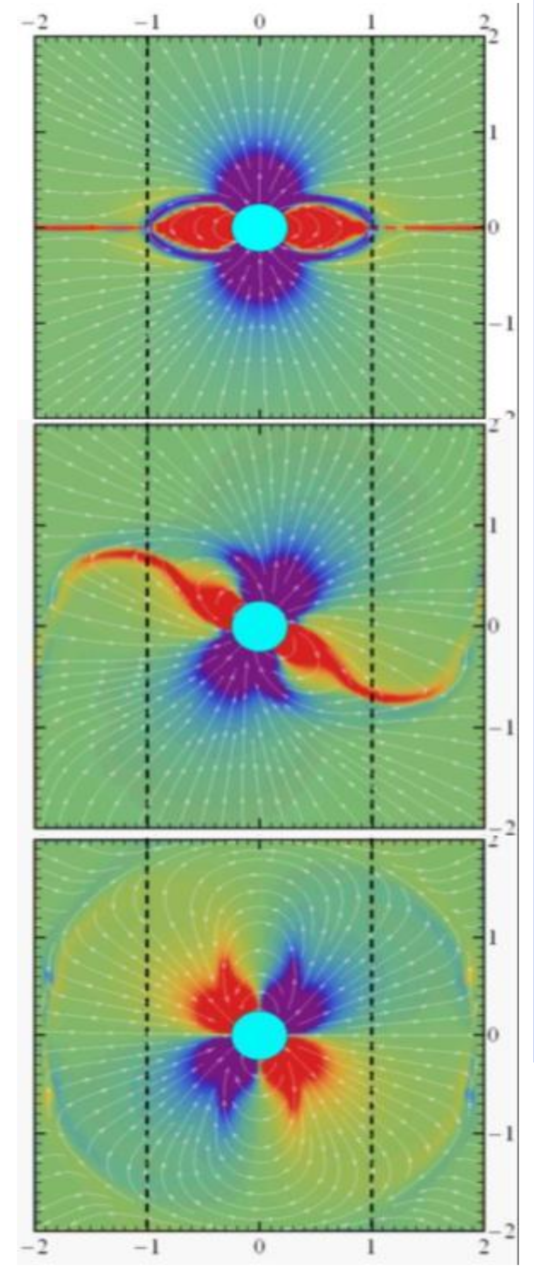

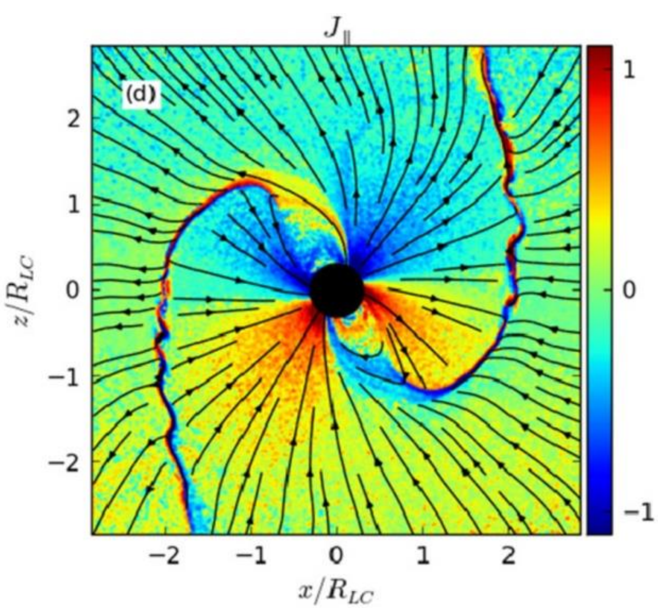

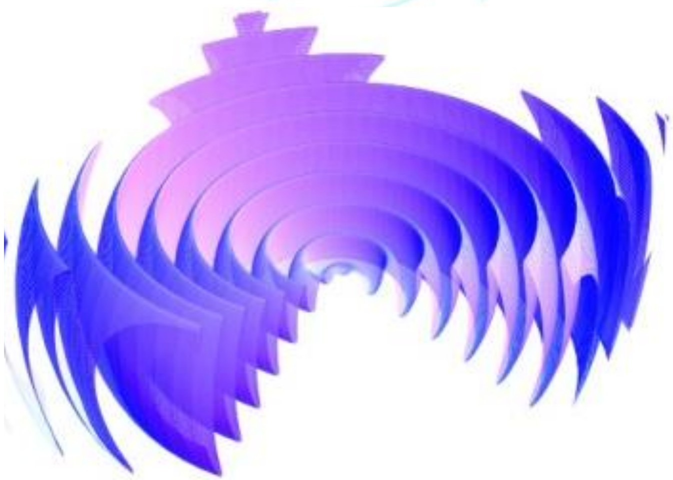

Light Curve Modelling of Pulsars

Caustics / Photon Bunching

- **Traditional models**

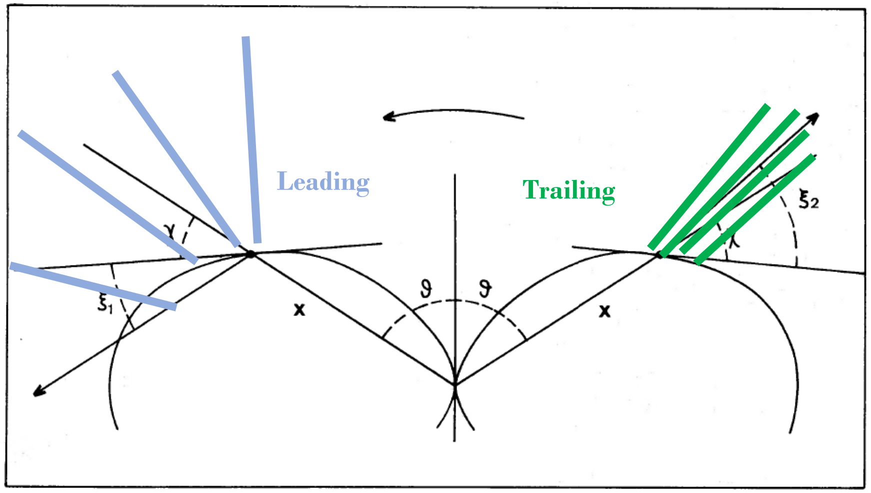

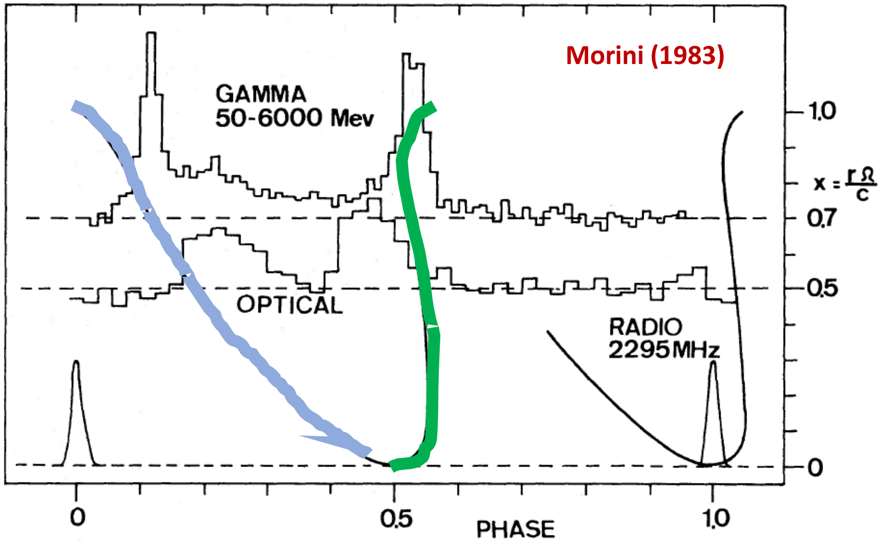

Morini (1983)
Romani & Yadigaroglu (1995)
Dyks et al. (2004)

Bunching of photons (from different field lines / heights) in phase due to:

1. **B-field structure**
2. **Aberration when transforming from co-rotating to lab frame**
3. **Time-of-flight delays**

Caustics / Photon Bunching

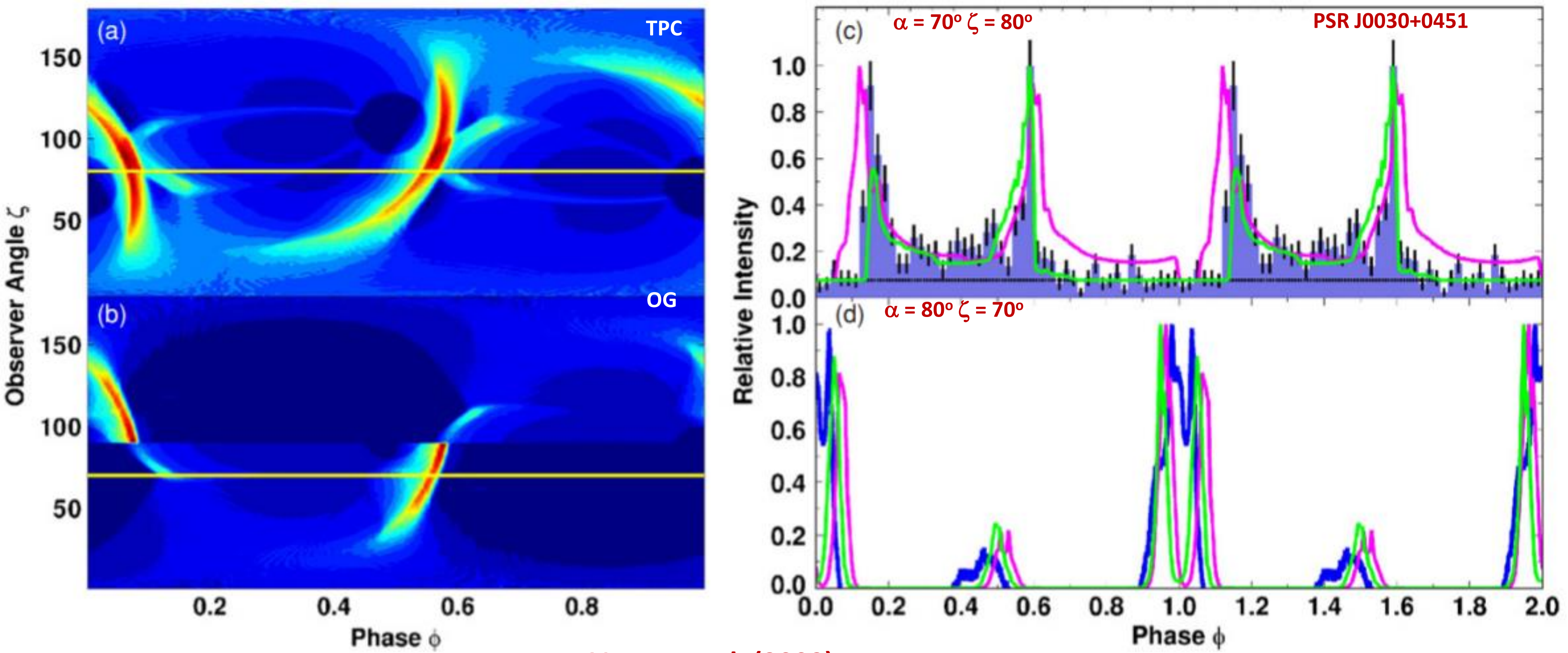

Venter et al. (2009)

Probing Pulsar Geometry

- E.g., a **single-peaked γ-ray LC**
- Cut γ-ray caustic almost tangentially
- Use radio light curve information: rotating vector model (RVM), phase shift

$$\tan(\psi - \psi_0) = \frac{\sin\alpha \sin(\phi - \phi_0)}{\sin\zeta \cos\alpha - \cos\zeta \sin\alpha \cos(\phi - \phi_0)},$$

$$h_{\rm P.A.} = \frac{P\,c}{8\pi}\Delta\phi = \frac{1}{4}R_{\rm LC}\Delta\phi$$

Weltevrede et al. (2010)
Cf. Rookyard et al. (2015)

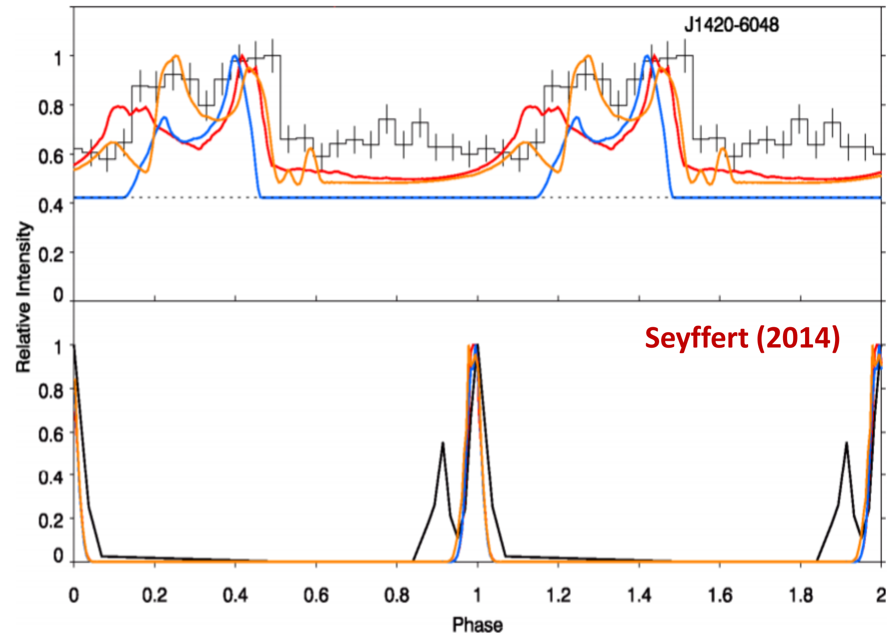

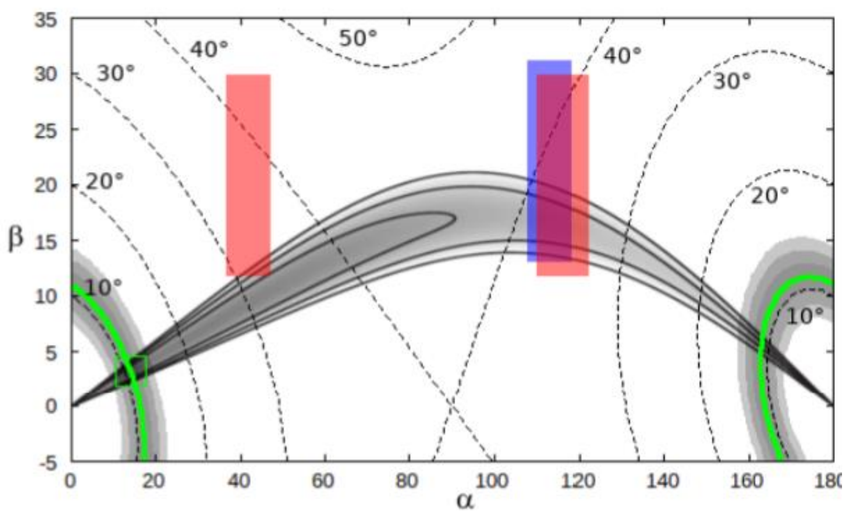

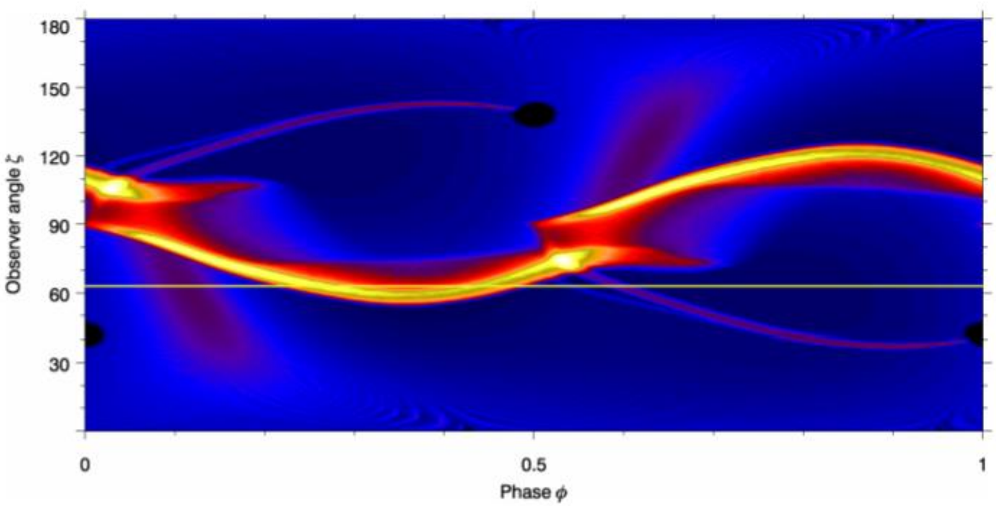

Probing Pulsar Geometry

- E.g., a **γ-ray-quiet pulsar**
- Double-torus fitting: $\zeta = 32.5^o \pm 4.3^o$
- Thermal pulsed X-rays: low $\beta = \zeta - \alpha$
- Single radio peak: $\beta > 10^o$
- Radio visibility: $\beta < 30^o$
- γ-ray invisibility: $\alpha < 55^o$, $\zeta < 55^o$
- Best-fit radio LC: $(\alpha, \zeta) = (22^o, 8^o)$

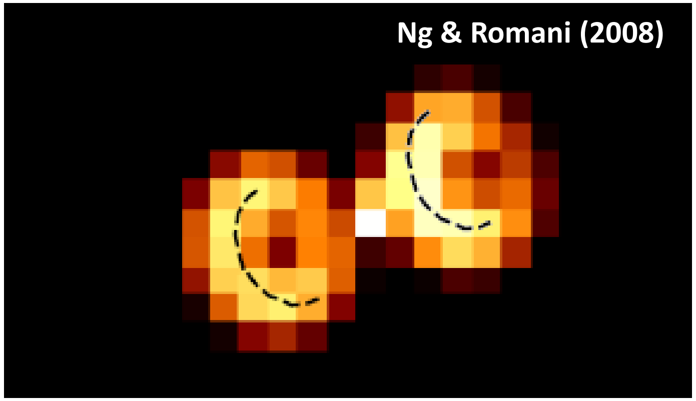

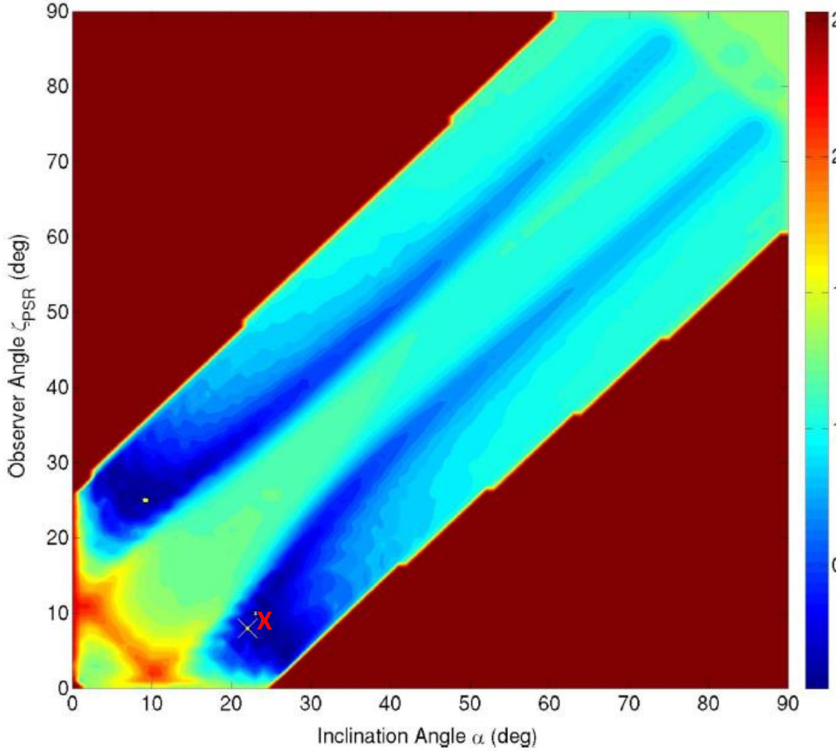

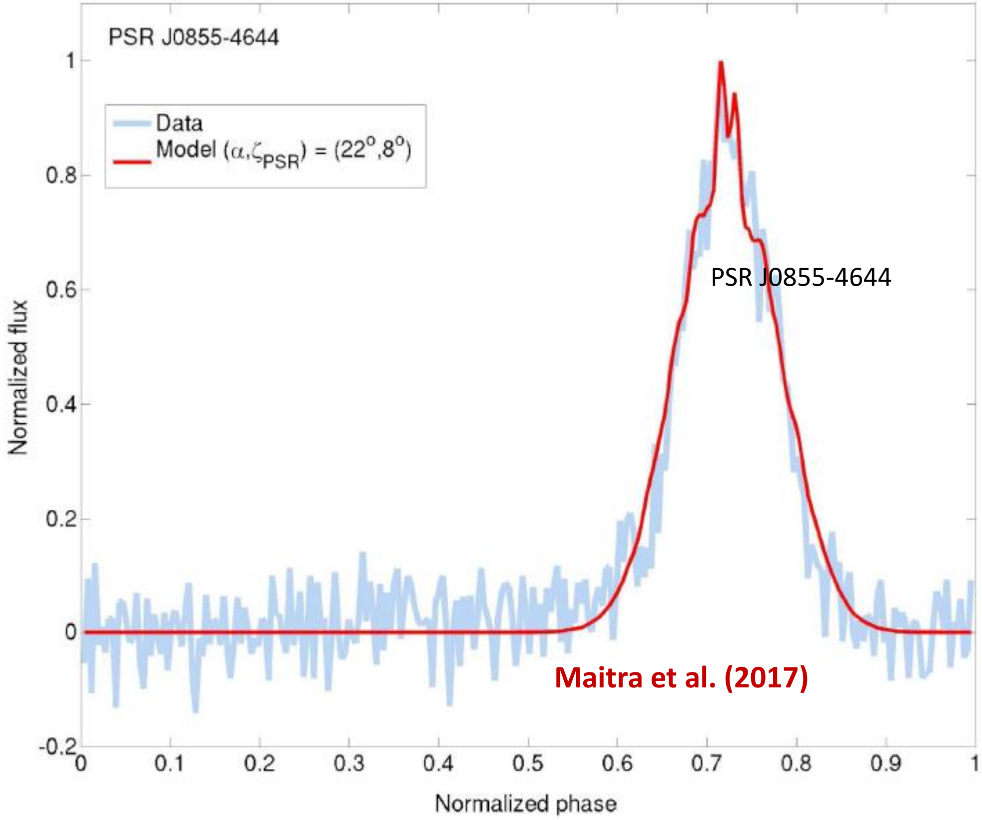

B / *E*-field Structure

- **Offset-dipole fields: geometric / emission models**

$$\boldsymbol{B}'_{\rm OPCs} \approx \frac{\mu'}{r'^3}\Big[\cos\theta'\hat{\mathbf{r}}' + \frac{1}{2}(1+a)\sin\theta'\hat{\boldsymbol{\theta}}' - \epsilon\sin\theta'\cos\theta'\sin(\phi'-\phi'_0)\hat{\boldsymbol{\phi}}'\Big],$$

Barnard et al. (2016)

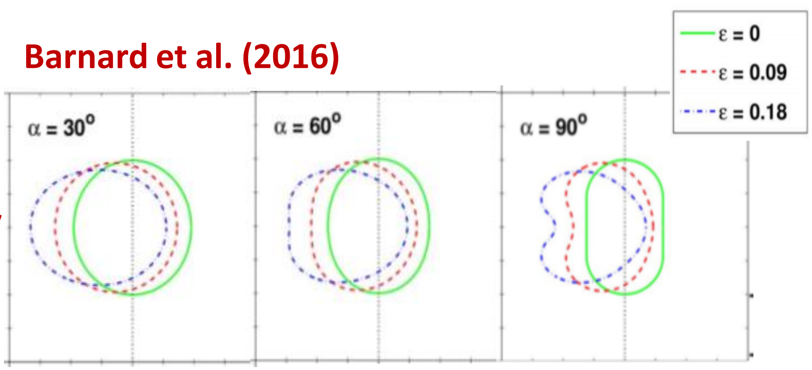

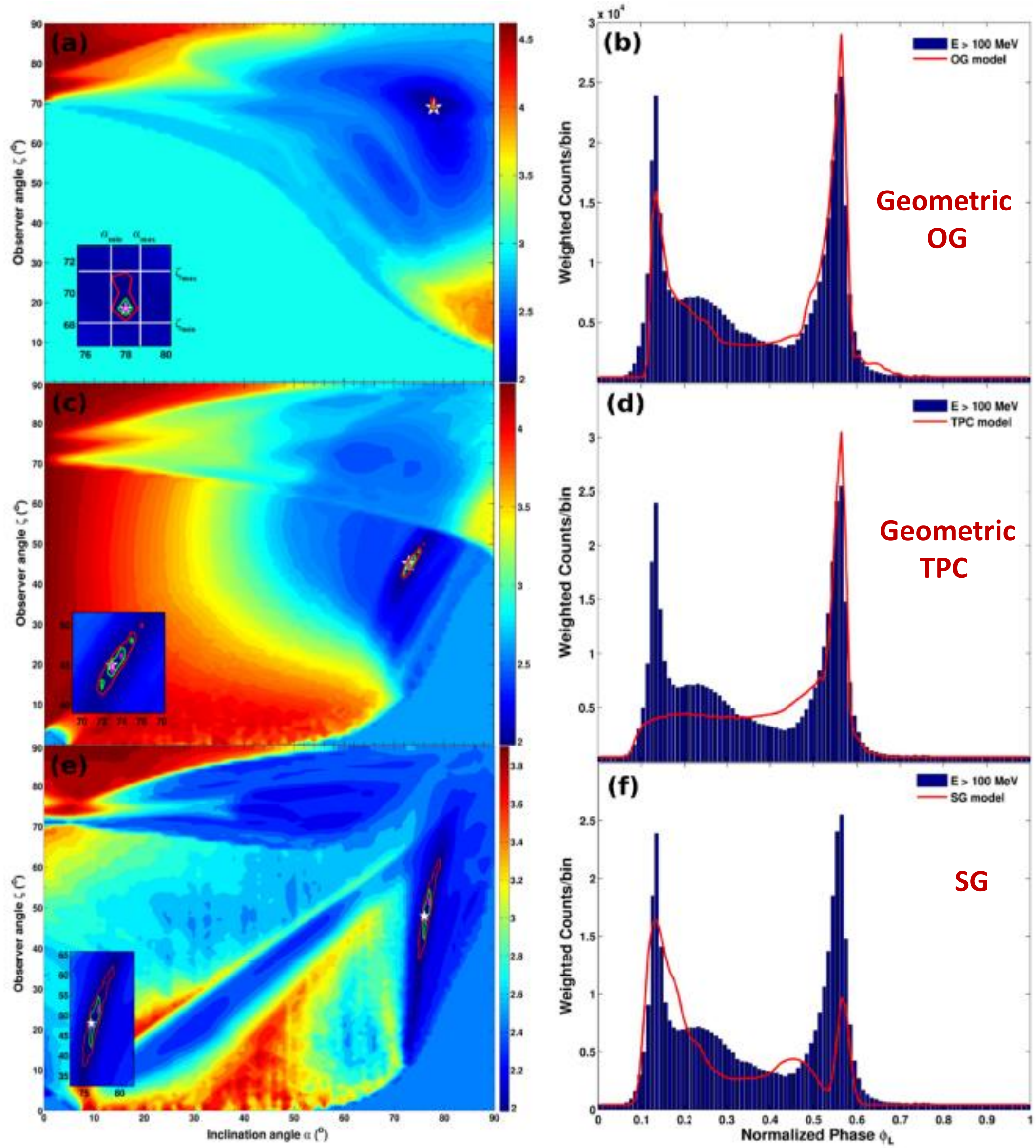

Energy-dependent Light Curve Modelling of Pulsars

Refinement of the Curvature Radius

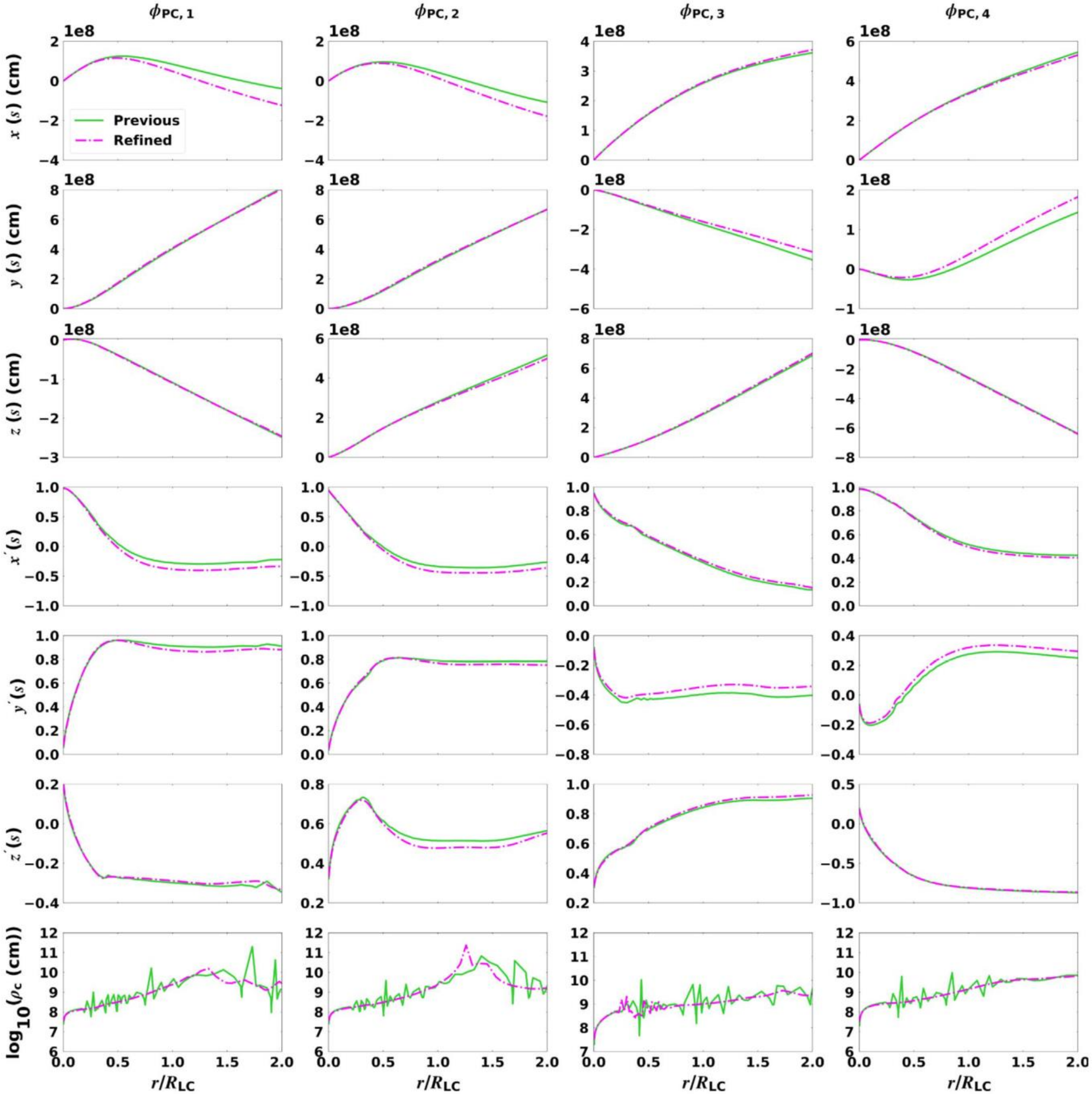

- 4 sample trajectories
- Refine x,y,z components
- Refine derivatives of trajectories
- Refine r_c

Previous

Refined

$$E_{\gamma,\mathrm{CR}} = \frac{3\lambda\!\!\!^{-}_c \gamma^3}{2\rho_c} m_e c^2$$

Credit: M. Barnard

Refinement of the Curvature Radius

Barnard et al. (2022)

- One and two-step function for the accelerating *E*-field (motivated by kinetic simulations).
- Refined calculation of the curvature radius of particle trajectories - impacts the transport, light curves, and spectra.
- Did a small parameter study to find optimal parameters, i.e., α, ζ_{cut}, R_{acc}, and selected the best spatial resolution.

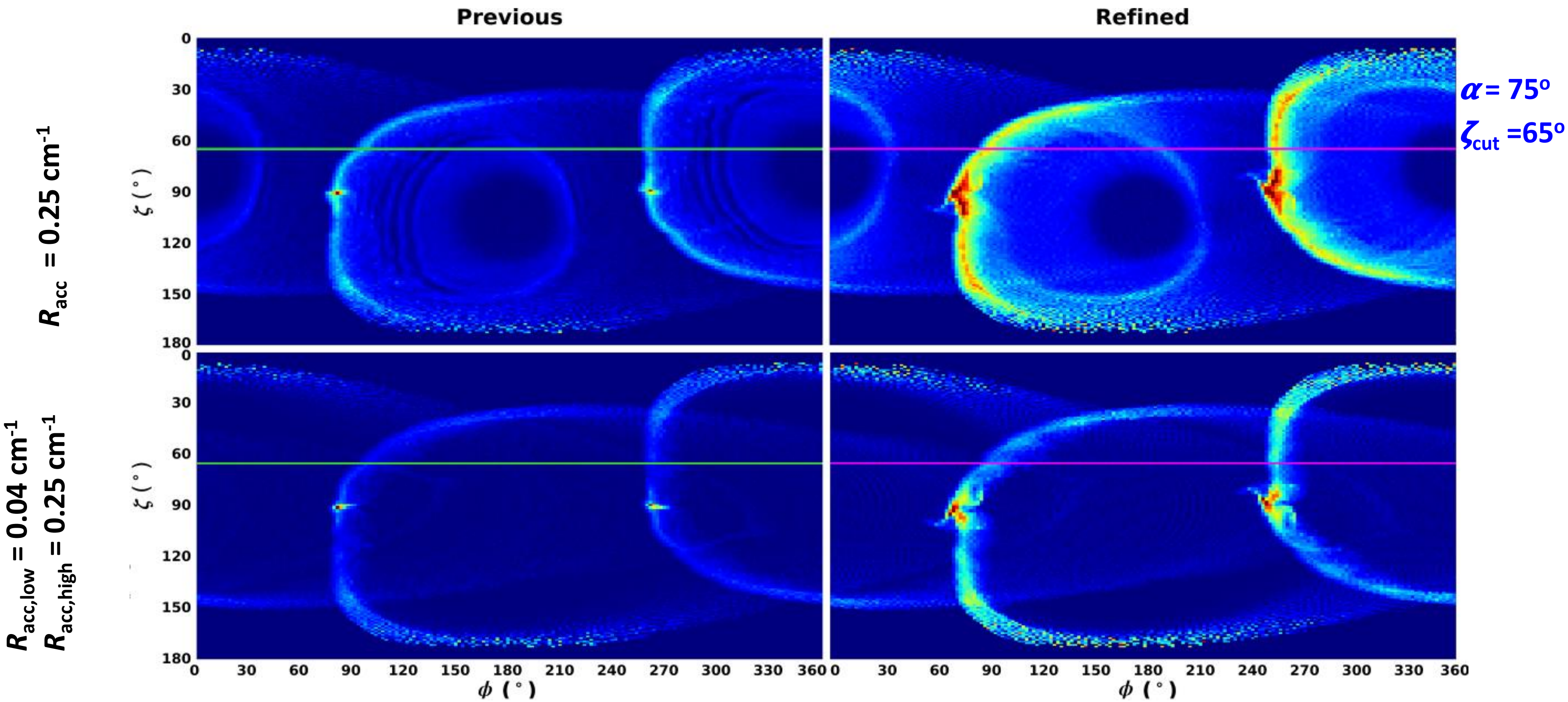

Energy-dependent CR Light Curves

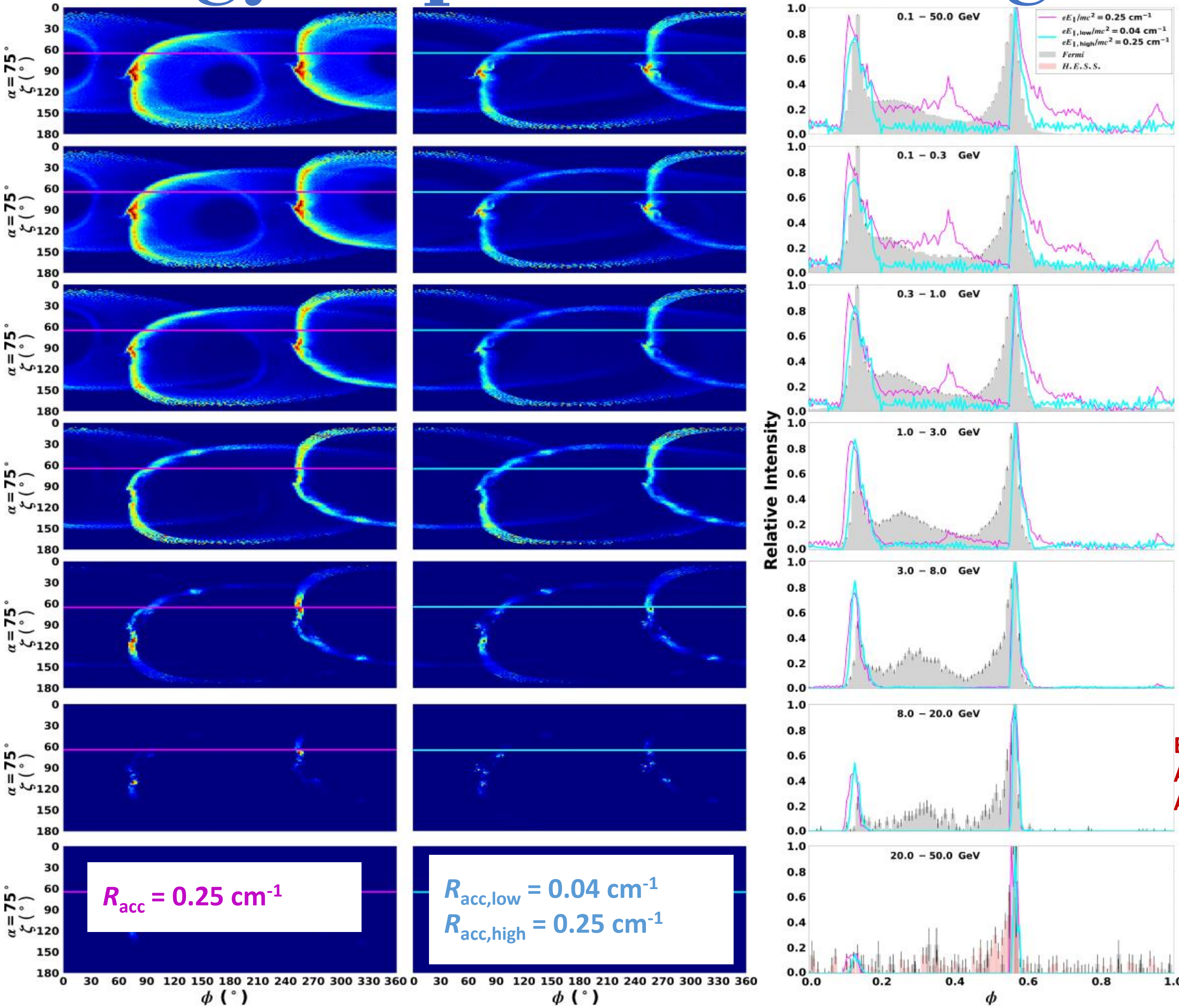

α = 75°

ζ_{cut} = 65°

Trends:

- P1/P2
- Widths
- Phase

Barnard et al. (2022)
Abdo et al. (2010,2013)
Abdalla et al. (2018)

Phase-avg. / Phase-resolved Spectra

Barnard et al. (2022)

$\alpha = 75^o$

$\zeta_{cut} = 65^o$

R_{acc} = 0.25 cm^{-1}
Norm = $5J_{GJ}$

$R_{acc,low}$ = 0.04 cm^{-1}; $R_{acc,high}$ = 0.25 cm^{-1}
Norm = $8.5J_{GJ}$

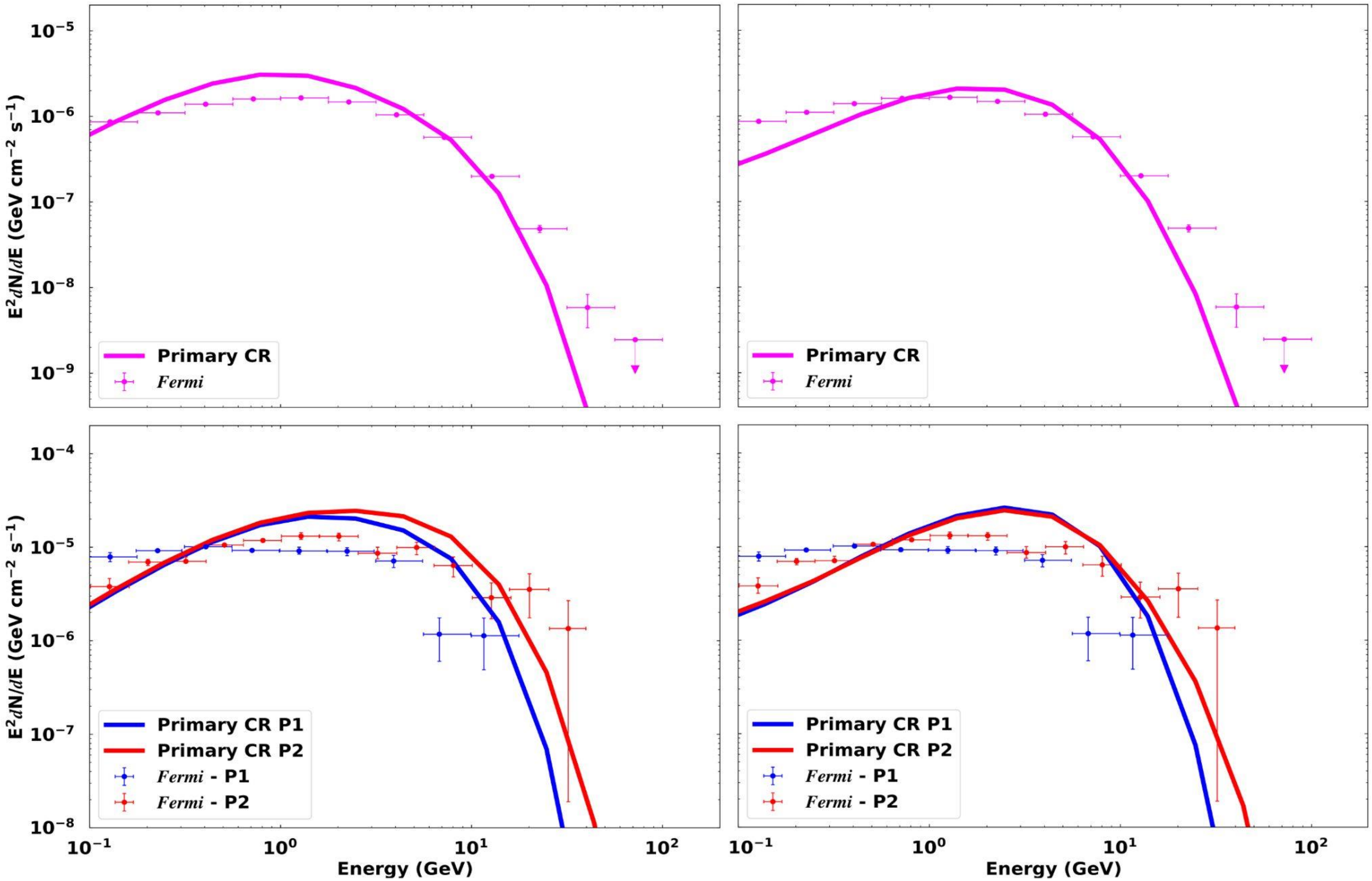

Abdo et al. (2010,2013)

Local Environment: P1/P2

$$E_{\gamma,\mathrm{CR}} = \frac{3\lambda\!\!\!^{-}_{c}\gamma^{3}}{2\rho_{c}} m_{e}c^{2}$$

$\alpha = 75^{\circ}$

$\zeta_{cut} = 65^{\circ}$

$R_{acc} = 0.25\ \mathrm{cm}^{-1}$

Barnard et al. (2022)

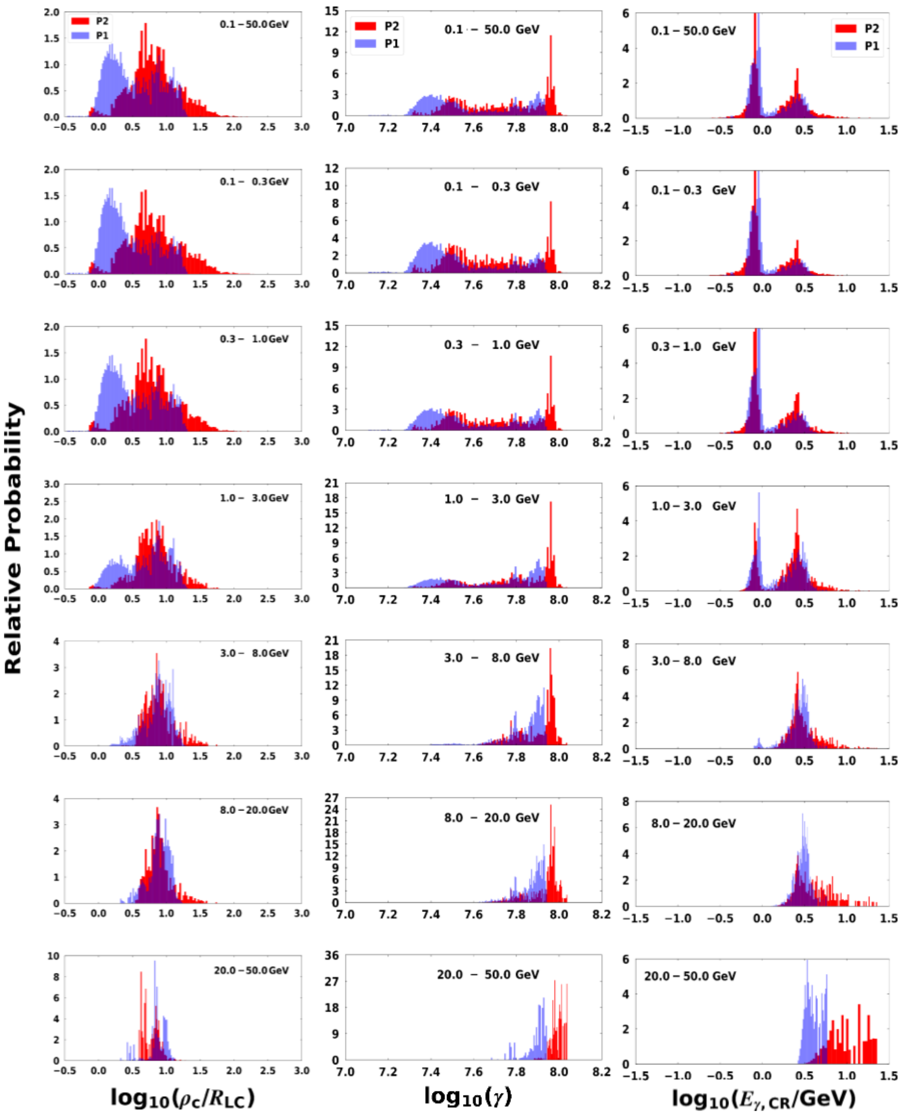

P1
P2

Tails of histograms on the left (same E's)

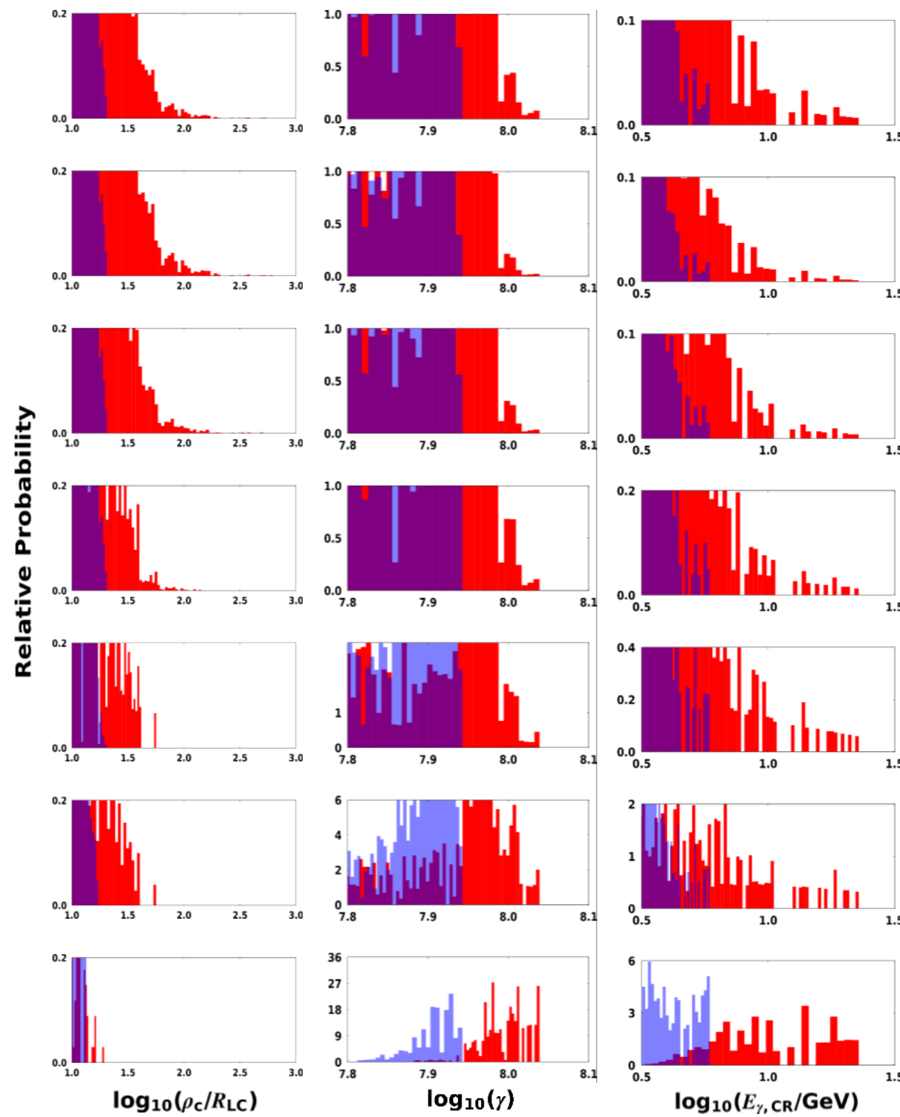

Spectral Modelling of the Broadband Emission from Pulsars

Energy-dependent LCs: Vela Pulsar

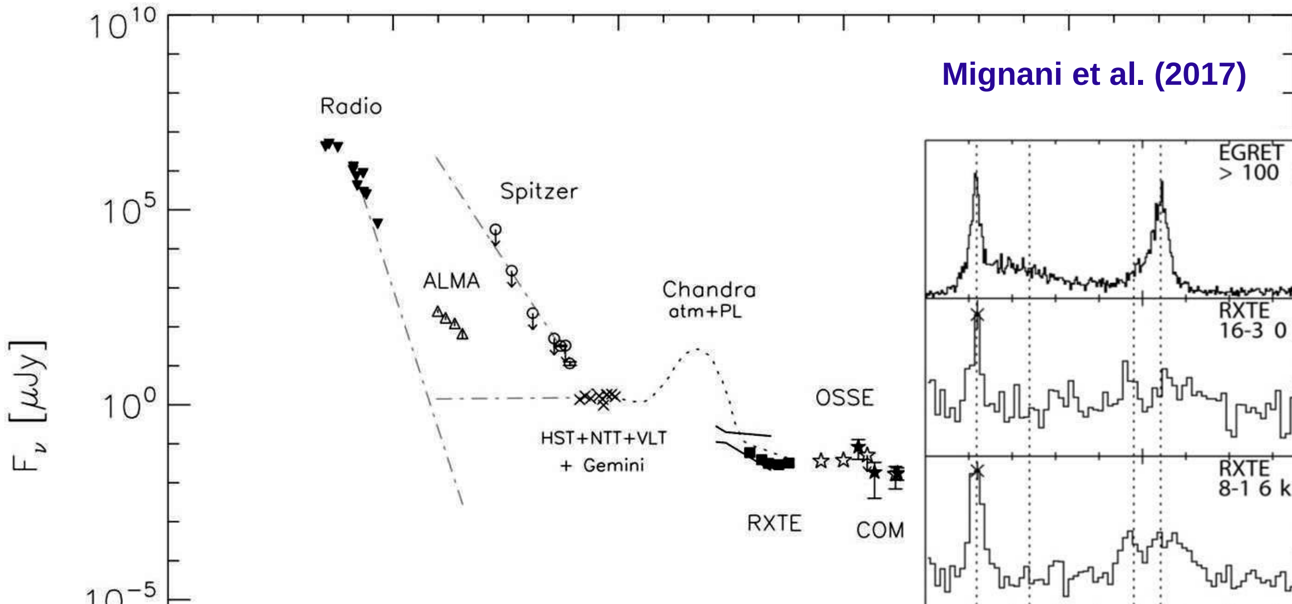

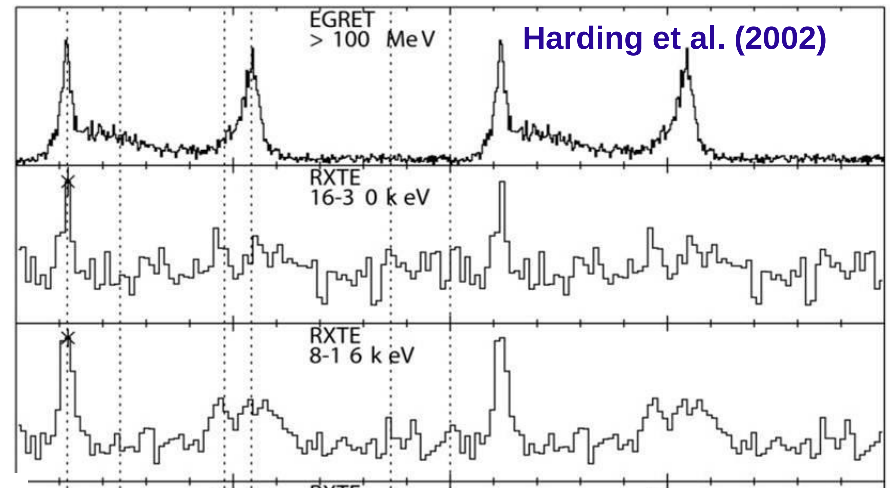

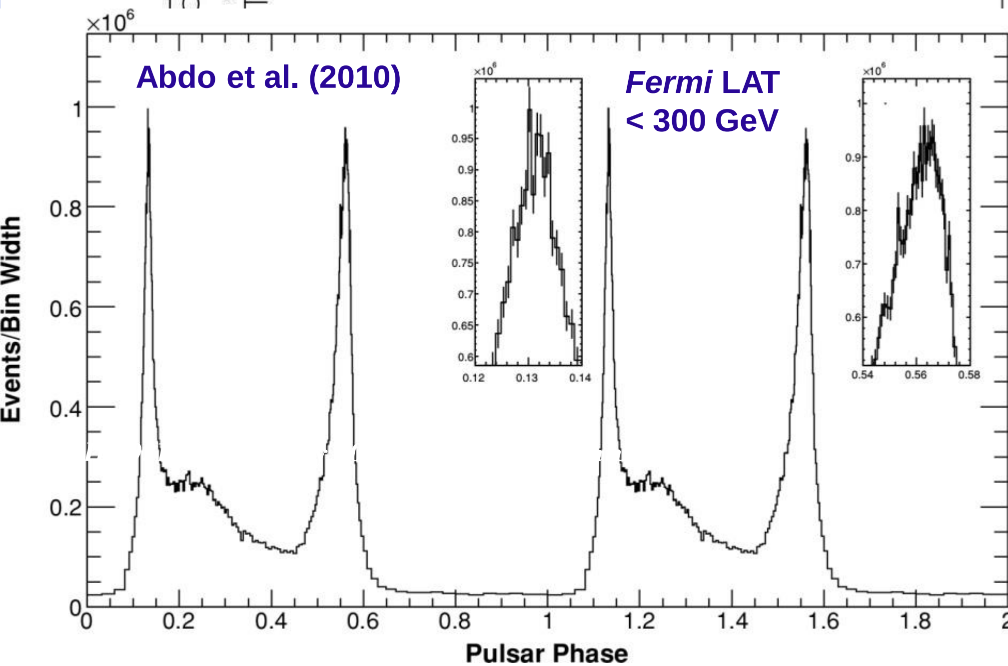

Pulsed TeV Emission from Vela PSR

- **3 – 7 TeV.**
- **Only P2 detected at 5.6σ level, P1 not visible.**

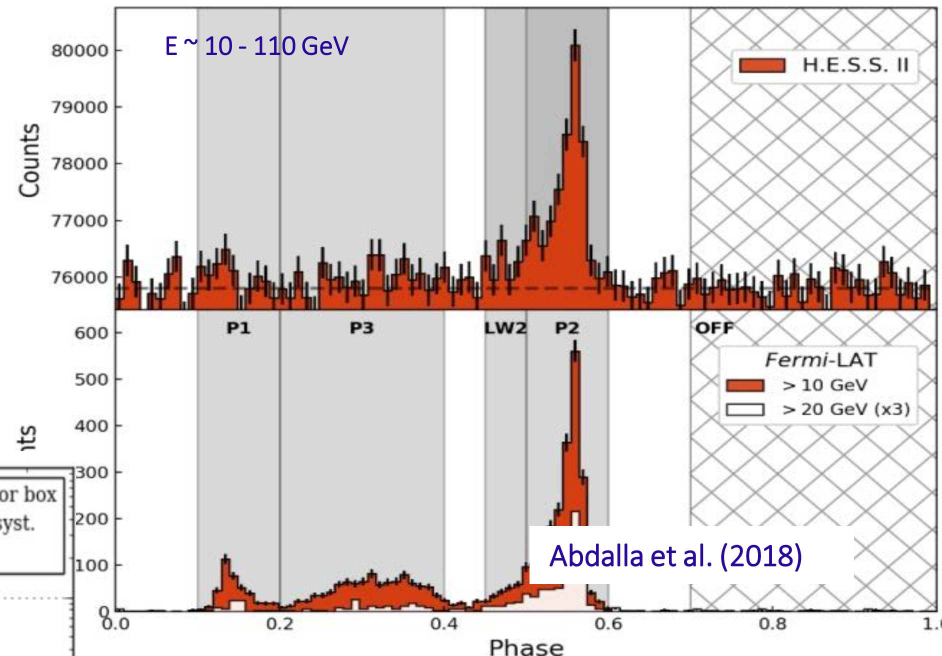

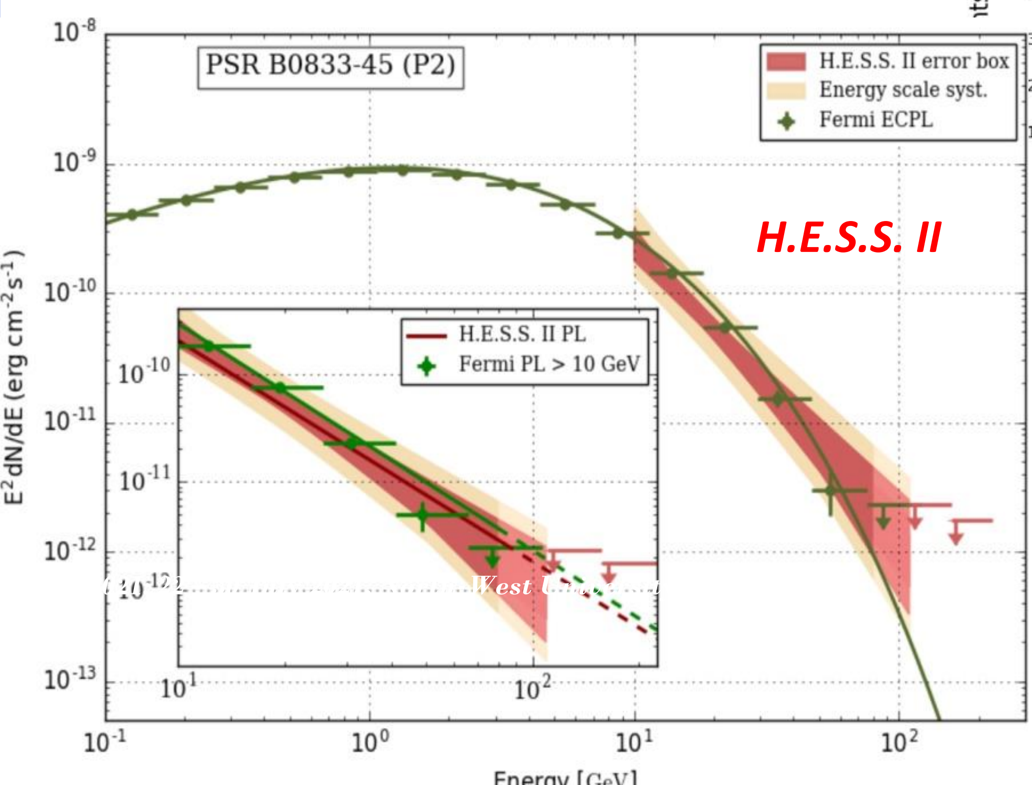

<u>MOTIVATION:</u>

Curved spectrum favoured by H.E.S.S. (>3σ).

CR tail or a different component?

Separatrix / Current Sheet Emission Model

- **Force-free magnetosphere**
- **Pairs and primaries from steady cascade in offset-PC field** (Harding & Muslimov 2011a,b).
- **Primaries accelerated only in extended SG and CS (out to $r = 2R_{LC}$) assuming a constant E-field.**
- **No pair acceleration. Chosen pair multiplicity.**
- **Empirical radio core / cone model.**
- **Resonant cyclotron absorption of radio photons** (cf. Lyubarski & Petrova 1998).
- **Solve particle dynamics.**
- **CR, SR, ICS, SSC radiation mechanisms.**
- **Inertial observer frame.**

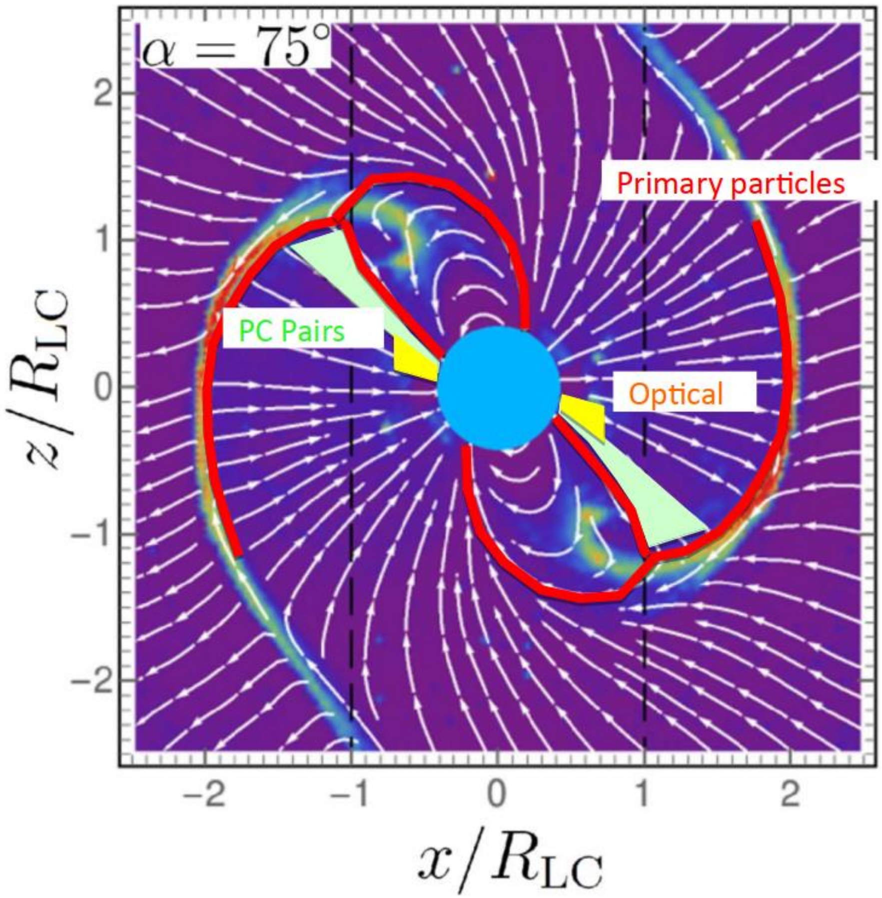

Harding & Kalapotharakos (2015), Harding et al. (2018)

Separatrix / Current Sheet Emission Model

- **Force-free 0.2 – 2 R_{LC}**
- **Vacuum Retarded Dipole below 0.2 R_{LC}**
- **Polar cap pairs produce SR in UV / optical at lower altitudes ➡ eV**
- **Synchro-curvature from primaries ➡ GeV**
- **Primaries scatter pair SR ➡ TeV**
- **Pair SSC ➡ MeV**

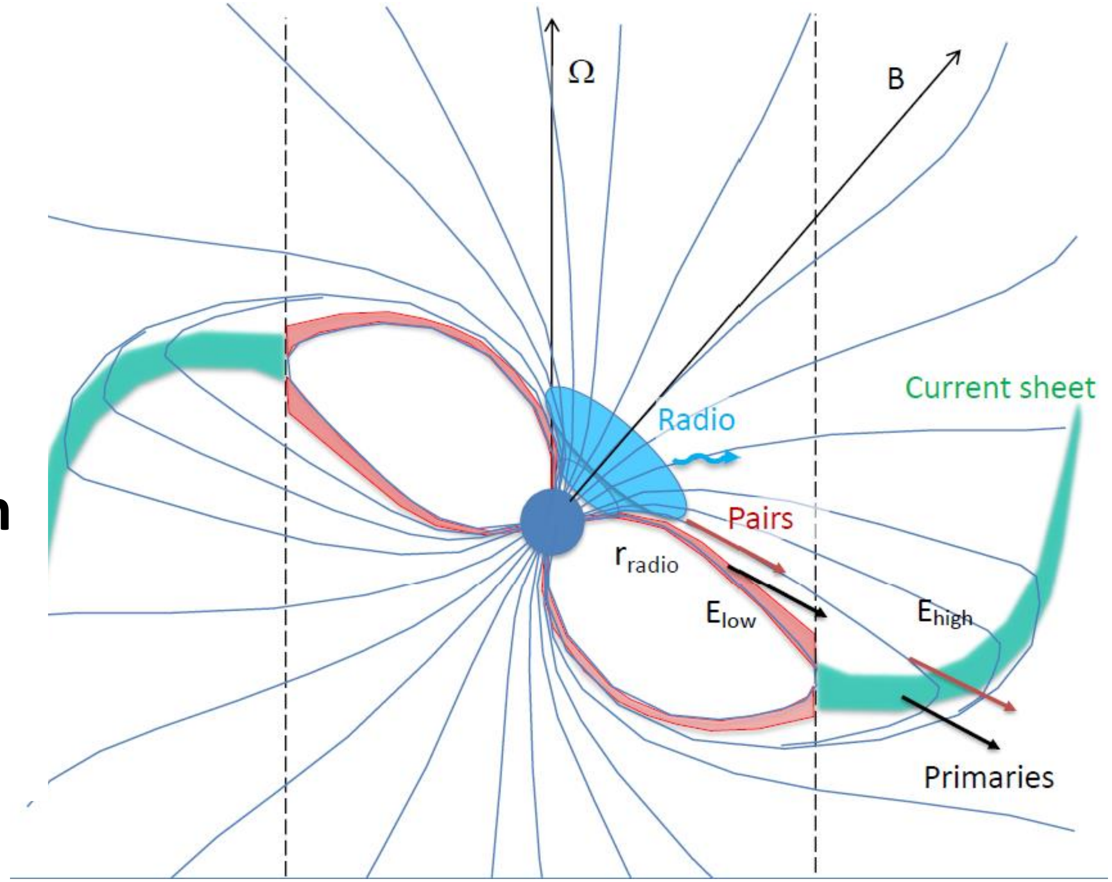

Credit: A Harding

Polar Cap Pair Cascades

- **First-principle calculation**
- **Primaries radiate gamma rays**
- **These are converted to electron-positron pairs in the strong *B*-field**
- **Sensitive to photon energy and *B*-field geometry**
- **Injected into magnetosphere: SR**

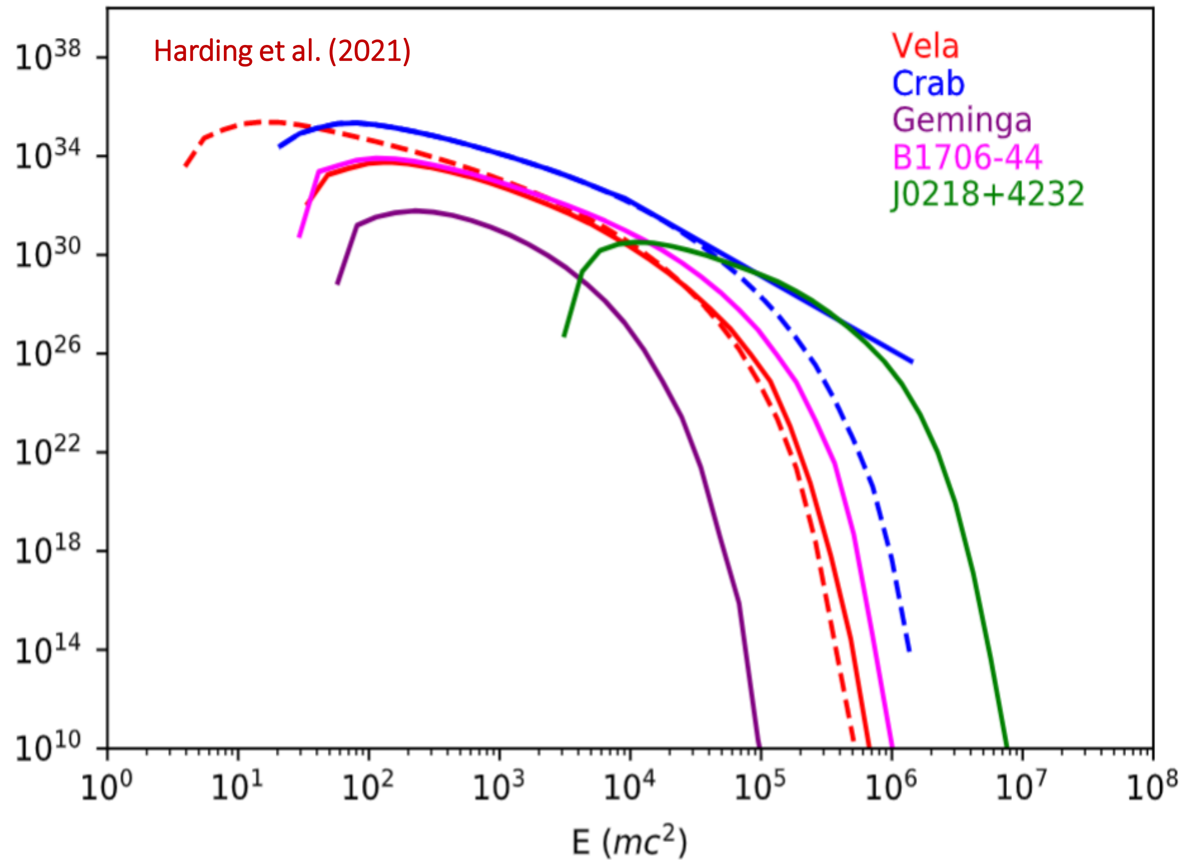

Results: Crab Spectrum

- **Pair emission near current sheet**
- **>10 TeV component detectable by HAWC?**
- **Violation of MAGIC data?**
- **γ–γ absorption?**
- **MeV gap?**

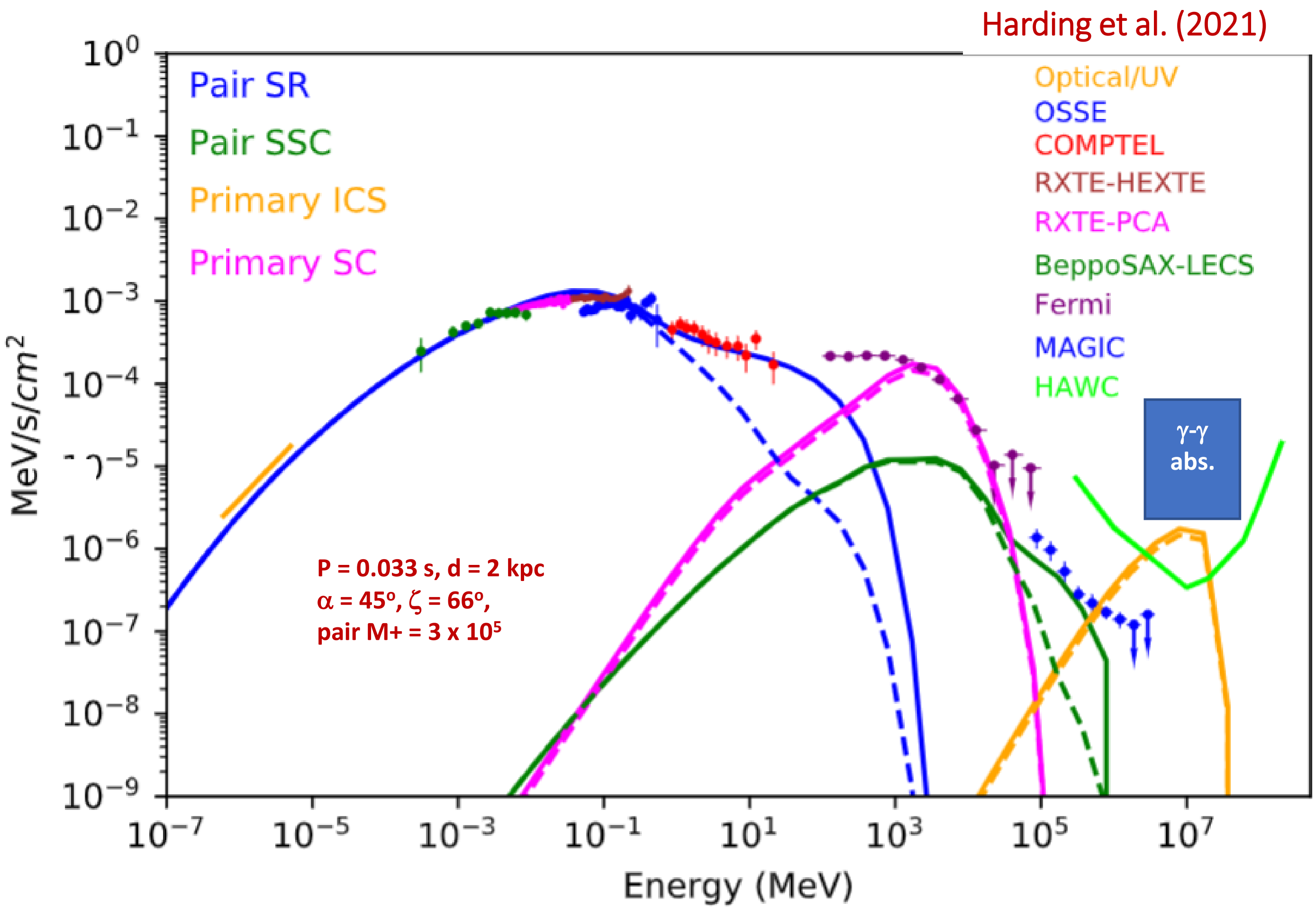

Results: Vela Spectrum

- **Detectable primary IC component around 10 TeV!**
- **Pair SR matches optical data**
- **TeV emission requires high γ_{max}, pointing to CR in GeV band**

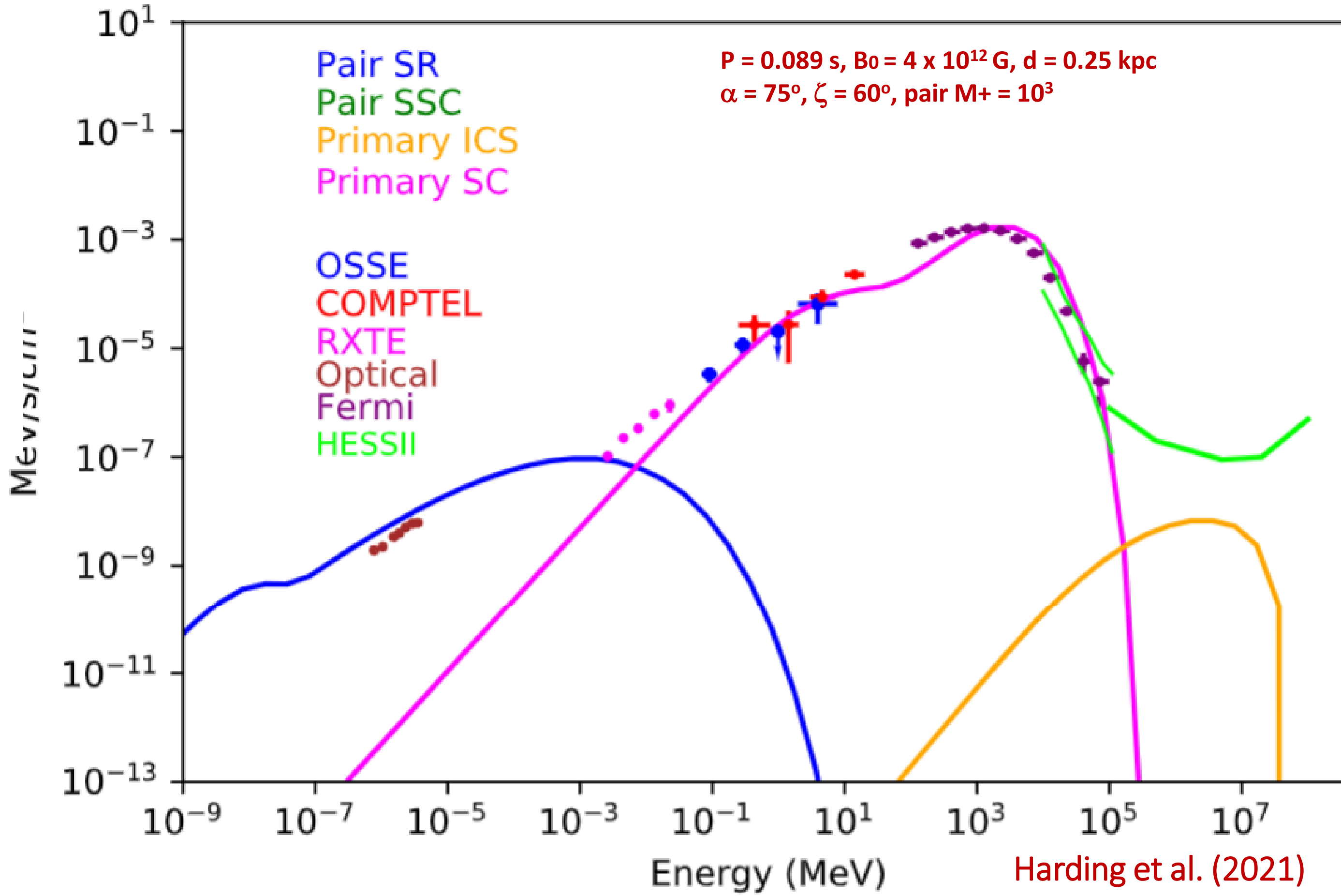

Harding et al. (2021)

Results: Vela LCs

- **Reasonable multi-wavelength LCs**
- **P1/P2 vs. E effect: higher-energy photons in P2 – larger ρ_c**
- **Only P2 in TeV: highest-energy particles responsible**
- **Azimuthally-dependent emissivity in current sheet may solve radio-to-γ lag**

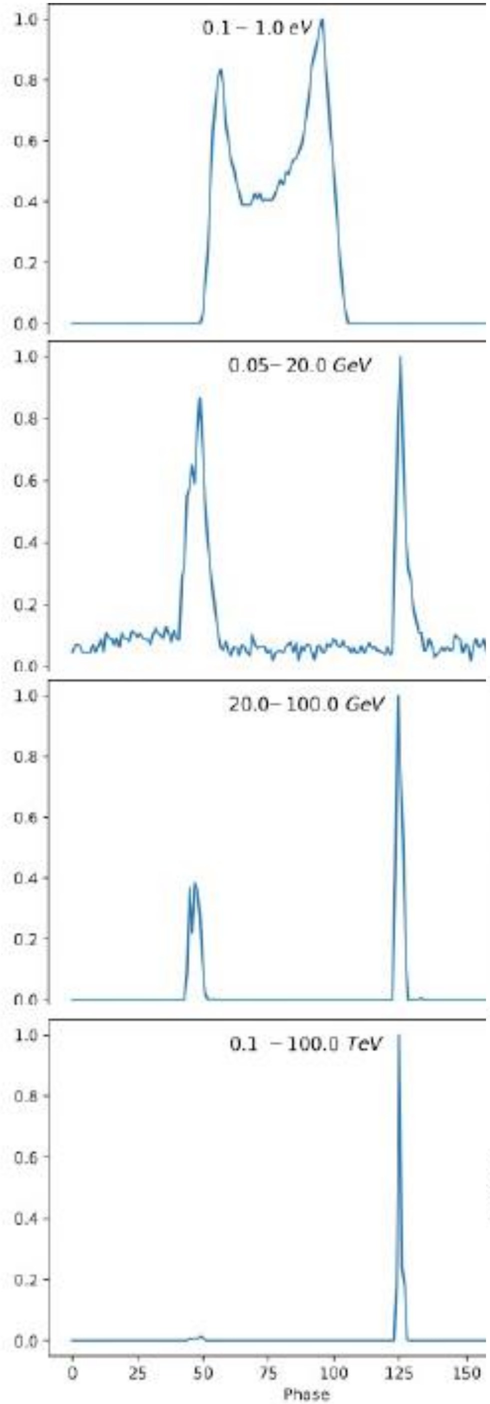

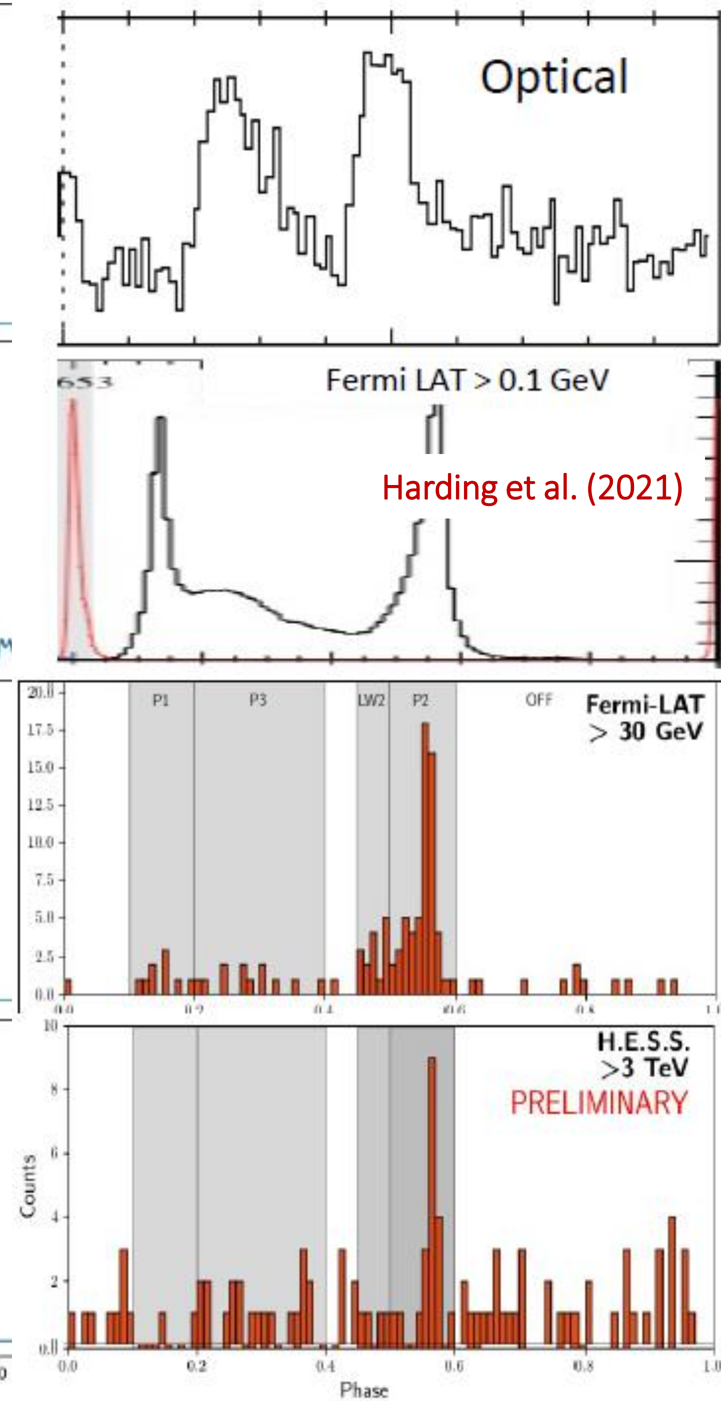

Multipolar *B*-Fields

Multipolar *B*-fields

- **Miller et al. (2019) and Riley et al. (2019) reported strong evidence of multipolar *B*-fields via X-ray LC modelling**
- **Dual-band LC fitting (X-ray & g-ray) proved constraining for 11-parameter model that assumes offset-dipole and offset-quadrupole B-field components (Kalapotharakos et al. 2020)**

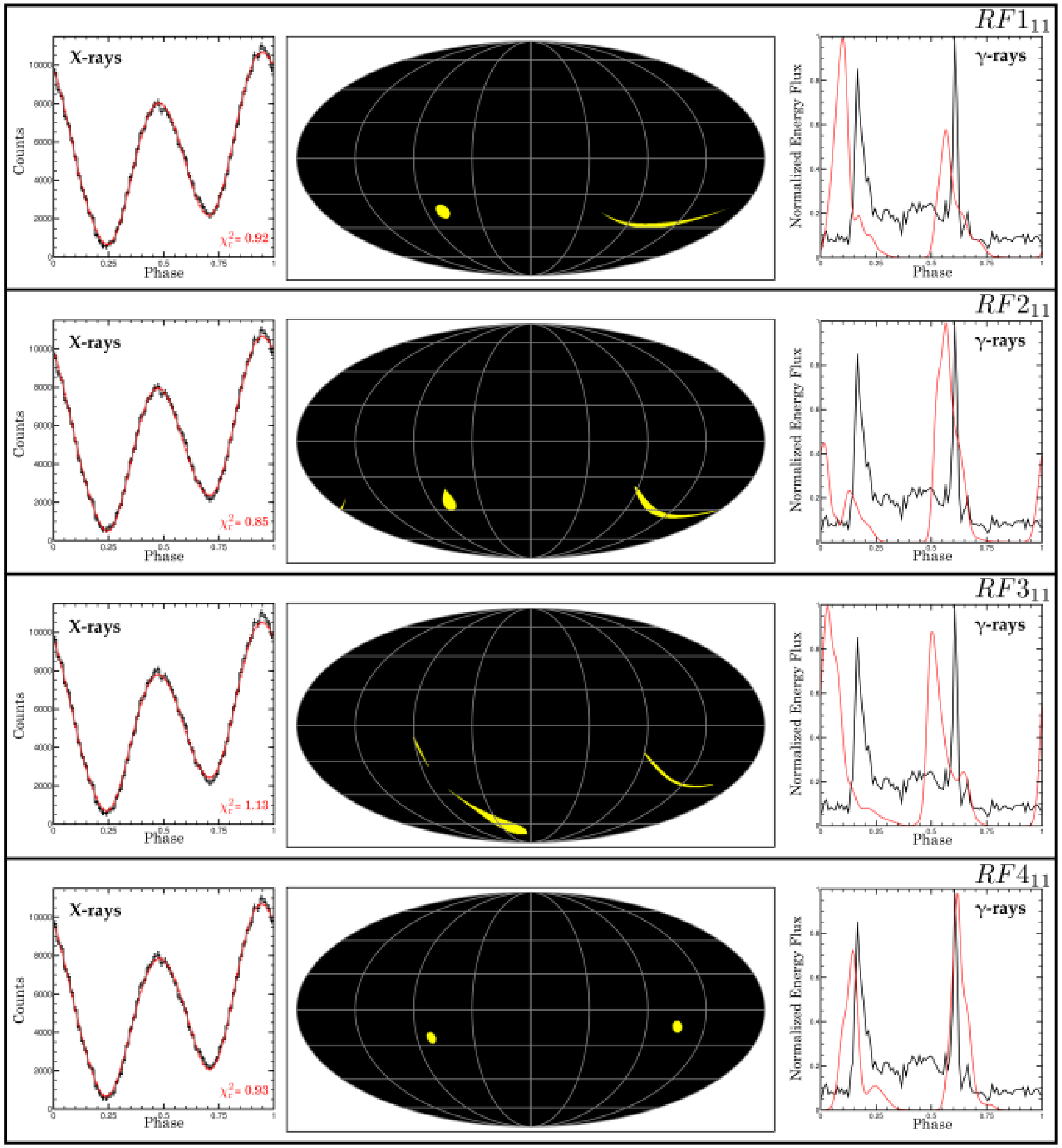

Spider Binaries

Spider Binaries

- Black widow (BW) & Redback (RB) spiders: devour male partners.
- Similar behaviour among MSP binary systems.
- Tight binaries $P_{orb} < 24$ h.
- Intense pulsar wind heats tidally-locked companion and excites companion wind / ablates it.
- Flares on companion star: variable heating. Hot 'day side'.
- Interaction of pulsar and companion winds forms an intra-binary shock – site for particle acceleration.
- BWs: smaller, lower-mass semi-degenerate companions ($<0.05M_{sun}$) than RBs ($\sim 0.1 - 0.5M_{sun}$) cf. Roberts (2013).

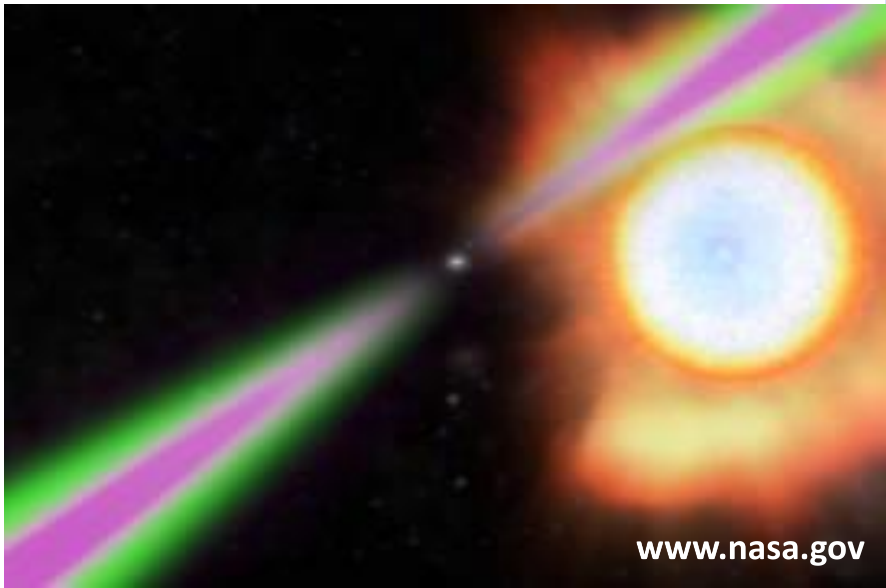

Optical Photometry

- Optical photometry on *Fermi* UnID source revealed orbital modulation (Romani & Shaw 2011)
- Optical spectroscopy / radial velocity curve: T_{comp} ~ 2 800 K – 6 900 K
- Approximate binary parameters
- Need to constrain surface heating pattern

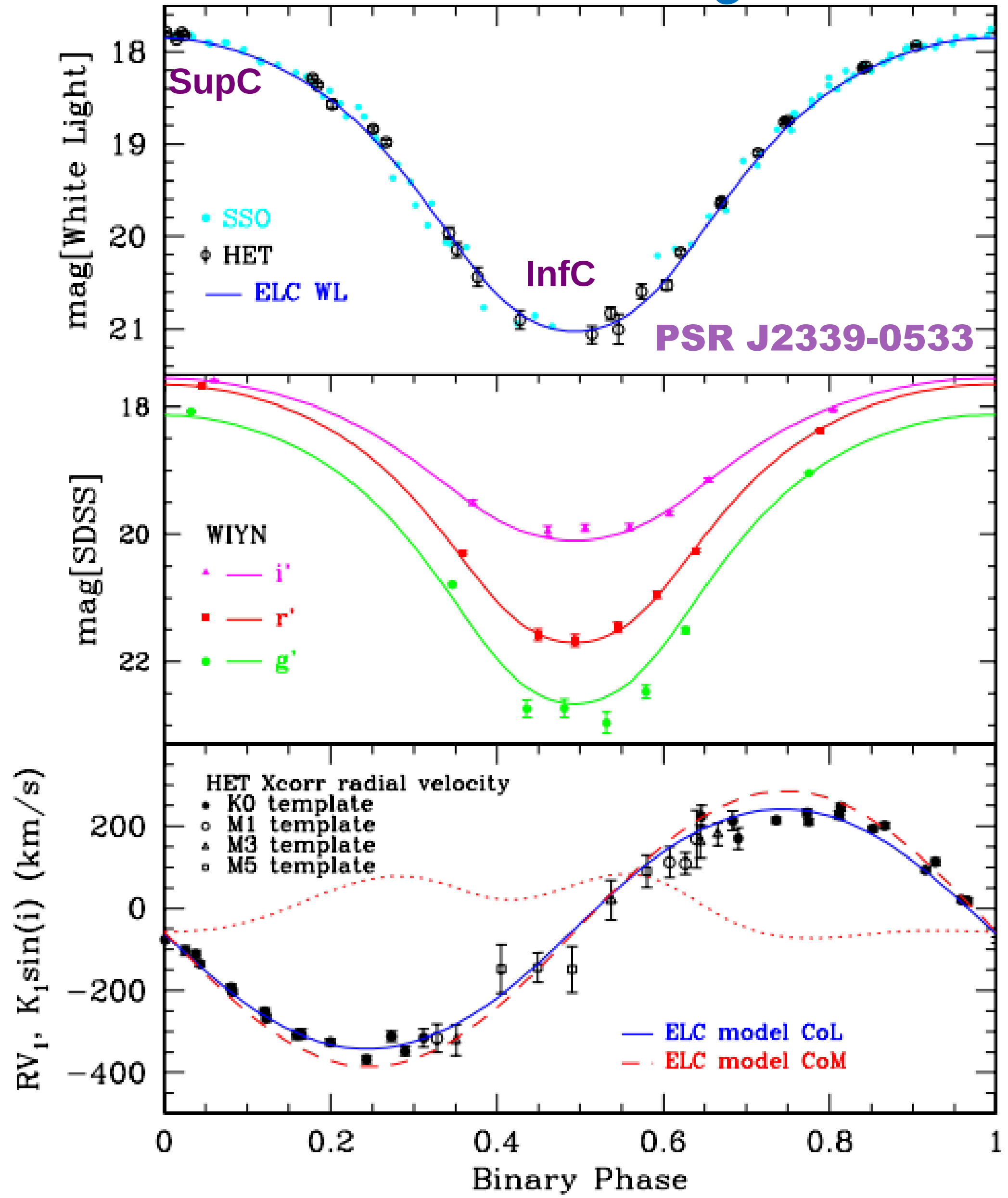

X-ray Modulation

- Archival *CXO* data
- $F(0.5\text{-}8\ \text{keV}) = (2.3^{+1.2}_{-0.3})\times 10^{-13}\ \text{erg/cm}^2\text{/s}$
- $G_{PL} = 1.09^{+0.40}_{-0.13}$
- Hardness ratio a minimum at companion inferior conjunction (eclipsing pulsar)

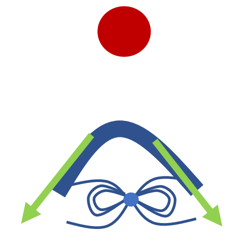

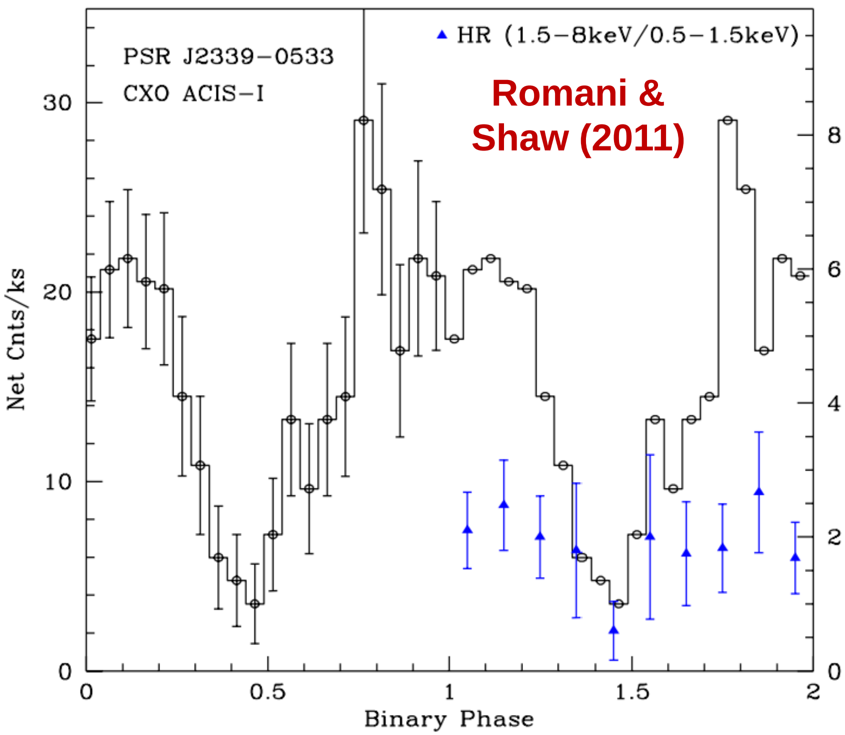

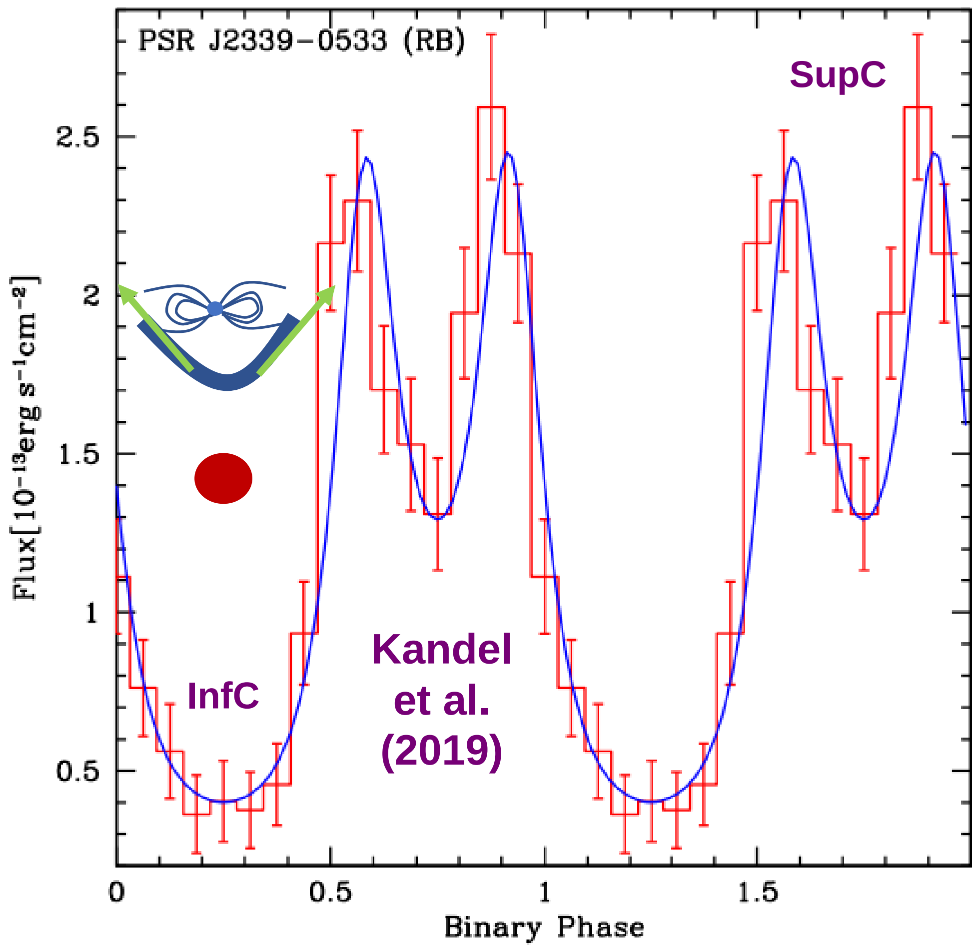

Intra-binary Shock

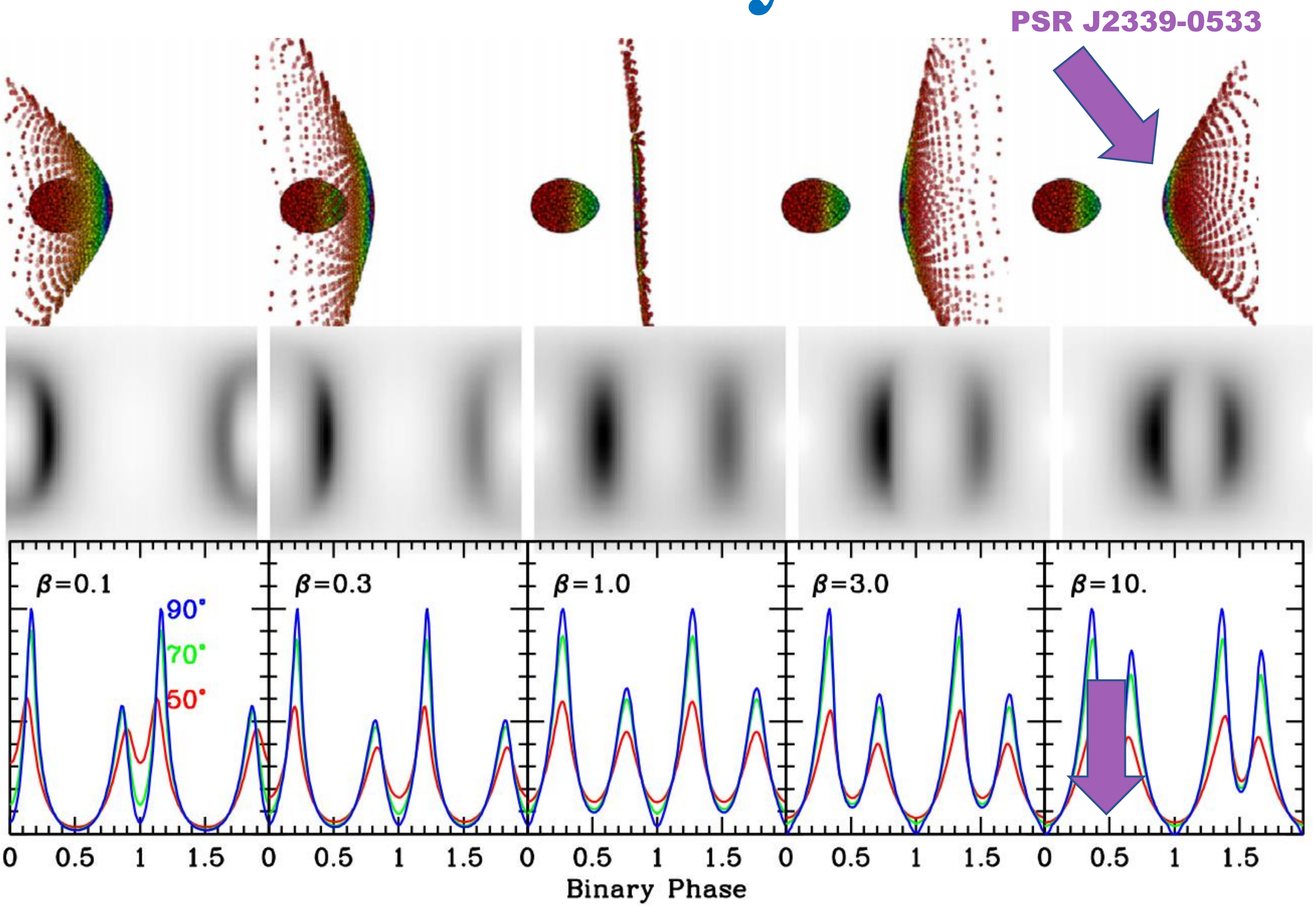

Romani & Sanchez (2016)

Particle Transport

$$\frac{\partial N_e}{\partial t} = -\vec{V} \cdot \left(\vec{\nabla} N_e\right) + \kappa(E_e)\nabla^2 N_e + \frac{\partial}{\partial E_e}\left(\dot{E}_{e,tot} N_e\right) - \left(\vec{\nabla} \cdot \vec{V}\right) N_e + Q$$

Solid Angle & Diffusion:

Van der Merwe et al. (2020)

$$Q_{PSR}(E_e) = Q_0 E_e^{-\Gamma} \exp\left(-\frac{E_e}{E_{cut}}\right)$$

$$Q_1 = \left(\frac{1}{4\pi}\int_0^{2\pi}\int_{\lambda_1}^{\lambda_2} \sin\lambda \, d\lambda \, d\phi\right) Q_{PSR} = \frac{1}{2}\left(\cos\lambda_1 - \cos\lambda_2\right) Q_{PSR}$$

$$Q_i = \frac{1}{t_{diff}} \frac{dN_{e,i-1}}{dE_e} + \frac{1}{2}\left(\cos\lambda_i - \cos\lambda_{i+1}\right) Q_{PSR}, \quad i > 1$$

Normalisation - Current and Energetics:

$$\dot{N}_{GJ} = \frac{B_{PSR} 4\pi^2 R_{PSR}^3}{2ceP^2} \qquad \dot{N}_{II} = M_{\pm} \dot{N}_{GJ}$$

$$\int_{E_{min}}^{\infty} Q_{PSR} \, dE_e = (M_{\pm} + 1)\dot{N}_{GJ} \qquad \int_{E_{min}}^{\infty} E_e Q_{PSR} \, dE_e = \eta_p \dot{E}_{rot}$$

subGeV Modulation

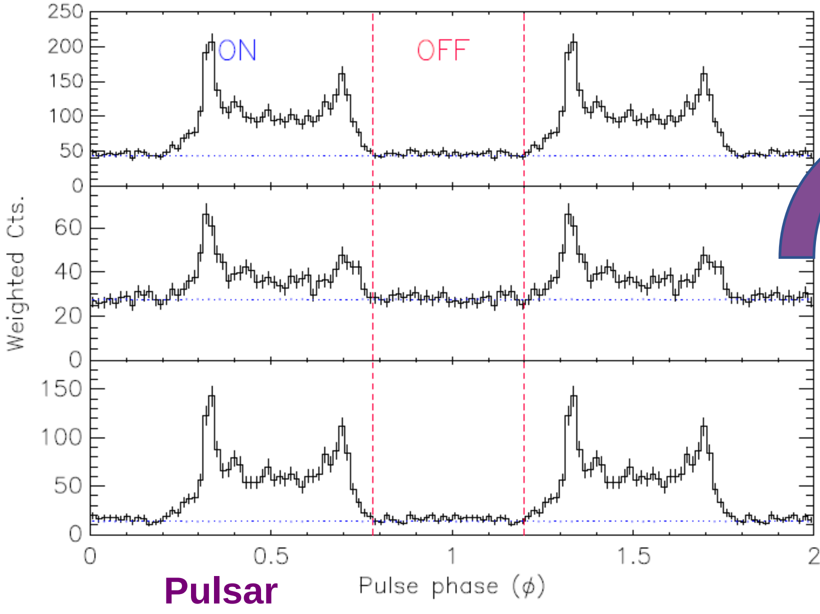

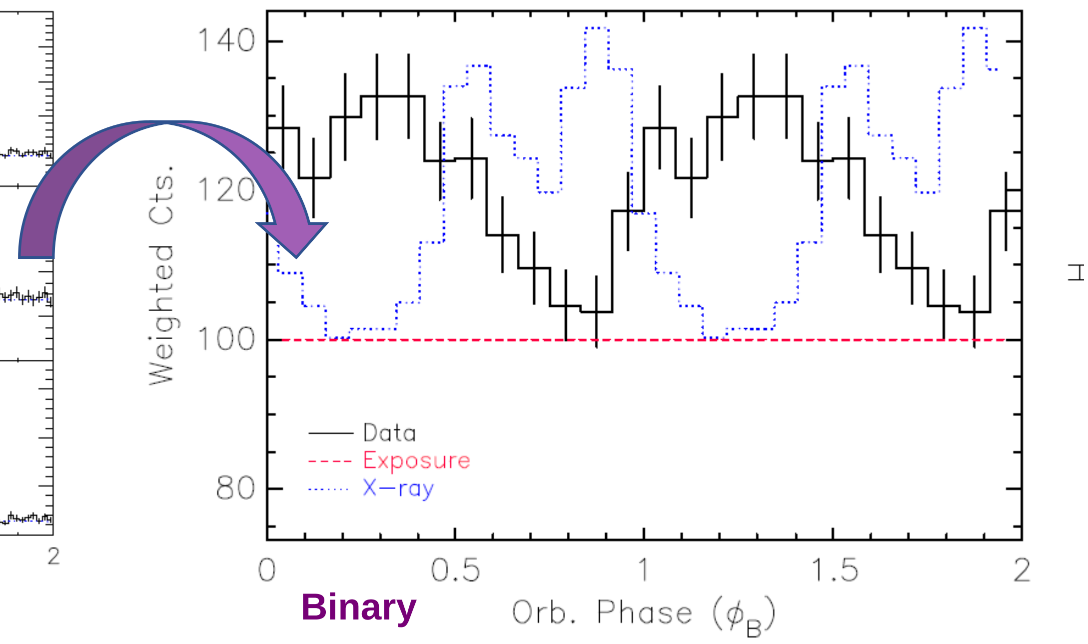

- **100 – 600 MeV orbital modulation**
- **Peaks near pulsar superior conjunction**
- **Detected in on-pulse interval: variation in pulsed 2.9 ms signal itself (An & Romani 2020)**

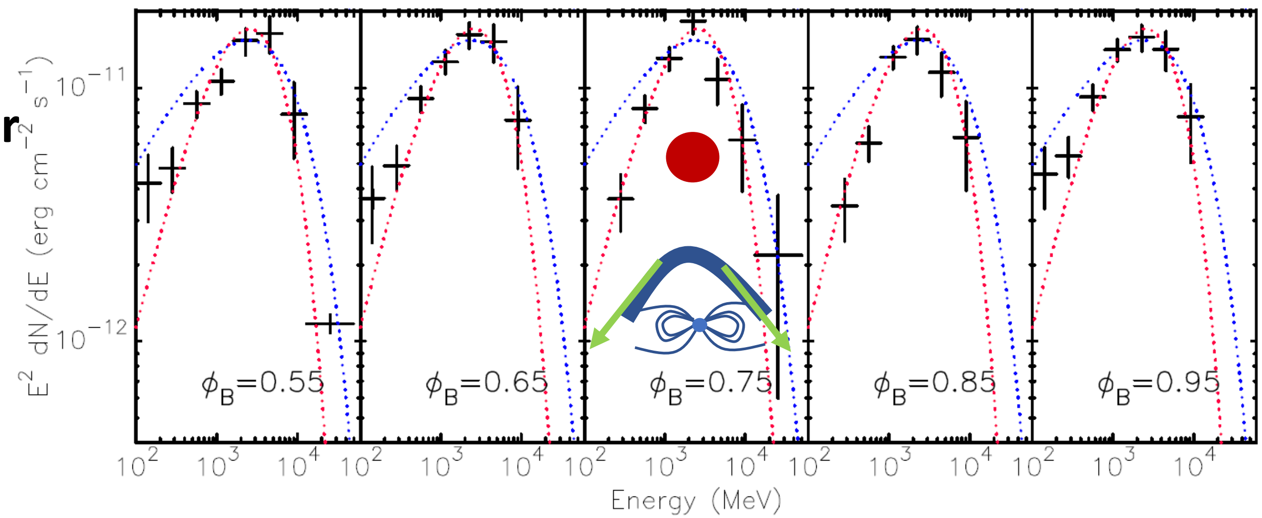

Spectral Modelling

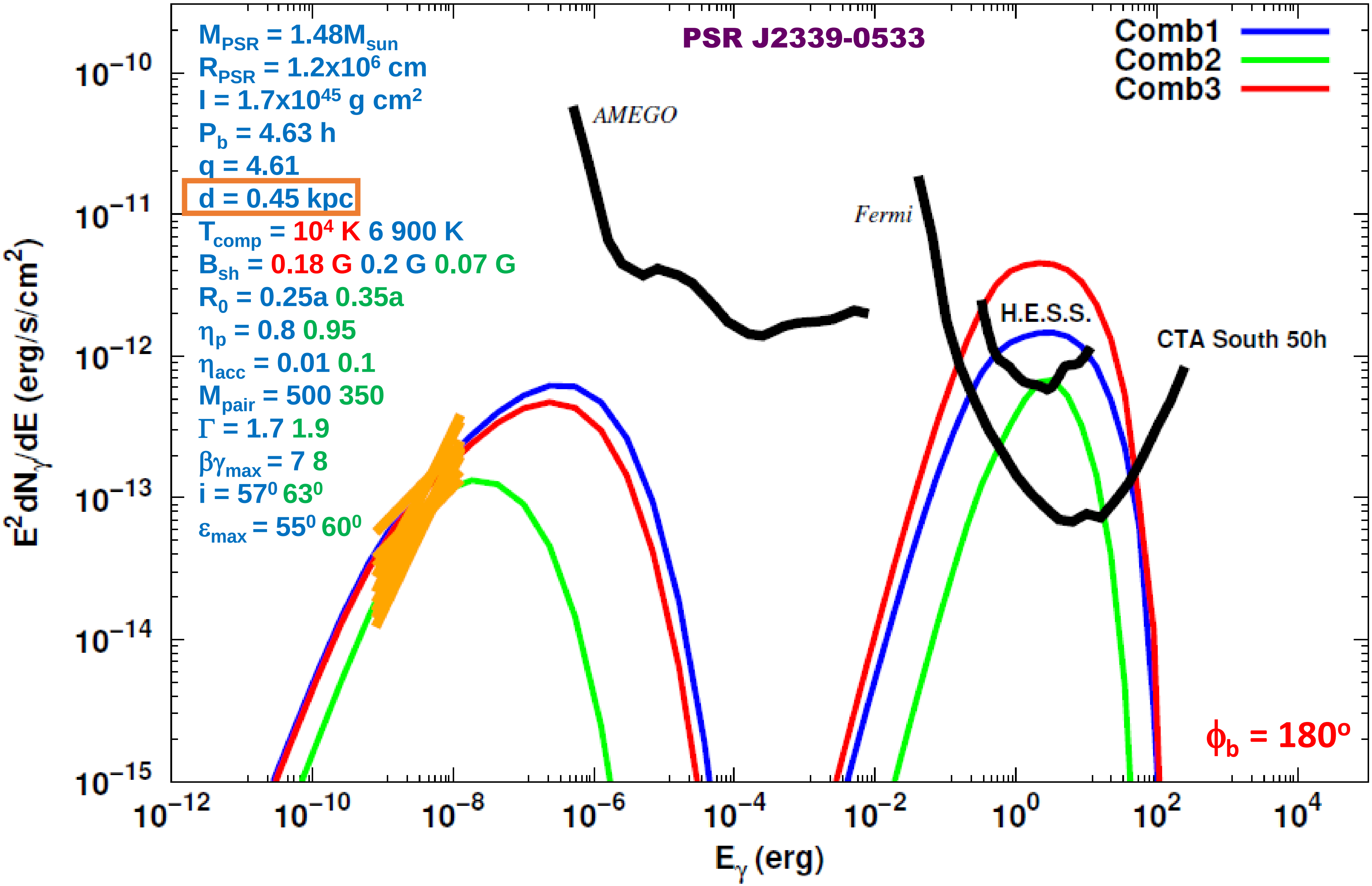

Orbital Light Curve Modelling

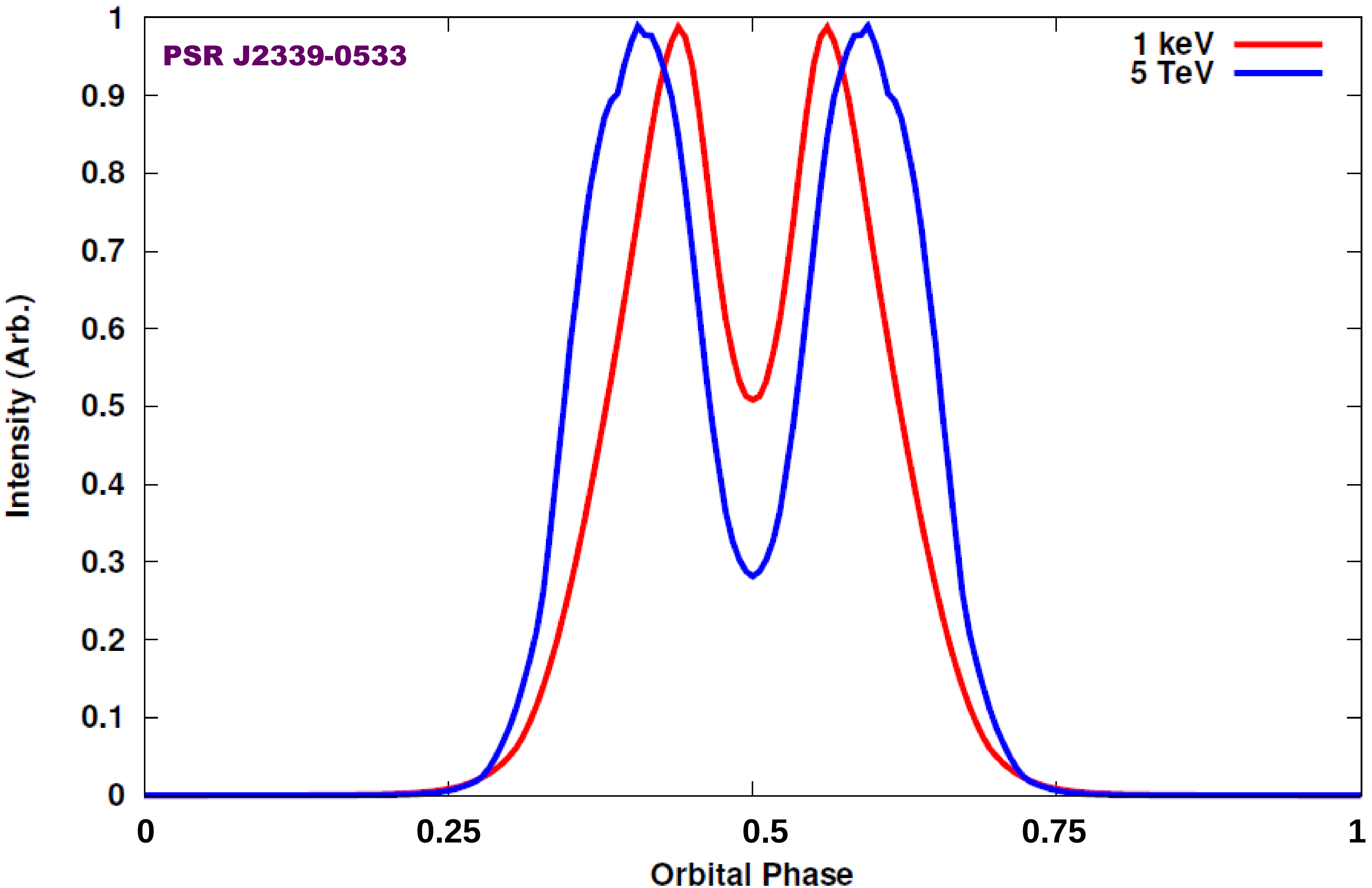

Pulsar Wind Nebulae

PWN Background

- Supernova explosion: remnant neutron star
- Rotation-powered / magnetic-powered pulsar (PWN or MWN)
- Radio: SR shell for SNR and flat-spectrum central PWN
- Composite SNRs (plerions)
- Dissipate rotational energy via relativistic wind of positrons and electrons
- May encounter inward reverse shock of SNR

Spatial Dependence of PWNe

- **Torus + jets**
- **Change in properties with central distance**

X-ray band (*Chandra* images)

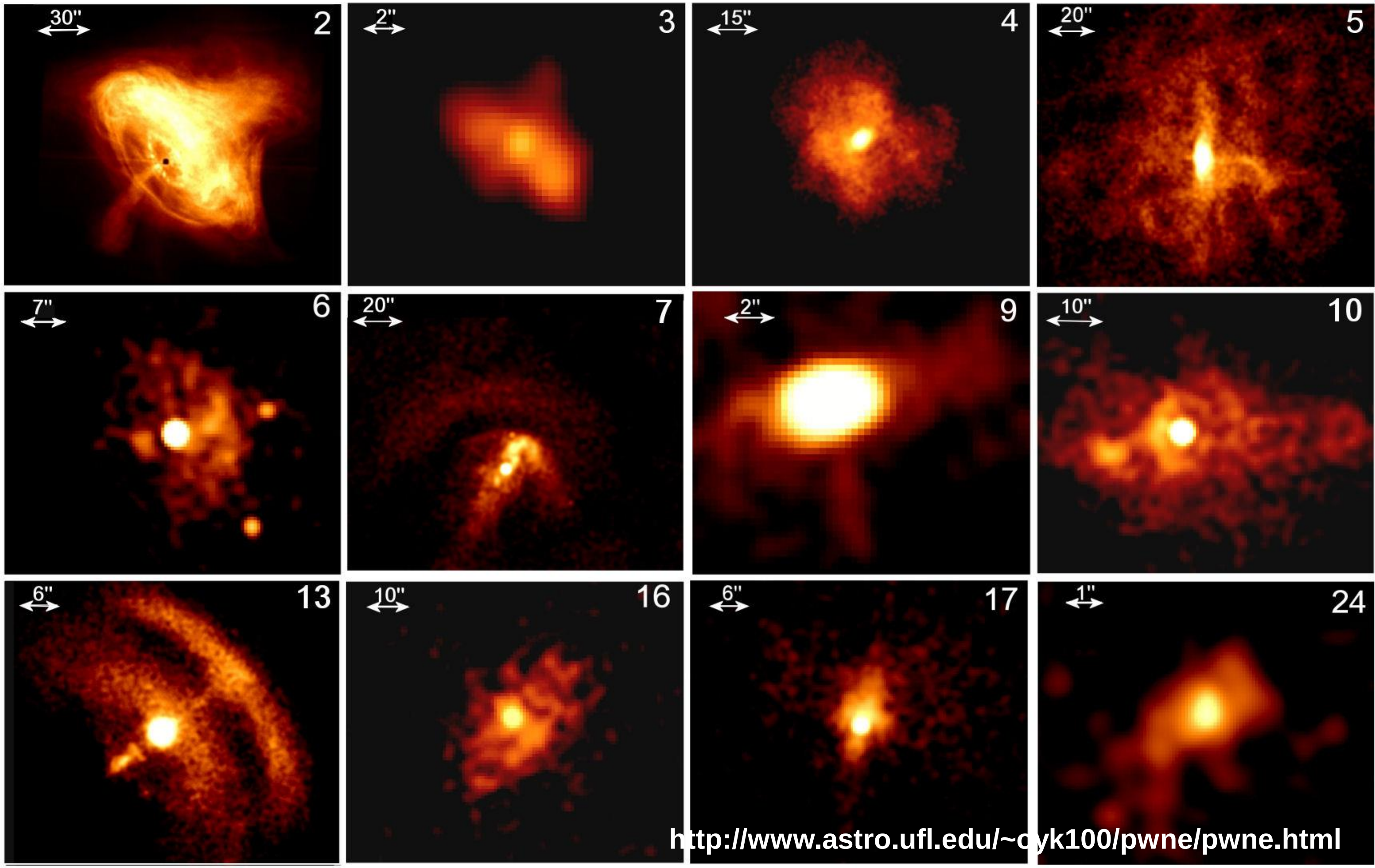

http://www.astro.ufl.edu/~dyk100/pwne/pwne.html

Spatial Dependence of PWNe

- **TeV radial profile**

$$y = \begin{cases} a(x - r_0)^n + c & (x < r_0) \\ c & (x \geq r_0) \end{cases}$$

Abdalla *et al.* (2018)

HESS J1825-137

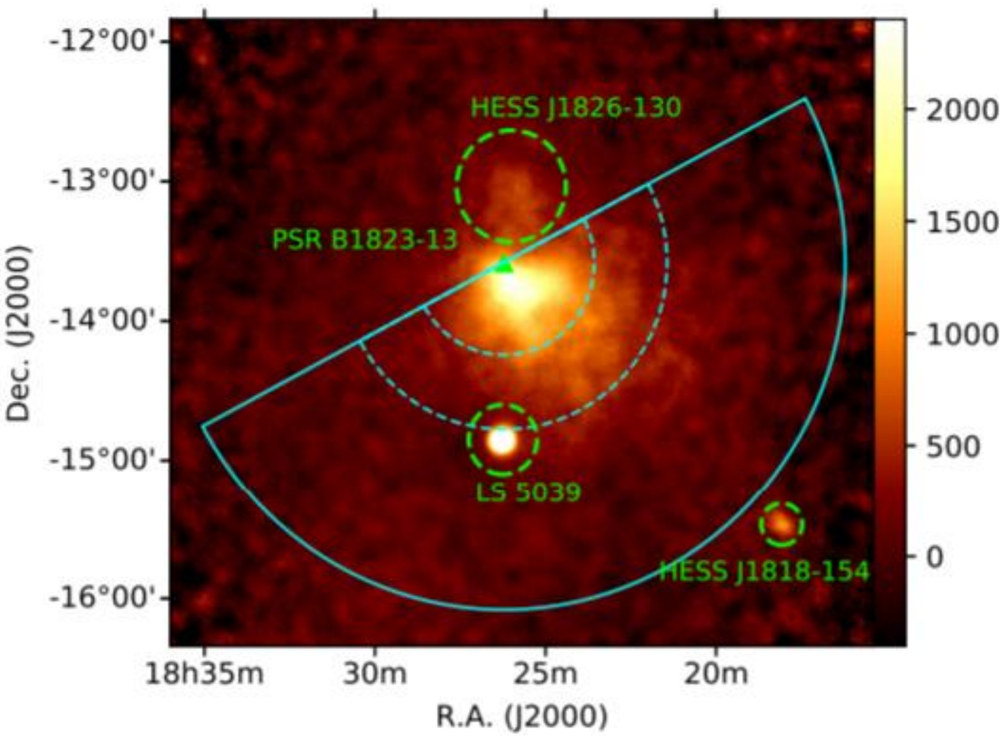

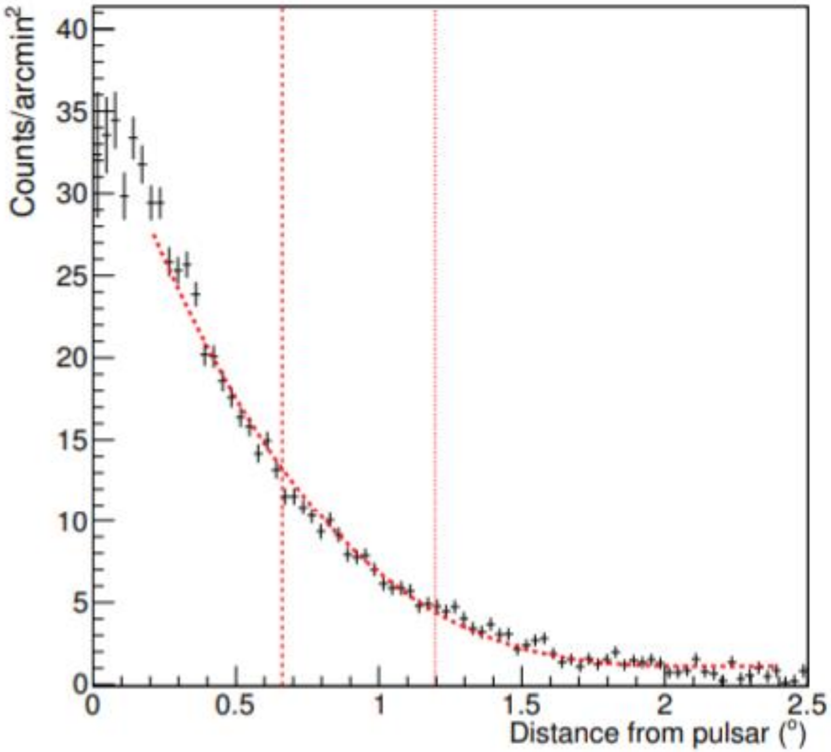

Spatial Dependence of PWNe

- **Spectral steepening with distance**
- **First direct evidence of electron cooling (at the time cir. 2006)**

Abdalla *et al.* (2018)

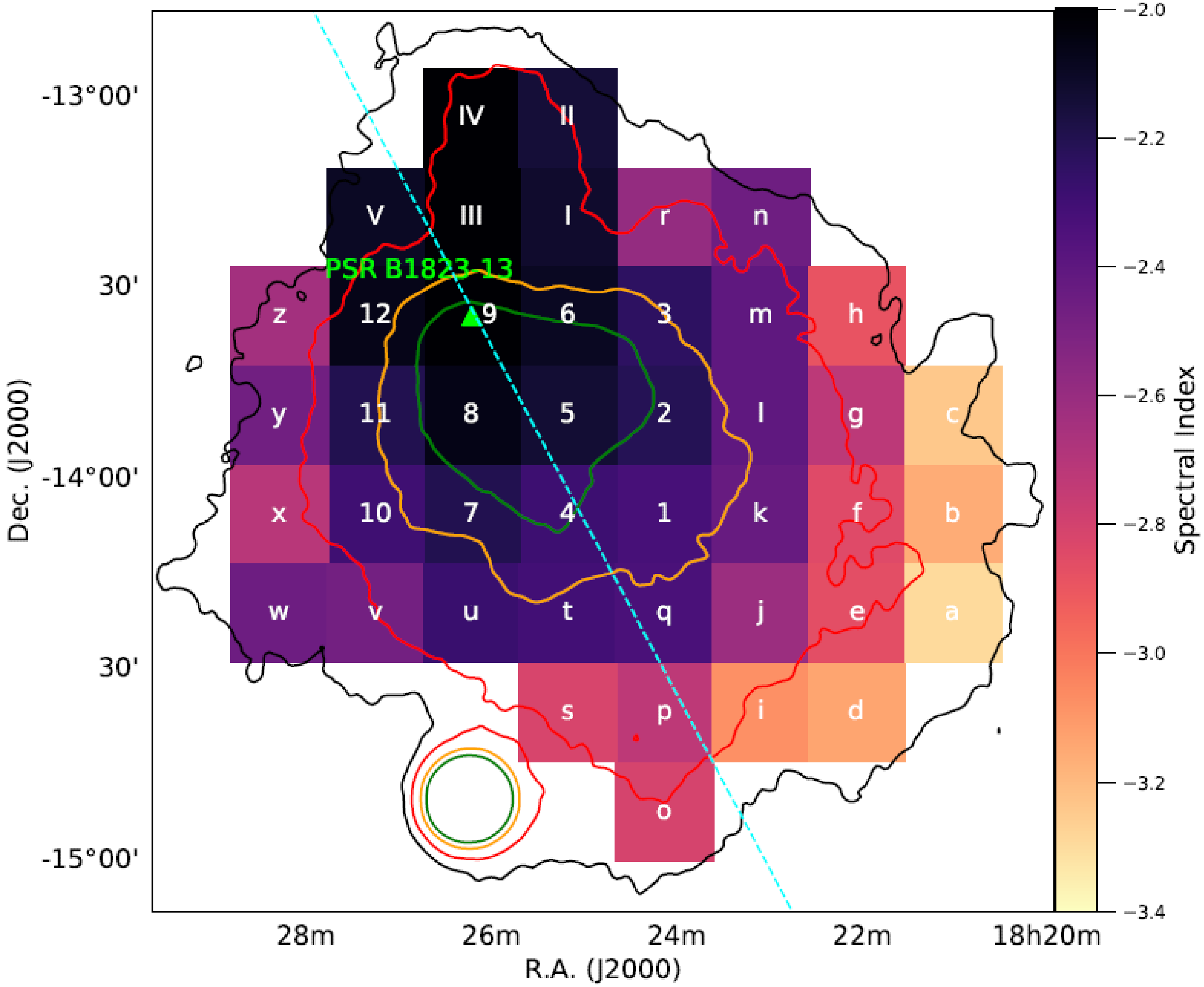

Temporal Dependence of PWNe

- **Spin-down**
- **Also variability on shorter timescales**
- **E.g., Vela PWN**

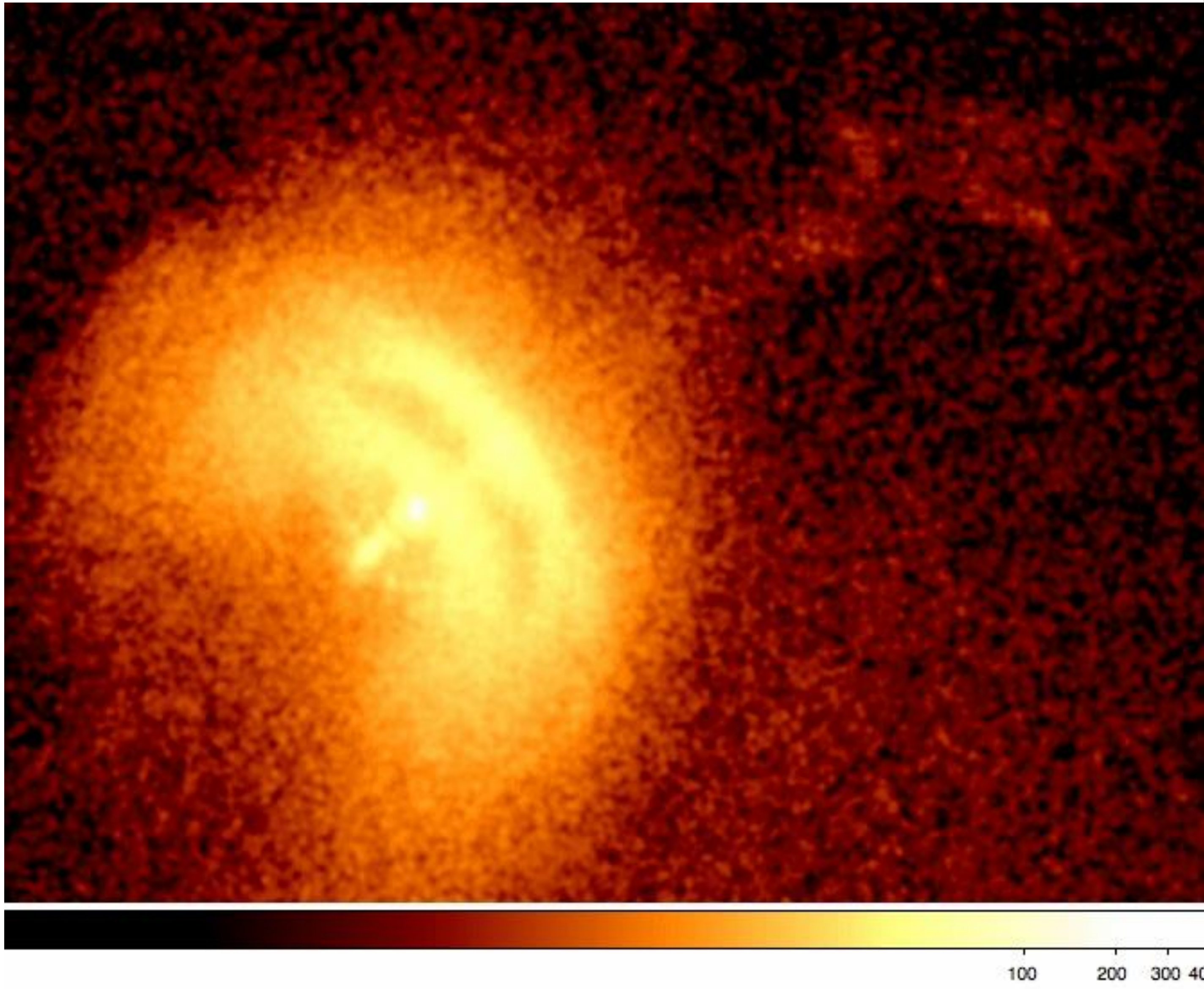

www.astro.ufl.edu/~oyk100/pwne/pwne.html

Kes 75 Background

- One of the youngest composite supernova remnants (~700 yr).
- Contains the pulsar wind nebula (PWN) of young glitching PSR J1846–0258.
- Youngest pulsar in Galaxy (360 – 530 yr)

Recent Observations

- *Chandra*: rapid PWN expansion (~0.2% in yr) = 1 million m/s!
- PWN expanding into a relatively low-density environment.
- ~10% flux decrease in 7 years
- Absence shell emission to the east: very strong density gradient of surrounding medium

Reynolds et al. (2018)

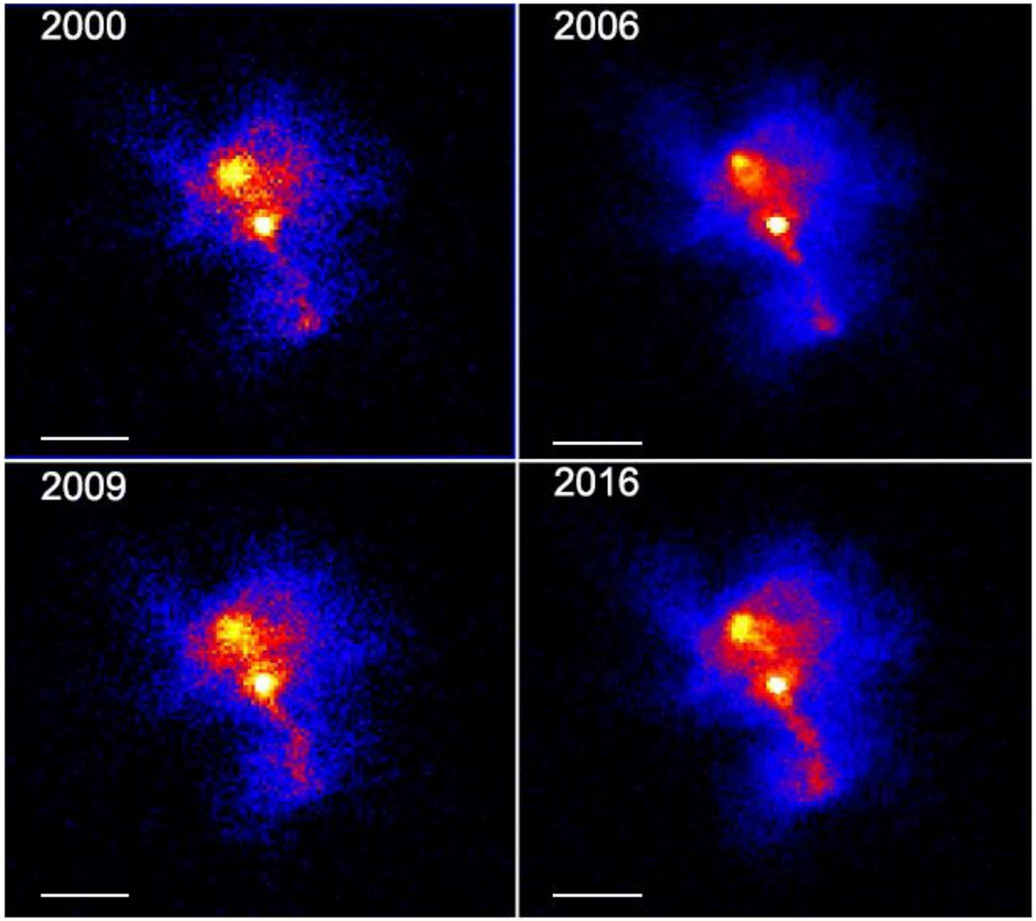

Transport Equation (I)

$$\frac{\partial N_\mathrm{e}}{\partial t} = -\mathbf{V} \cdot (\nabla N_\mathrm{e}) + \kappa \nabla^2 N_\mathrm{e} + \frac{1}{3}(\nabla \cdot \mathbf{V}) \left(\left[\frac{\partial N_\mathrm{e}}{\partial \ln E} \right] - 2N_\mathrm{e} \right) + \frac{\partial}{\partial E}(\dot{E}_\mathrm{rad} N_\mathrm{e}) + Q(\mathbf{r}, E, t)$$

Van Rensburg et al. (2018)

Injection spectrum

$$Q(E_\mathrm{e}, t) = \begin{cases} Q_0(t) \left(\frac{E_\mathrm{e}}{E_\mathrm{b}} \right)^{\alpha_1} & E_\mathrm{e} < E_\mathrm{b} \\ Q_0(t) \left(\frac{E_\mathrm{e}}{E_\mathrm{b}} \right)^{\alpha_2} & E_\mathrm{e} \geq E_\mathrm{b}. \end{cases}$$

Venter & de Jager (2007)

Time-dependent normalization:

$$\epsilon L(t) = \int_{E_\mathrm{min}}^{E_\mathrm{b}} Q E_\mathrm{e} dE_\mathrm{e} + \int_{E_\mathrm{b}}^{E_\mathrm{max}} Q E_\mathrm{e} dE_\mathrm{e}$$

$$L(t) = L_0 \left(1 + \frac{t}{\tau_c} \right)^{-(n+1)/(n-1)}$$

Pacini & Salvati (1973)

Transport Equation (II)

- SR & IC radiative losses
- Adiabatic losses
- Convection
- Diffusion
- Limiting energy

$$V(r) = V_0 \left(\frac{r}{r_0}\right)^{\alpha_V}$$

$$\kappa = \kappa_0 \left(\frac{E}{E_0'}\right)^{q}$$

$$B(r,t) = B_{\rm age} \left(\frac{r}{r_0}\right)^{\alpha_B} \left(\frac{t}{t_{\rm age}}\right)^{\beta_B}$$

$$\frac{\partial \mathbf{B}}{\partial t} = \nabla \times (\mathbf{V} \times \mathbf{B})$$

$$\Rightarrow \quad \alpha_V + \alpha_B = -1$$

Kennel & Coroniti (1984a)

$$E_{\rm max} = \frac{e}{2}\sqrt{\frac{L(t)\sigma}{c(1+\sigma)}}$$

Line-of-Sight (LOS) Calculation

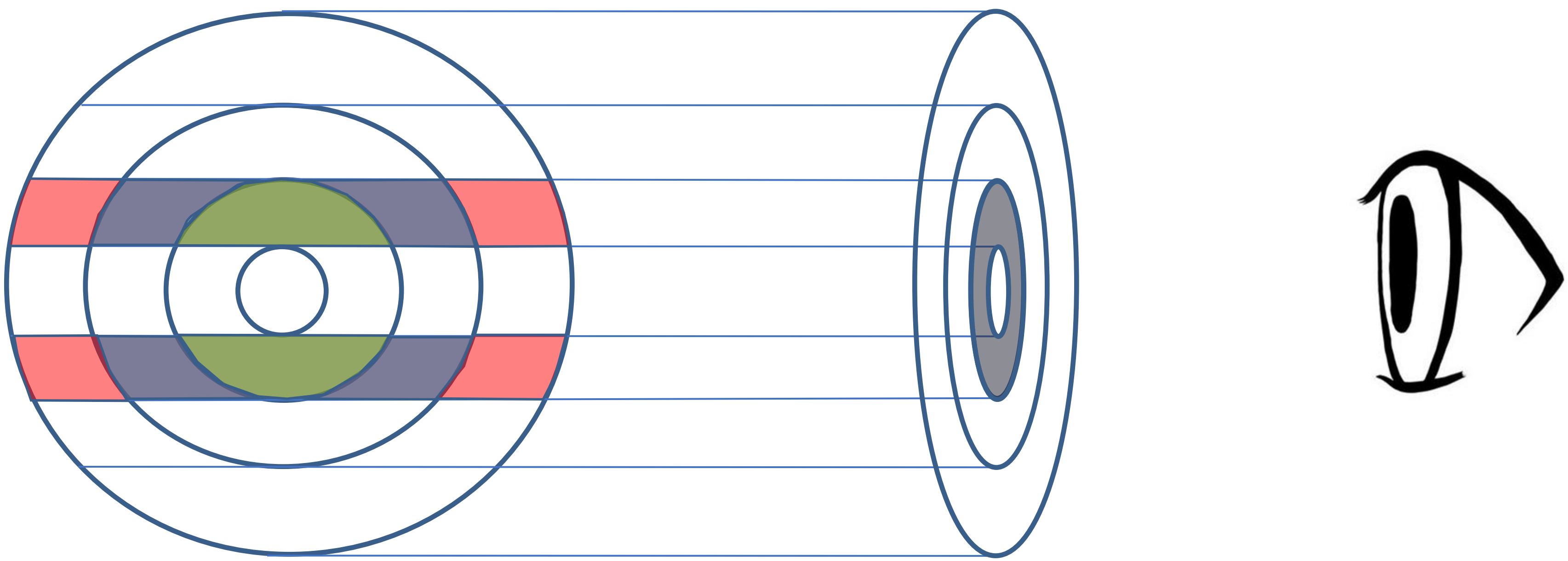

Credit: C van Rensburg

Fitting Results

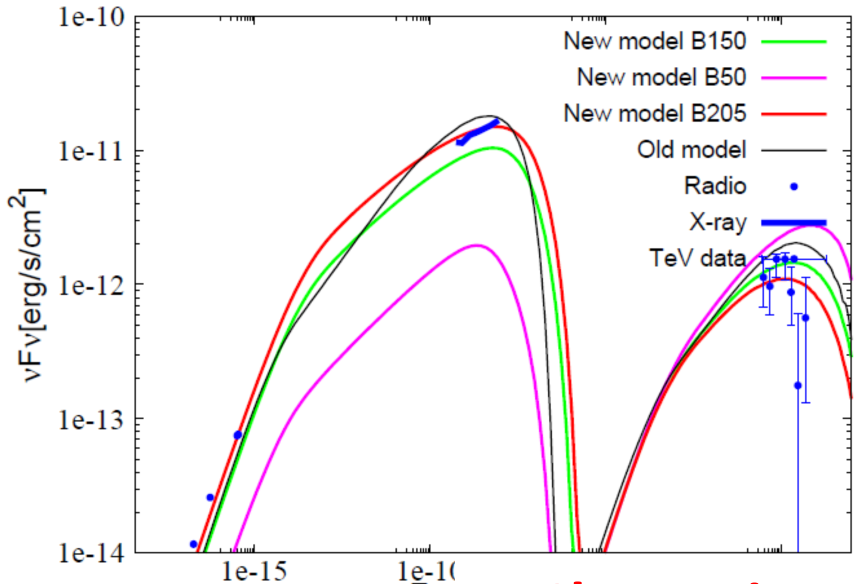

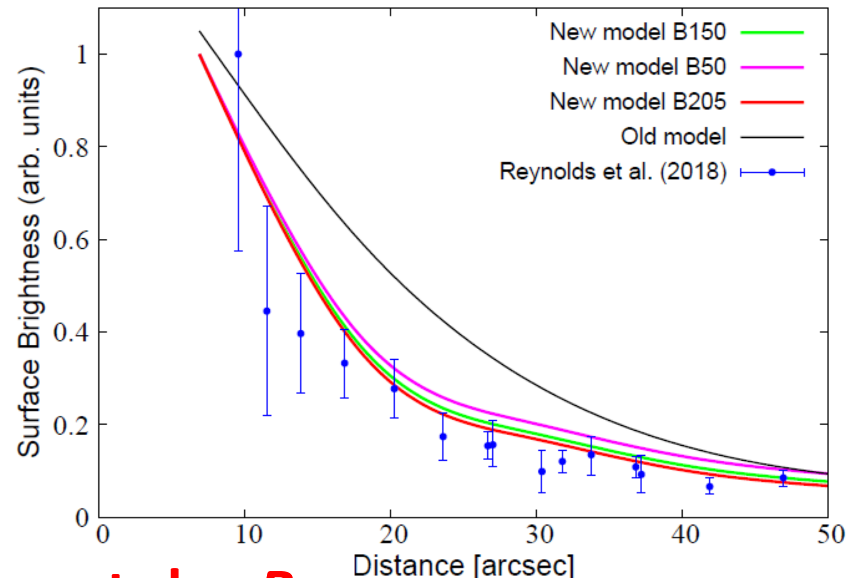

Change in present-day *B*

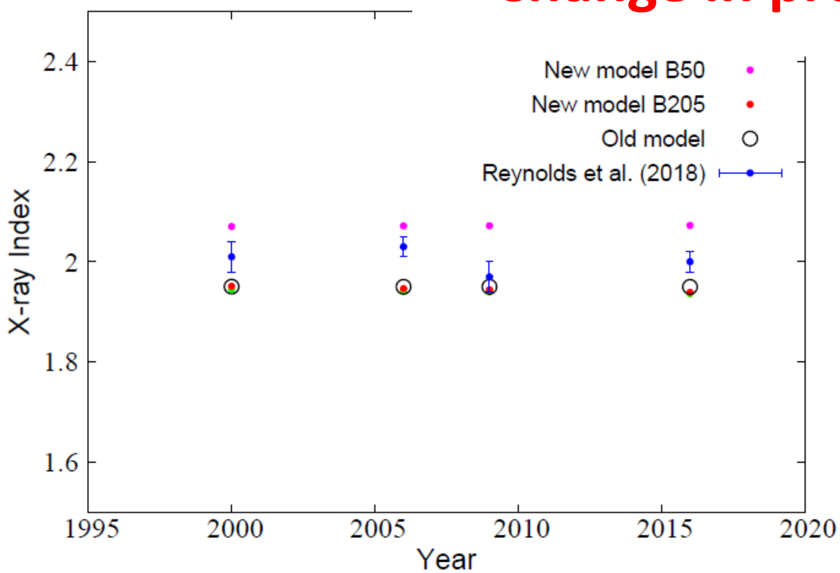

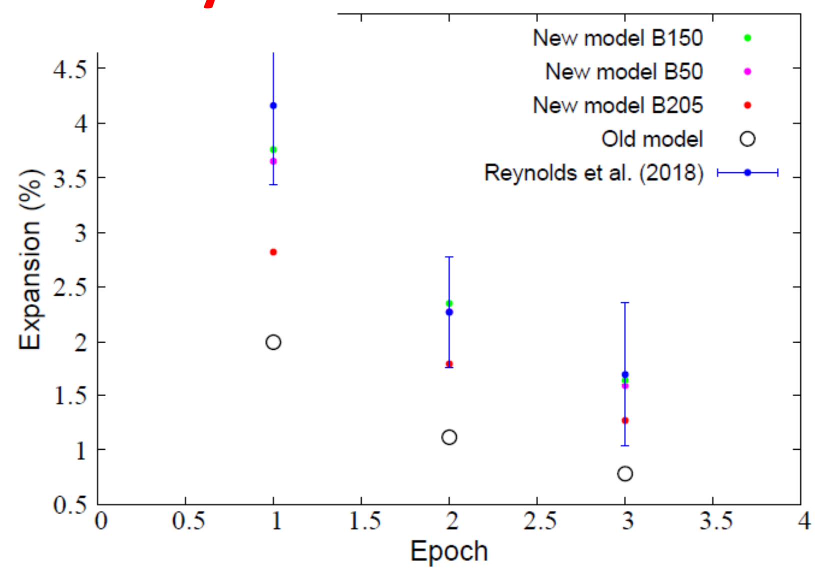

Pulsars in Globular Clusters

Globular Clusters (GCs)

- ~160 Galactic clusters (Harris 1996, 2010)
- $10^4 - 10^6$ stars
- Spherical distribution about Galactic Centre with $\langle d \rangle$ ~12 kpc

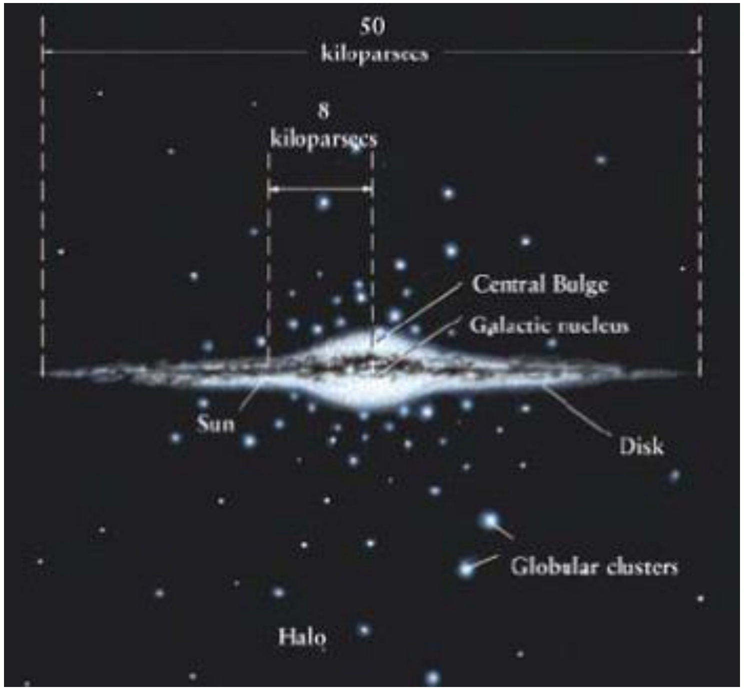

- Exotic stellar members (BHs, MSPs, WDs, CVs, etc.)
- Multi-wavelength objects

Millisecond Pulsars in GCs

150 radio MSPs in 28 GCs*

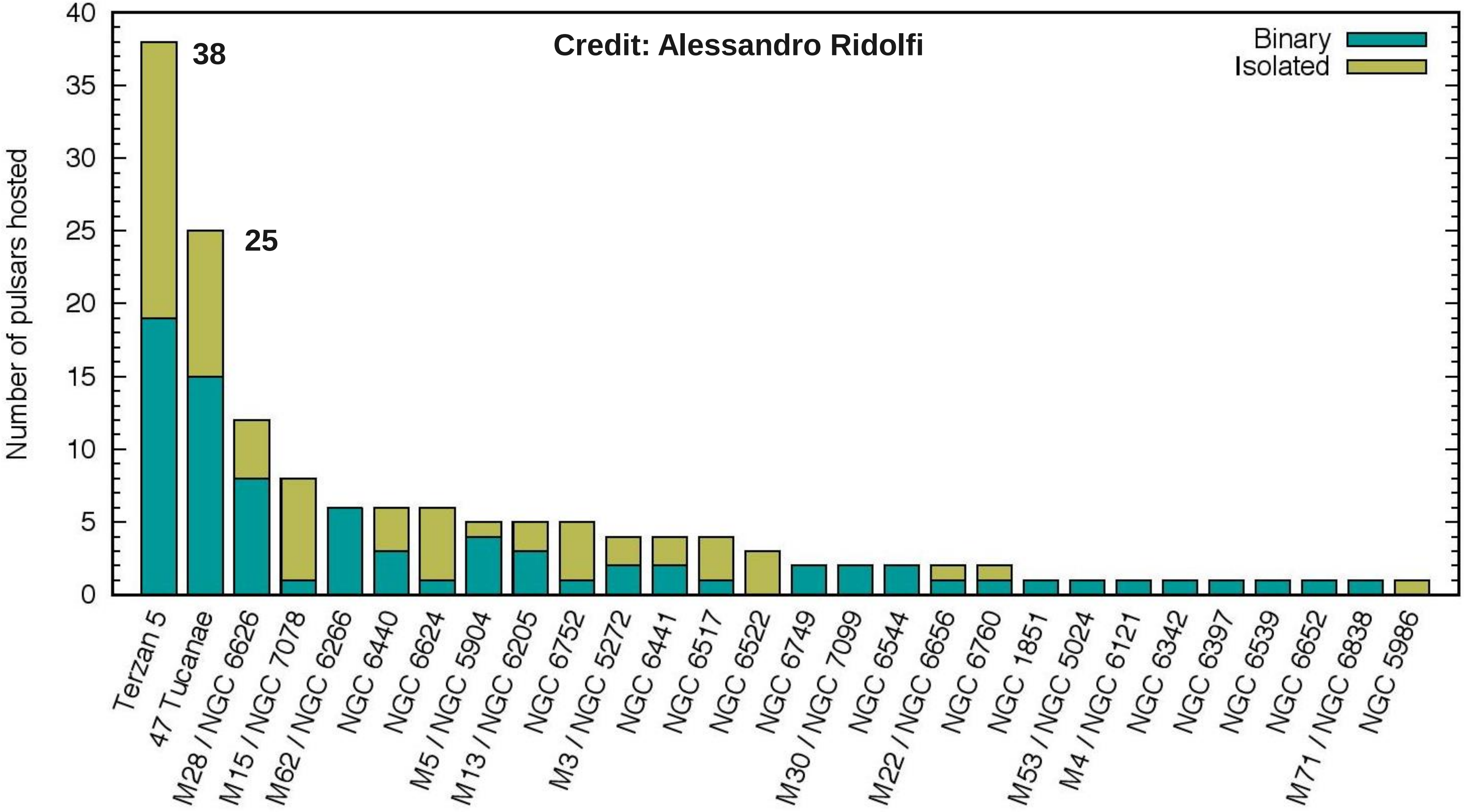

*www.naic.edu/~pfreire/GCpsr.html

Spectral Components Expected from GC MSPs

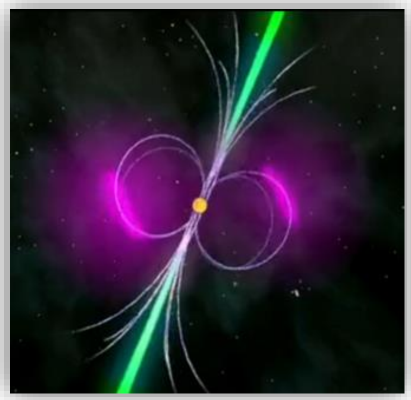

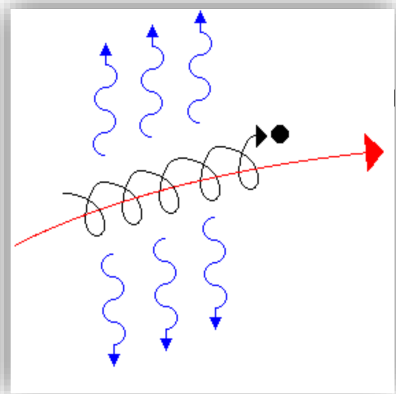

http://i.space.com/images/i/000/013/110/i02/nasa-fermi-pulsar-J1823-2021a.jpg?1320348068

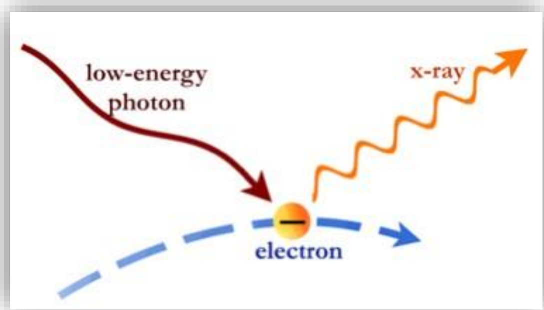

http://www.astro.wisc.edu/~bank/img/inversecompton.jpg

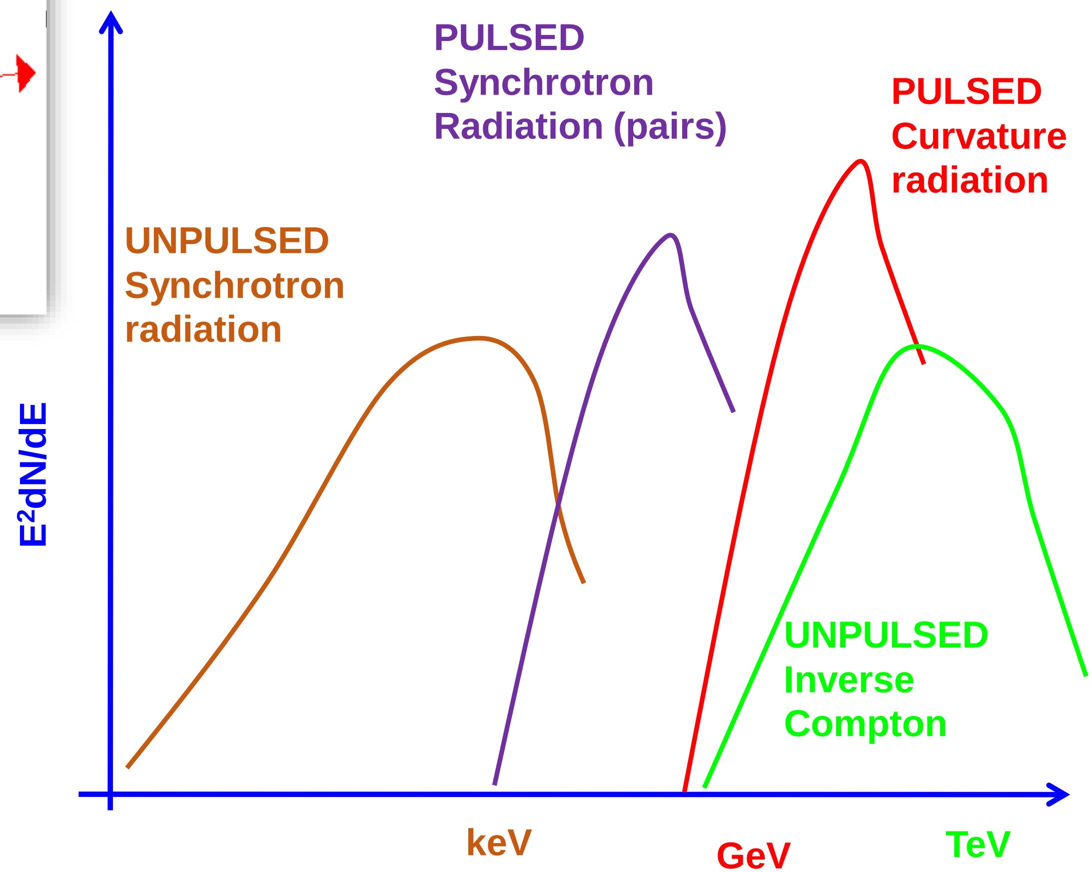

SED & Parameter Constraints

Cluster parameters:

$R_c, R_h, R_t \; \alpha \; d$
$F_g \; \alpha \; d^2$
$u(r) \; \alpha \; N_* R^2 T^4 \int_0^{R_t} \rho(R_c, R_h, R_t)$

Kopp et al. (2013)
Ndiyavala-Davids et al. (2021)

CR/SR parameters:

$E_{||}, N_{MSP}$, *gap width*, M_+

Injection spectrum:

$E_{min}, E_{max}, \Gamma, N_{MSP}$
$\alpha \; N_{MSP} \, \eta_p \langle \dot{E} \rangle$

Diffusion parameters:

$\kappa = \kappa_0 E^{\delta}$

SR parameters:

$E \; \alpha \; B^2$
$N_e(u_i, B, \kappa) \; \alpha \; N_{MSP} \, \eta_p \langle \dot{E} \rangle$

IC parameters:

$u(r), u_{CMB}, u_{BG}$
$N_e(u_i, B) \; \alpha \; N_{MSP} \, \eta_p \langle \dot{E} \rangle$

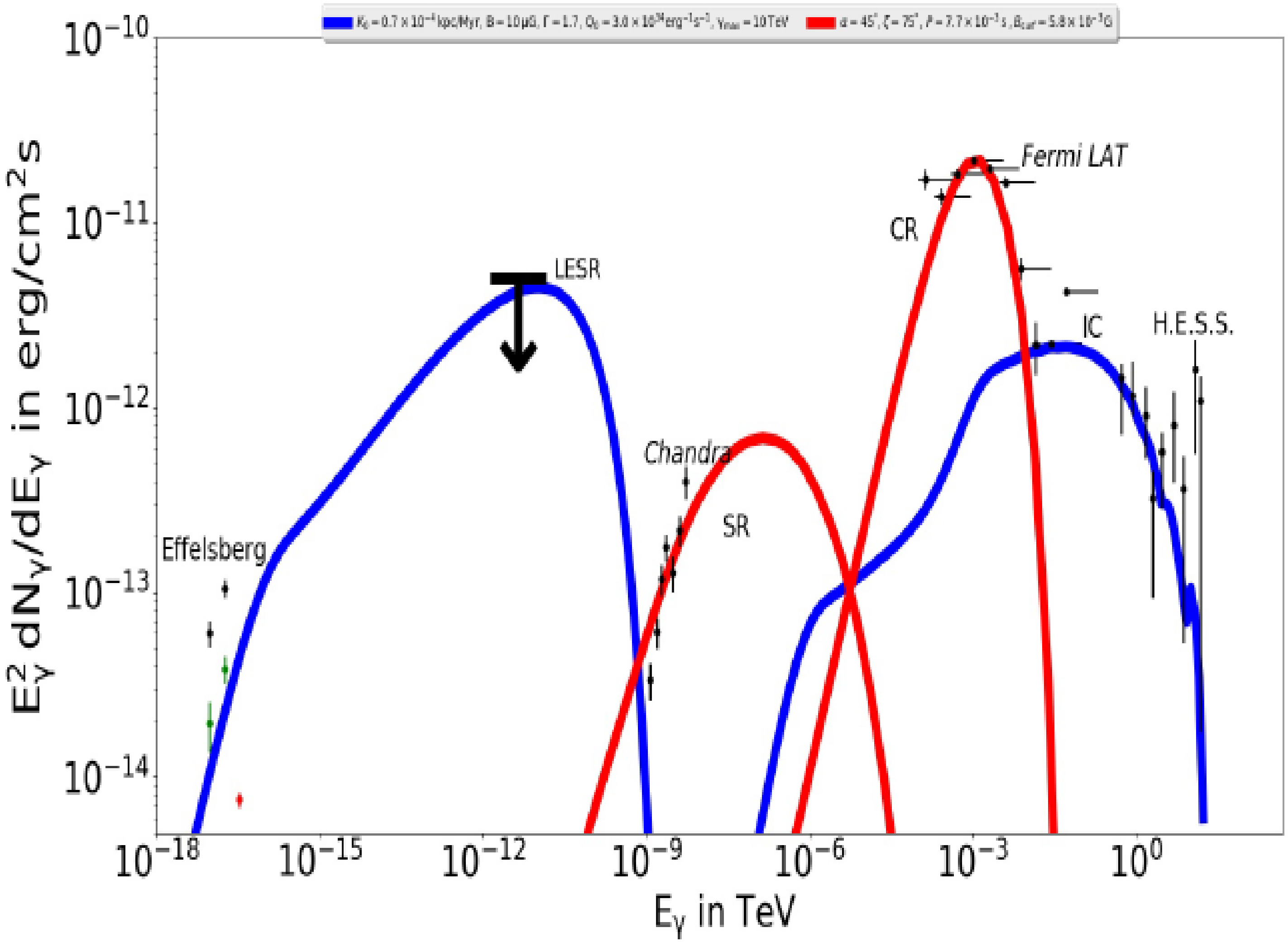

White Dwarf Pulsar

AR Sco Observations

- Marsh et al. (2016) detected optical and radio pulsations from the binary white dwarf (WD) system AR Scorpii

- Orbital period of 3.55 hours and a "pulsar" spin period of 1.95 min

- Constrained the mass of the WD to $\sim 0.8 M_{\odot}$ and the M-dwarf companion to $\sim 0.3 M_{\odot}$

- Stiller et al. (2018) obtained a $\dot{P} = 7.18 \times 10^{-13}\ ss^{-1}$

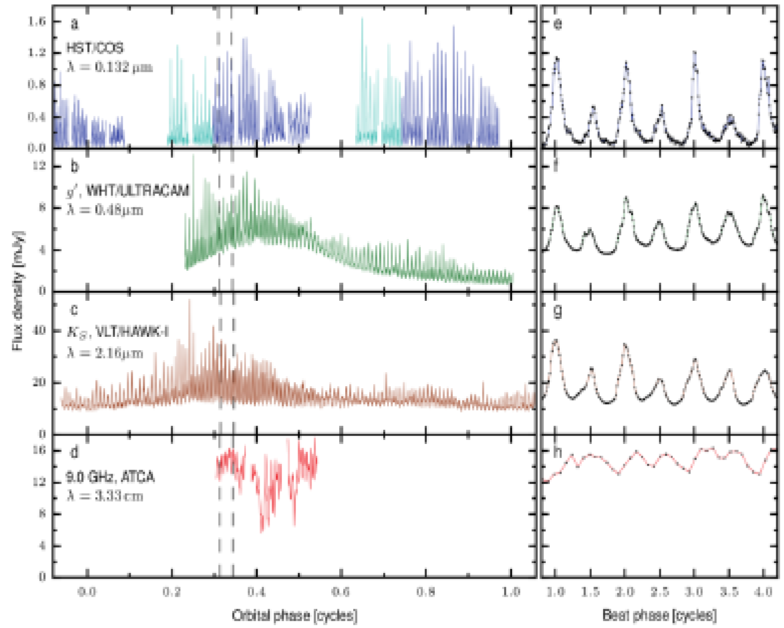

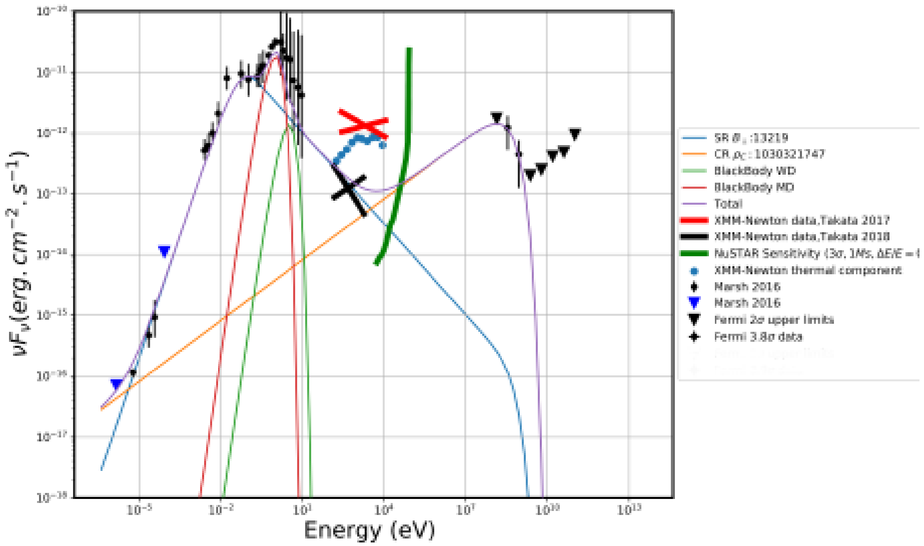

Credit: L du Plessis

AR Sco Observations

- Optical and UV emission lines show no indication of an accretion disc
- The optical and UV are non-thermal emission and pulsed at the WD spin period
- This gives a light cylinder radius of $R_{\rm LC} = 5.6 \times 10^{11}\ cm$ and an orbital semi-major axis of $a = 8.5 \times 10^{10}\ cm$
- Buckley et al. (2017) found that the system exhibits strong linear optical polarisation (up to $\sim 40\%$) and estimated the WD B-field to be $\sim 500\mathrm{MG}$

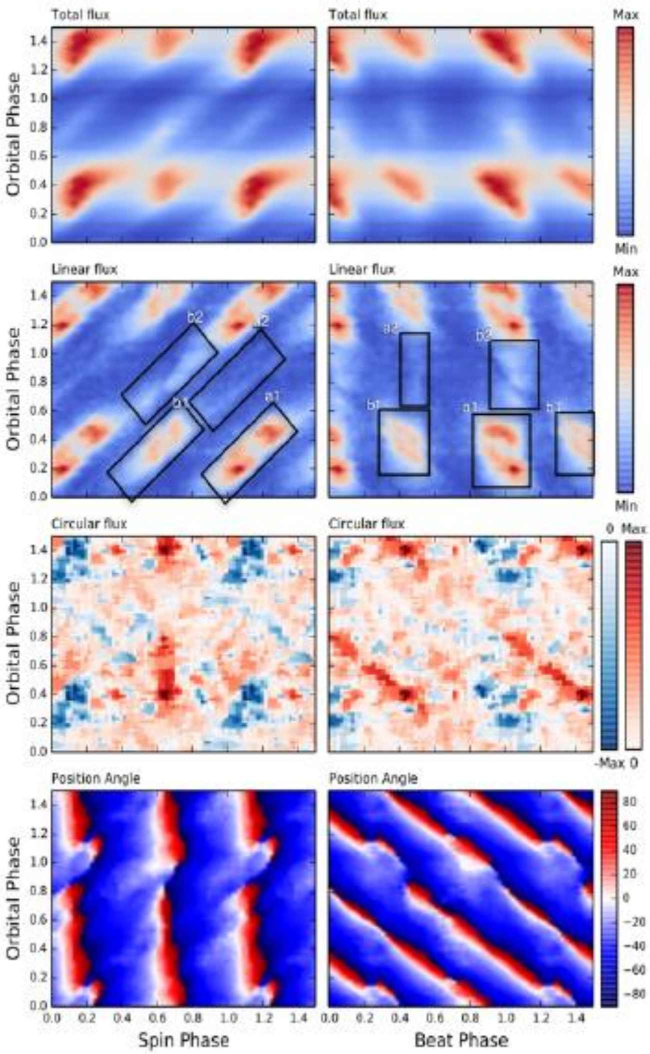

Figure: Optical data from Potter and Buckley (2018)

Credit: L du Plessis

Radiation-reaction Force

- Use equation from Landau and Lifshitz for general radiation-reaction force:

$$\begin{aligned}\mathbf{f} = &\frac{2e^3\gamma}{3mc^3}\left\{\left(\frac{\partial}{\partial t}+\mathbf{v}\cdot\nabla\right)\mathbf{E}+\frac{1}{c}\mathbf{v}\times\left(\frac{\partial}{\partial t}+\mathbf{v}\cdot\nabla\right)\mathbf{H}\right\}\\ &+\frac{2e^4}{3m^2c^4}\left\{\mathbf{E}\times\mathbf{H}+\frac{1}{c}\mathbf{H}\times(\mathbf{H}\times\mathbf{v})+\frac{1}{c}\mathbf{E}\,(\mathbf{v}\cdot\mathbf{E})\right\}\\ &-\frac{2e^4\gamma^2}{3m^2c^5}\mathbf{v}\left\{\left(\mathbf{E}+\frac{1}{c}\mathbf{v}\times\mathbf{H}\right)^2-\frac{1}{c^2}(\mathbf{E}\cdot\mathbf{v})^2\right\}.\end{aligned} \tag{3}$$

$$\frac{d\mathbf{p}}{dt} = q\left(\mathbf{E}+\frac{c\mathbf{p}\times\mathbf{B}}{\sqrt{m^2c^4+\mathbf{p}^2c^2}}\right)$$

- The first term of Equation 3 requires 9, 18 or 36 evaluations of the B-field per stage to find the derivatives.
- This first term is $\sim 10^8 - 10^{10}$ times smaller than the largest component.
- The super-relativistic form of Equation 3 is given by:

$$f_x = -\frac{2e^4\gamma^2}{3m^2c^4}\left\{(E_y - H_z)^2 + (E_z + H_y^2)\right\} \tag{4}$$

- Equation 3 and 4 converge at a Lorentz factor around $10^4 - 10^5$.

$$\begin{aligned} P_{rad} &= \mathbf{F}_{rad}\cdot\mathbf{v},\\ E_{rad} &= \int \mathbf{F}_{rad}\cdot\mathbf{v}.dt \end{aligned} \tag{5}$$

Credit: L du Plessis

Adaptive Time-step Evaluation

- Discovered numerical instability from adaptive time step.
- We investigated new higher precision adaptive time step methods.

$$\Delta t_{n+1} = \Delta t_n \left(\frac{TOL}{T_{\mathrm{err}}}\right)^{-\frac{1}{kp}} \left(\frac{TOL}{T_{\mathrm{err;n-1}}}\right)^{-\frac{1}{kp}} \left(\frac{\Delta t_n}{\Delta t_{n-1}}\right)^{-\frac{1}{kp}}. \qquad (7)$$

- Δt is the time step, TOL is the chosen tolerance for the truncation error T_{err}, p is the order of the chosen numerical method and $k = 8$.
- We used a limiting function to constrict the new time step.

$$\Delta t_l = \Delta t_n \left[1 + \kappa arctan\left(\frac{\Delta t_{n+1} - \Delta t_n}{\kappa \Delta t_n}\right)\right]. \qquad (8)$$

- $\kappa \in [0.7, 2.0]$.

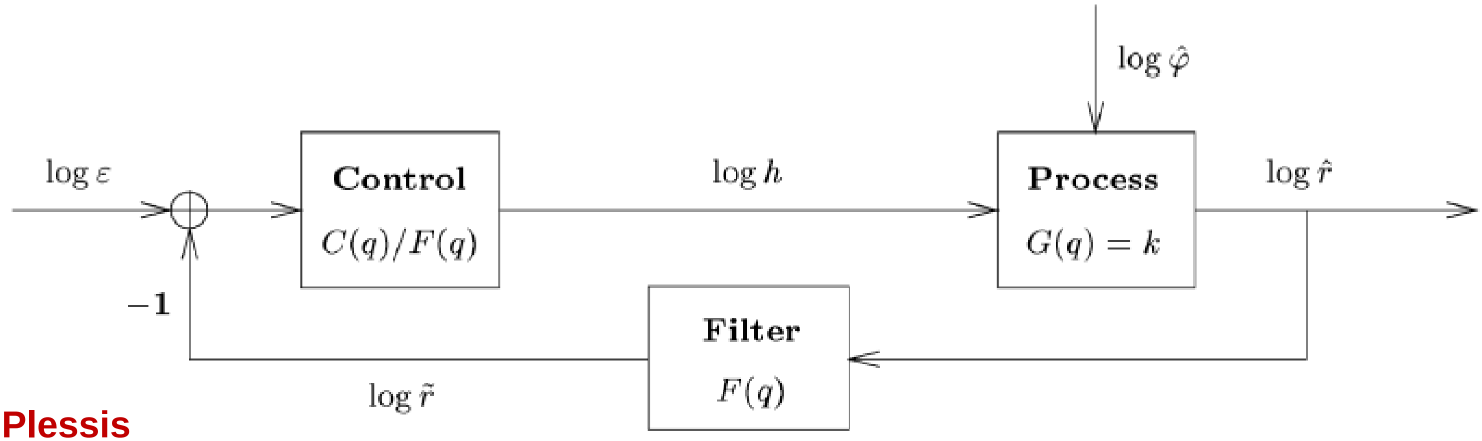

Credit: L du Plessis

Calibration of Code

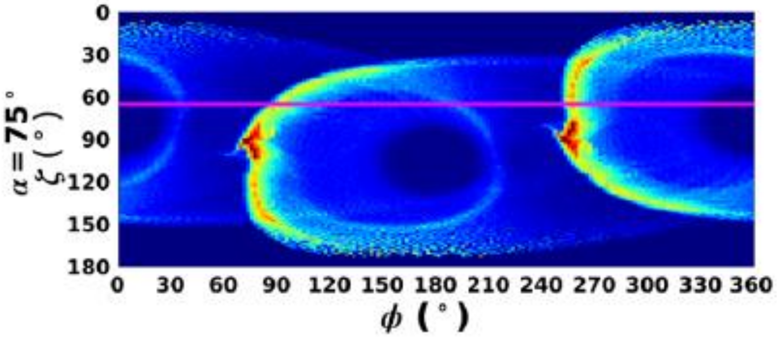

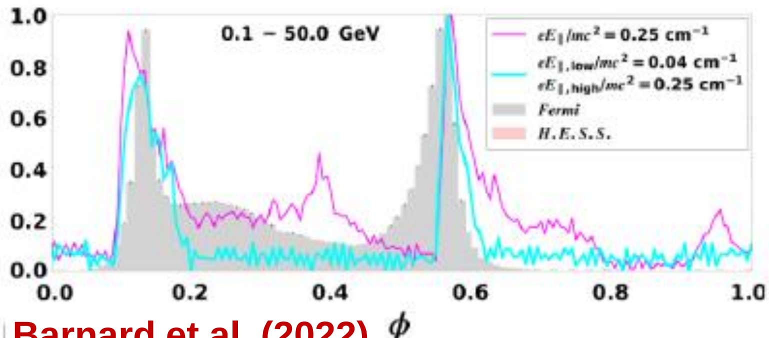

Barnard et al. (2022)

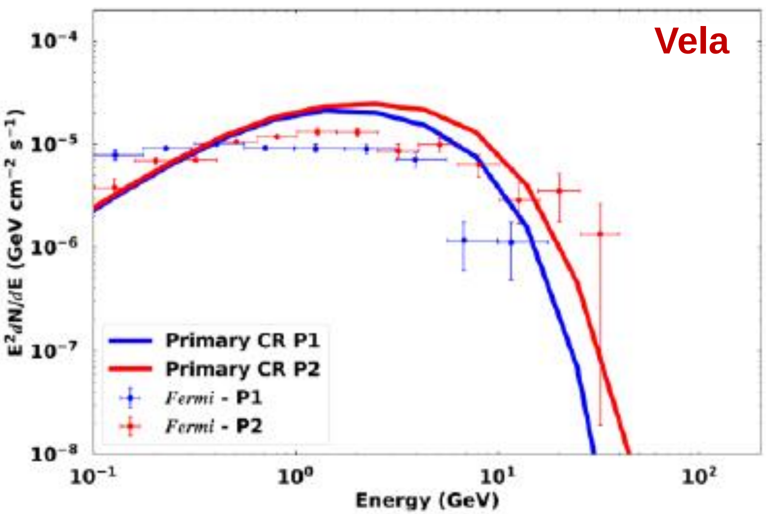

Credit: L du Plessis

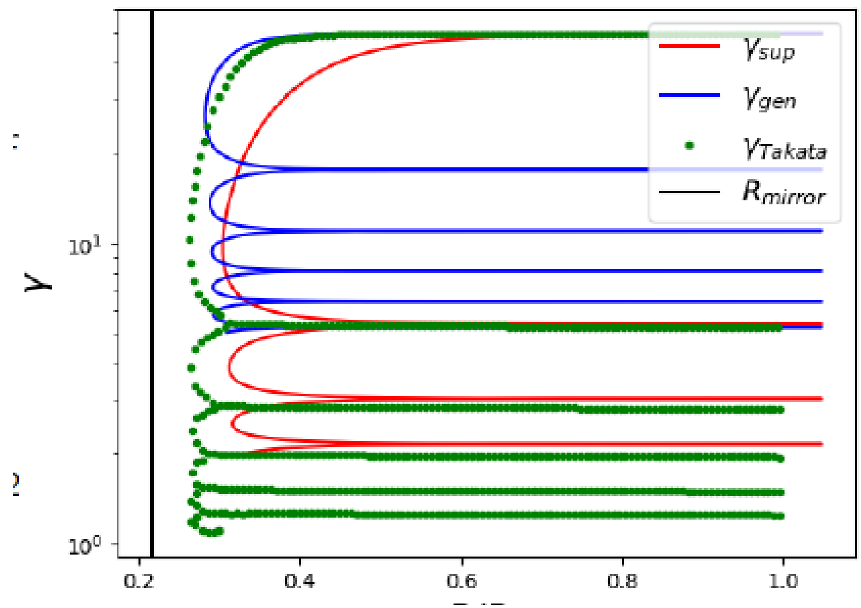

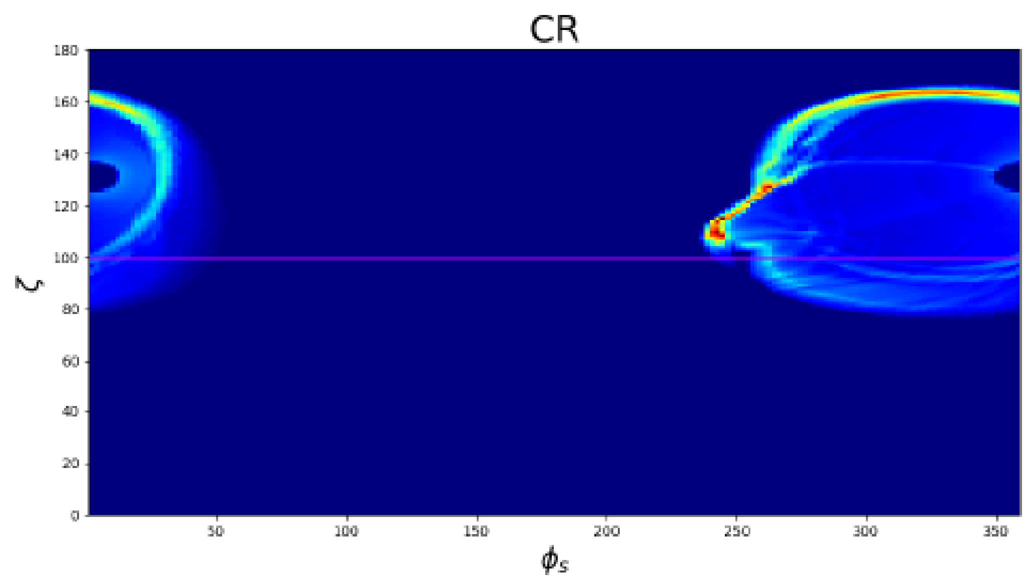

RUNTIME!! Strong B-field

AR Sco

MeerKAT Obser-vations

Open Time Round 1, 2, 3, 4

A search for persistent radio emission associated with localised FRBs

MeerKAT Open Time Proposal

Overvie

Fast Radio

Investigating the properties of localised

Monthly Notices of the ROYAL ASTRONOMICAL SOCIETY

MNRAS **00**, 1 (2022) https://doi.org/10.1093/mnras/stac1601

Advance Access publication 2022 June 16

A MeerKA transient e

J. O. Chibueze

C. Venter,[1] I. H

M. C. Bezuiden

M. Mickaliger,[3]

C. R. H. Walke

E. O. Angüner,[1]

D. Berge,[21] M.

R. Brose,[14] F. B

T. Chand,[1] A. C

MNRAS **000**, 1–13 (2022) Preprint 15 February 2023 Compiled using MNRAS LaTeX style file v3.0

Discovery of an apparently non-repeating fast radio burst with the hallmarks of a repeater

M. Caleb,[1,2,3★] L. N. Driessen,[4,1] A. C. Gordon,[5] N. Tejos,[6] J. O. Chibueze,[7,8] B. W. Stappers,[2] K. M. Rajwade,[9,2] F. Cavallaro,[10,11] Y. Wang,[1,12,13] P. Kumar,[14,15] W. A. Majid,[16,17] R. S. Wharton,[16] C. J. Naudet,[16] M. C. Bezuidenhout,[7] F. Jankowski,[2,18] M. Malenta,[2] V. Morello,[2] S. Sanidas,[2] M. P. Surnis,[2,19] E. D. Barr,[20] W. Chen,[20] M. Kramer,[20,2] W. Fong,[5] C. D. Kilpatrick,[5] J. Xavier Prochaska,[21,22] S. Simha,[21] C. Venter,[7] I. Heywood,[23,24] A. Kundu,[7] F. Schussler[25]

[1] *Sydney Institute for Astronomy, School of Physics, The University of Sydney, NSW 2006, Australia*

[2] *Jodrell Bank Centre for Astrophysics, University of Manchester, Oxford Road, Manchester M13 9PL, UK*

[3] *ASTRO3D: ARC Centre of Excellence for All-sky Astrophysics in 3D, ACT 2601, Australia*

[4] *CSIRO, Space and Astronomy, PO Box 1130, Bentley, WA 6102, Australia*

[5] *Center for Interdisciplinary Exploration and Research in Astrophysics (CIERA) and Department of Physics and Astronomy, Northwestern University, Evanston, IL*

[6] *Instituto de Física, Pontificia Universidad Católica de Valparaíso, Casilla 4059, Valparaíso, Chile*

Open Time Round 1, 2, 3, 4

- Search for persistent radio emission from the one-off fast radio burst (FRB) 20190714A, as well as from two repeating FRBs, 20190711A and 20171019A, using MeerKAT.
- For FRB 20171019A, simultaneous observations with H.E.S.S. and searched for signals in the uv, optical, and X-ray bands.
- UV flux upper limit of 1.39×10^{-16} erg cm^{-2}s^{-1}Å^{-1}.
- X-ray limit of $\sim6.6\times10^{-14}$ erg cm^{-2} s^{-1}
- F(E > 120 GeV) $< 1.7\times10^{-12}$ erg cm^{-2} s^{-1}.
- Radio UL ~15 μJy beam^{-1} for persistent emission at the locations of both FRBs 20190711A and 20171019A.

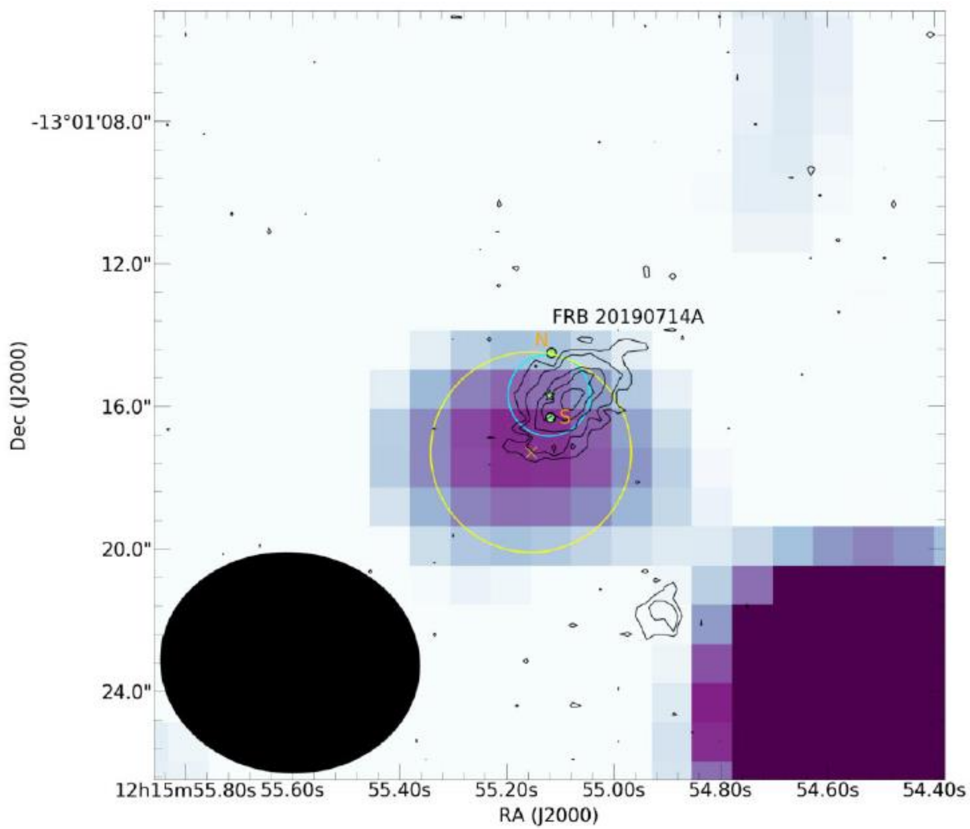

Some Open Questions

- <u>**Debates:**</u>
  - ➢ **SR vs. CR responsible for GeV spectrum?**
  - ➢ **OG vs. SG – break degeneracy using TeV emission**
- **Spectral shape of emitting particles (primaries / pairs)?**
- **Which emission mechanisms contribute to the broadband SED?**
- **Local and global electrodynamical properties?**
- **Pulsar (magnetosphere) geometry? Novel systems?**

Spectral and energy-dependent light curve modelling

(Polarimetry)

Overlaps?

<u>Quantum processes</u>

- **One-photon pair production**
- **Two-photon pair production**
- **Photon splitting**
- **Critical *B*-fields B > 4e13 G: effect on radiation physics**

Overlaps?

Computational power needed!

- Diverse data sets
- Diverse models addressing different scales / quantities
- E.g., statistics, searching, classifying
- E.g., triple integrals, coupled differential equations, Maxwell's equations, trajectories (SR, beaming), Monte Carlo, pair production, polarisation, binning…

Overlaps?

Storage of information

- **MeerKAT: 2 TB/h**
- **On-the-fly analysis, discarding a lot of data due to space limitations**
- **IDIA / CHPC: storage constraints**
- **Data mining (Machine Learning)**

Conclusions

- Lots of outstanding theoretical issues in pulsar science
- Lots of new (multi-messenger) and high-quality data
- Quantum effects in physical processes
- Computational requirements sometimes prohibitive
- New ideas? Overlaps?

Thanks!

NRF National Research Foundation | RISA Research and Innovation Support and Advancement

This work is based on the research supported wholly/in part by the National Research Foundation (NRF) of South Africa (grant number 99072). The grantholder acknowledges that opinions, findings, and conclusions or recommendations expressed in any publication generated by the NRF supported research is that of the author(s), and that the NRF accepts no liability whatsoever in this regard.

"The heavens declare the glory of God; the skies proclaim the work of his hands." (Ps. 19:1)